Science Advances
AAAS

advances.sciencemag.org/cgi/content/full/6/46/eabc6871/DC1

# Supplementary Materials for

## HSF1 physically neutralizes amyloid oligomers to empower overgrowth and bestow neuroprotection

Zijian Tang, Kuo-Hui Su, Meng Xu, Chengkai Dai*

*Corresponding author. Email: chengkai.dai@nih.gov

Published 11 November 2020, *Sci. Adv.* **6**, eabc6871 (2020)
DOI: 10.1126/sciadv.abc6871

**This PDF file includes:**

Figs. S1 to S8
Tables S1 to S3

## SUPPLEMENTAL MATERIALS AND METHODS

### Cell lines

HEK293T cells were purchased from GE Dharmacon, and HeLa and A2058 cells were purchased from ATCC. They were all authenticated by ATCC. Immortalized *Rosa26-CreER$^{T2}$*; *Hsf1$^{fl/fl}$* MEFs (male) were described previously (*21*). Primary mouse astrocytes were prepared from the brains of P1 newborn mice as described previously (*58*) with a minor modification, wherein trypsin was replaced with Accumax Cell Dissociation Solution. All cell cultures were maintained in DMEM supplemented with 10% HyClone™ bovine growth serum. These cell lines have been routinely tested for mycoplasma contamination using MycoAlert™ Mycoplasm Detection kits.

Primary human neurons were cultured in complete neuronal medium. For the PLA, human neurons were plated on 8-well Nunc™ Lab-Tek™ II CC2™ Chamber Slides coated with both 20μg/ml laminin and 50μg/ml poly-L-Lysine. Half of the culture medium was changed every four days. After 12 days in culture, neurons were transduced with lentiviral particles overnight in the absence of polybrene and cultured for another four days, followed by transfection with A$\beta_{1\text{-}42}$ peptides overnight.

### Dual HSF1 reporter assay

Plasmids were co-transfected with the dual reporter system, comprising the heat shock element (HSE)-secreted embryonic alkaline phosphatase (SEAP) and CMV-Gaussia luciferase (GLuc) reporter plasmids, into HEK293T cells using TurboFect™ transfection reagents. After 48 hr, SEAP and luciferase activities in culture supernatants were quantitated using a NovaBright™ Phospha-Light™ EXP Assay Kit for SEAP and a Pierce™ Gaussia Luciferase Glow Assay Kit, respectively. Luminescence signals were measured by a CLARIOstar microplate reader (BMG LABTECH), and SEAP activities were normalized against GLuc activities.

### *In vitro* kinase assays

The AKT kinase assays were performed in 30μl kinase buffer comprising 25mM MOPS pH 7.2, 12.5mM β-glycerol-phosphate, 25mM MgCl2, 5mM EGTA, 2mM EDTA, 0.25mM dithiothreitol, 250μM ATP. Reactions were incubated at 30ºC for 30 min with 1,200 rpm mixing in an Eppendorf Thermomixer® C (Eppendorf North America). Reactions were stopped by adding 30μl of 2x SDS-PAGE sample buffer with 3% 2-mercaptoethanol.

### Real-time quantitative RT-PCR

The extraction of total RNAs and qRT-PCR were described previously (*21*). Signals were detected by an Agilent Mx3000P qPCR System (Agilent Genomics). ACTB was used as the internal control. The sequences of individual primers for each gene are listed in Table S3.

### Chromatin immunoprecipitation (ChIP)

ChIP experiments were performed according to the procedures described previously (*5*). Rabbit anti-HSF1 Abs H-311 or rabbit monoclonal anti-DYKDDDDK Tag Abs (D6W5B) were used for ChIP. Normal rabbit IgG served as the negative control. The sequences of individual primers for each gene are listed in Table S3.

### Cytosolic and nuclear fractionation

Cytosolic and nuclear fractions were separated using a NE-PER™ Nuclear and Cytoplasmic Extraction Kit. Equal amounts of the same fractions were loaded for SDS-PAGE.

**Measurement of cell size and quantitation of nuclei and DNA content**
The sizes of cultured astrocytes were measured by a Scepter™ 2.0 Handheld Automated Cell Counter (Millipore) equipped with 60 μm sensors. Nuclei and DNAs were extracted from 30mg pulverized frozen mouse brain tissues. Nuclei were extracted using a Detergent-free Nuclei Isolation Kit and counted using the Scepter™ 2.0 Cell Counter. DNAs were extracted using a NucleoSpin® TriPrep Kit and quantitated by a NanoDrop™ 2000 Microvolume Spectrophotometer (Thermo Fisher Scientific).

**Measurement of global protein translation rate**Cultured astrocytes were labeled with 50nM 6-FAM-dc-puromycin *in vitro* for 30 min and analyzed by flow cytometry.

**Congo red staining**
Following deparaffinization or air drying, paraffin-embedded brain or frozen liver sections were stained with 0.5% CR dissolved in PBS at RT for 20 min followed by differentiation in alkaline solutions (0.01% NaOH in 50% alcohol). Nuclei were counterstained with hematoxylin.

**Peptide and antibody transfection**
$A\beta_{42-1}$ or $A\beta_{1-42}$ peptides and A11 or OC antibodies were transfected into primary mouse astrocytes, immortalized MEFs, or primary human neurons using the Xfect™ Protein Transfection Reagent.

**Mitochondria fractionation**
$1x10^6$ astrocytes were used to isolate the cytoplasmic and mitochondrial fractions using a Mitochondrial Isolation Kit according to the manufacturer's instructions. Equal amounts of the same fractions were loaded for SDS-PAGE.

**Quantitation of mitochondrial mass**
After detaching cells with trypsin from culture plates, live cells were incubated with the culture medium containing 100nM MitoView™ Green dyes, which are not dependent on the mitochondrial membrane potential, for 15 min at 37°C. After washing once with PBS, stained cells were analyzed by a BD FACSCalubur™ flow cytometer (BD Biosciences) using the FL1 channel. The data were analyzed using the FlowJo™ v10 software (FlowJo LLC.).

**siRNA and shRNA knockdown**
siRNAs were transfected at 10nM final concentration using Mission® siRNA transfection reagent or jetPRIME® transfection reagent. HEK293T cells stably expressing lentiviral *HSF1*-targeting (hA6) shRNAs were described previously (*21*). The target sequences of siRNAs and shRNAs are listed in Table S3.

**Separation of detergent-soluble and -insoluble cell/tissue fractions**
All centrifugation was performed in Eppendorf Benchtop 5424 Microcentrifuges at 4°C. First, $1x10^6$ cells or 1mg pulverized snap-frozen tissues were incubated with the whole-cell lysis buffer (100 mM NaCl, 30 mM Tris-HCl pH 7.6, 1% Triton X-100, 1 mM EDTA, 1x Halt™ phosphatase inhibitor cocktail, and 1x Halt™ protease inhibitor cocktail) on ice for 20 min. Following a brief centrifugation at 500xg for 5 min at $4^0$C, the lysates were separated into pellets (P1) and supernatants (S1). The P1, which contains nuclei, membrane debris, and large aggregates, was then treated with 50μl DNA digestion buffer (three units DNase I in 40 mM Tris-HCl, pH 8.0, 10 mM NaCl, 6 mM $MgCl_2$, 10 mM $CaCl_2$ and 1% Triton X-100) at RT for 20 min to digest genomic DNAs, followed by membrane re-solubilization with 2% SDS for 30 min at RT. The re-solubilized P1 was centrifugated at 16,813xg for 10 min at $4^0$C to obtain pellets (P2), which contain large aggregates and some SDS-resistant materials that cannot be resolubilized, and supernatants (S2), which mainly contain resolubilized membrane-

associated proteins and are therefore designated as the membrane-associated fractions. The combined S1 and P2 were further centrifuged at 16,813xg for 10 min at $4^0$C to obtain pellets (P3) and supernatants (S3). The P3, which contains both large aggregates from the P2 and small aggregates pelleted from the S1, is thus designated as the detergent-insoluble fractions. By contrast, the S3, which now contains all soluble proteins, is designated as the detergent-soluble fractions. For downstream SDS-PAGE and ELISA, the detergent-insoluble fractions were further re-solubilized by sonication for 10 min in PBS containing 2% SDS at high intensity using a Bioruptor® Sonication System (Diagenode Inc.) or a Q125 sonicator (Qsonica, LLC).

**Apoptosis detection**

Four independent approaches were applied to detect apoptosis in cultured cells and frozen tissues, including quantitation of caspase 3 activity using either a Caspase-3 Colorimetric Assay Kit or a Caspase 3 DEVD-R110 Fluorometric and Colorimetric Assay Kit, immunostaining with rabbit monoclonal anti-cleaved Caspase-3 (Asp175) (5A1E) Abs, detection of DNA fragmentation (TUNEL) in frozen sections using a NeuroTACS™ II In Situ Apoptosis Detection Kit, and measurement of mitochondrial membrane potential changes by FACS using a JC-1 Mitochondrial Membrane Potential Detection Kit. For the JC-1 staining, both floating and adherent cells were collected for analyses.

**Immunoblotting and Immunoprecipitation**

Whole cell lysates were extracted in lysis buffer, which comprises 100 mM NaCl, 30 mM Tris-HCl pH 7.6, 1% Triton X-100, 1 mM EDTA, 1x Halt™ phosphatase inhibitor cocktail, and 1x Halt™ protease inhibitor cocktail. Following incubation on ice for 20 min, lysates were centrifuged at 15,000 rpm for 10 min in an Eppendorf Benchtop 5424 Microcentrifuge at 4°C.

For immunoblotting, nitrocellulose membranes were incubated with primary antibodies (1:1,000 dilution in the blocking buffer) overnight at 4°C, followed by incubation with peroxidase-conjugated secondary antibodies (1: 2,500 dilution in the blocking buffer) at RT for 1 hr. Signals were generated using SuperSignal West Pico PLUS or Femto chemiluminescent substrates and captured by either X-ray films or an iBright™ FL1000 imaging system (Life Technologies Corporation). Uncropped blot images are provided as Fig. S8.

For IP, either 1mg whole cell and mouse tissue lysates or 500µg human AD brain lysates were incubated at 4°C overnight with primary antibodies, including: 10µl rabbit monoclonal anti-AKT (pan) (C67E7) Abs, 2µg rabbit polyclonal anti-amyloid oligomers (A11) or anti-amyloid fibrils (OC) Abs, 2µg mouse monoclonal anti-$A\beta_{17-24}$ (4G8) Abs, and 2µg rabbit anti-HSF1 (H-311) Abs or 2µg mouse monoclonal anti-HSP60 Abs clone LK1. Either normal rabbit or mouse IgG or rabbit anti-PI3K p110α (C73F8) were used as the negative controls. Protein G MagBeads were used to precipitate primary Abs. After washing with the lysis buffer three times, beads were boiled in 1x sample loading buffer for 5 min before loading on SDS-PAGE.

To minimize the cross-reactivity between secondary Abs and reduced, denatured IP Abs during immunoblotting, EasyBlot® anti-Rabbit or anti-Mouse IgG Kits, which also include EasyBlocker to reduce the background caused by Protein G, were applied.

**Dot blotting of $A\beta_{1-42}$**

1µM $A\beta_{1-42}$ was mixed with GST or HSF1 proteins at different molar ratios in 100µl PBS and incubated at RT for 4 hr. After centrifugation at 15,000 rpm for 10 min at 4°C in an Eppendorf

Benchtop 5424 microcentrifuge, 50µl of supernatants were loaded on a 96-well Bio-Dot® Microfiltration Apparatus with Immobilon® PVDF membranes (0.45µm pore size) pre-soaked in PBS. A vacuum was used to drain the samples. Following blocking with 5% non-fat dry milk in PBS, the membranes were incubated with 4G8, ab2539, or D54D2 Abs (1:1000) at 4°C overnight, followed by incubation with secondary Abs-HRP conjugates (1:2500) at RT for 1 hr.

**Immunofluorescence**

Following fixation with 4% formaldehyde in 1xPBS for 15 minutes at RT, cells were blocked with 5% normal goat serum in PBS containing 0.3% Triton X-100 for 1 hr at RT. Primary antibodies 1:100 diluted in 5% normal goat serum were incubated at 4°C overnight, followed by incubation with donkey anti-rabbit or anti-mouse IgG (H+L) CF®594 or CF®488A conjugates (1:200) at RT for 1 hr. For immunofluorescence staining of HSP60 in mouse brains, frozen sections were first incubated with mouse monoclonal anti-HSP60 Abs clone LK1 (1:100) at 4°C overnight, followed by incubation with anti-mouse IgG (H+L) CF®594 conjugates (1:200) at RT for 1 hr. To co-stain neurons, sections were further incubated with mouse anti-βIII Tubulin Abs clone 2G10-TB3 Alexa Fluor® 488 conjugates (1:100) at RT for 4 hr. A set of brain sections incubated only with conjugated secondary Abs served as the negative controls. Nuclei were counterstained with Hoechst 33342, and fluorescent signals were documented by a Zeiss LSM780 confocal microscope.

**Nissl staining**

Following deparaffinization, brain sections were stained with 0.1% Cresyl violet solution (NovaUltra™ Nissl Stain Kit) for 5 min, followed by differentiation in 95% alcohol for 1 min.

**Lentiviral production and transduction**

Lentiviral particles were produced in HEK293T cells by co-transfection of pLKO vectors, pCMV-dR8.2 dvpr, and pCMV-VSV-G using the TurboFect™ Transfection Reagent. Culture supernatants containing lentiviral particles were collected and filtered through sterile 0.45µm syringe filters. Lentiviral titers were determined using the Lenti-X™ GoStix™ Plus. To transduce target cells, different amounts of viral supernatants, based on the MOIs, were diluted in the culture medium containing 10µg/ml polybrene and incubated with target cells overnight.

# Figure S1

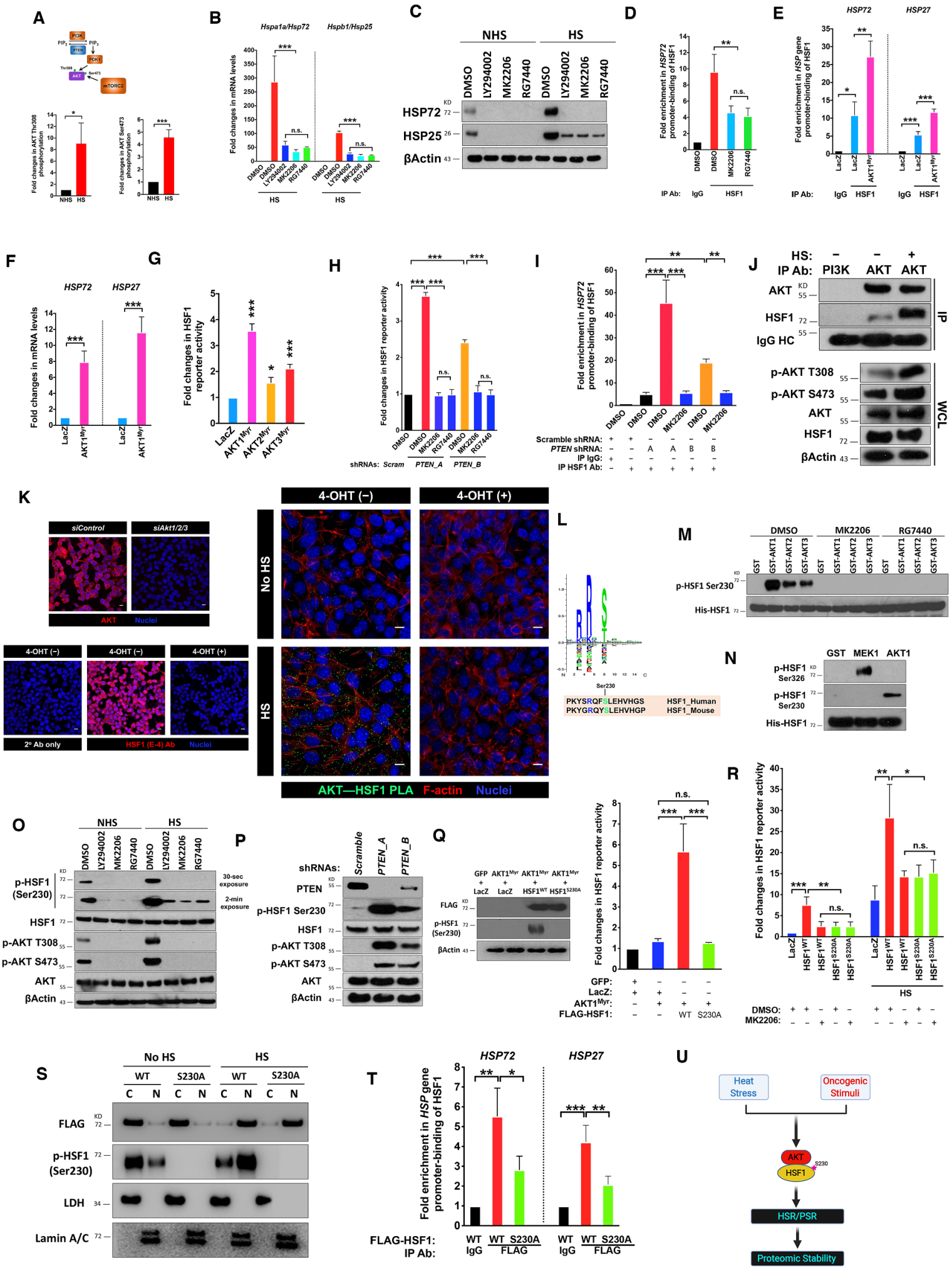
A
PI3K
PIP2
PIP3
PTEN
PDK1
Thr308
AKT
Ser473
mTORC2
Fold changes in AKT Thr308 phosphorylation
Fold changes in AKT Ser473 phosphorylation
NHS
HS
B
Hspa1a/Hsp72
Hspb1/Hsp25
Fold changes in mRNA levels
DMSO
LY294002
MK2206
RG7440
n.s.
C
NHS
HS
HSP72
HSP25
βActin
KD
D
Fold enrichment in HSP72 promoter-binding of HSF1
IP Ab:
IgG
HSF1
E
HSP72
HSP27
Fold enrichment in HSP gene promoter-binding of HSF1
LacZ
AKT1Myr
F
HSP72
HSP27
Fold changes in mRNA levels
G
Fold changes in HSF1 reporter activity
LacZ
AKT1Myr
AKT2Myr
AKT3Myr
H
Fold changes in HSF1 reporter activity
shRNAs:
Scram
PTEN_A
PTEN_B
I
Fold enrichment in HSP72 promoter-binding of HSF1
Scramble shRNA:
PTEN shRNA:
IP IgG:
IP HSF1 Ab:
J
HS:
IP Ab:
PI3K
AKT
AKT
AKT
HSF1
IgG HC
IP
p-AKT T308
p-AKT S473
AKT
HSF1
βActin
WCL
K
siControl
siAkt1/2/3
AKT
Nuclei
4-OHT (−)
4-OHT (+)
No HS
HS
2° Ab only
HSF1 (E-4) Ab
Nuclei
AKT—HSF1 PLA
F-actin
Nuclei
L
Ser230
PKYSRQFSLEHVHGS
HSF1_Human
PKYGRQYSLEHVHGP
HSF1_Mouse
M
DMSO
MK2206
RG7440
GST
GST-AKT1
GST-AKT2
GST-AKT3
p-HSF1 Ser230
His-HSF1
N
GST
MEK1
AKT1
p-HSF1 Ser326
p-HSF1 Ser230
His-HSF1
O
NHS
HS
p-HSF1 (Ser230)
30-sec exposure
2-min exposure
HSF1
p-AKT T308
p-AKT S473
AKT
βActin
P
shRNAs:
Scramble
PTEN_A
PTEN_B
PTEN
p-HSF1 Ser230
HSF1
p-AKT T308
p-AKT S473
AKT
βActin
Q
GFP
AKT1Myr
AKT1Myr
AKT1Myr
LacZ
LacZ
HSF1WT
HSF1S230A
FLAG
p-HSF1 (Ser230)
βActin
Fold changes in HSF1 reporter activity
GFP:
LacZ:
AKT1Myr:
FLAG-HSF1:
WT
S230A
R
Fold changes in HSF1 reporter activity
LacZ
HSF1WT
HSF1S230A
HS
DMSO:
MK2206:
S
No HS
HS
WT
S230A
C
N
FLAG
p-HSF1 (Ser230)
LDH
Lamin A/C
T
HSP72
HSP27
Fold enrichment in HSP gene promoter-binding of HSF1
FLAG-HSF1:
IP Ab:
WT
WT S230A
IgG
FLAG
U
Heat Stress
Oncogenic Stimuli
AKT
HSF1
S230
HSR/PSR
Proteomic Stability

## SUPPLEMENTARY FIGURE LEGENDS

**Figure S1: AKT directly activates HSF1.**
**(A**) Following heat shock at 43°C for 30 min, HEK293T cells were fixed and stained with phospho-AKT Thr308 and Ser473 antibodies. The fluorescence intensities were quantitated by flow cytometry (mean±SD, n=3 experiments, two-tailed Student's t test). NHS: no heat shock. (**B**) Following pre-treatment with 20μM inhibitors for 3 hr, NIH3T3 cells were heat shocked at 43°C for 30 min and recovered at 37°C for 8 hr. The mRNAs of *Hsp72* and *Hsp25* were quantitated by qRT-PCR (mean±SD, n=3 experiments, One-way ANOVA). (**C**) Following pre-treatment with 20μM PI3K or AKT inhibitors for 3 hr, NIH3T3 cells were heat shocked at 43°C for 30 min and recovered at 37°C for 8 hr. HSP induction was detected by immunoblotting (images of a single experiment). (**D**) Following treatment with 20μM AKT inhibitors for 3 hr, the binding of HSF1 to the *HSP72* promoter in HEK293T cells in the absence of heat shock was quantitated by chromatin immunoprecipitation (ChIP)-qPCR (mean±SD, n=3 experiments, One-way ANOVA). (**E)** and (**F**) Following transfection of HEK293T cells with LacZ or $AKT1^{Myr}$ plasmids for 48 hr, the binding of endogenous HSF1 to the *HSP72* and *HSP27* promoters were quantitated by ChIP-qPCR (**E**) and the transcripts of *HSPs* were quantitated by qRT-PCR (**F**) (mean±SD, n=3 experiments, One-way ANOVA). (**G**) Following co-transfection of plasmids encoding individual AKT isoforms along with the dual HSF1 reporter system in HEK293T cells for 48 hr, the reporter activities in culture media were measured, and SEAP activities were normalized against GLuc activities (mean±SD, n=3 experiments, One-way ANOVA). (**H**) HEK293T cells, stably expressing either scramble or *PTEN*-targeting shRNAs, were transfected with the dual HSF1 reporter system comprising the heat shock element (HSE)-secreted embryonic alkaline phosphatase (SEAP) and the CMV-Gaussia luciferase (GLuc) reporter plasmids. After 16 hr, transfected cells were treated with 20μM AKT inhibitors for 48 hr. The reporter activities in culture media were measured, and SEAP activities were normalized against GLuc activities (mean±SD, n=3 experiments, One-way ANOVA). (**I**) In HEK293T cells stably expressing either scramble or *PTEN*-targeting shRNAs, the binding of HSF1 to the *HSP72* promoter was quantitated by ChIP-qPCR with and without 20μM MK2206 treatment overnight (mean±SD, n=3 experiments, One-way ANOVA). (**J**) Following heat shock at 43°C for 30 min, the endogenous AKT-HSF1 interactions were detected by co-IP with the EasyBlot® reagents in HEK293T cells (representative images of three experiments). Rabbit monoclonal anti-PI3K p110α Abs served as the negative control. HC: heavy chain. WCL: whole cell lysate. (**K**) Following transfection of control or combined *Akt1/2/3*-targeting siRNAs for four days, immortalized *Rosa26-CreER$^{T2}$*; *Hsf1$^{fl/fl}$* MEFs without 4-OHT treatment were stained with rabbit monoclonal anti-pan AKT (C67E7) Abs (images of a single experiment). Following treatment with and without 1μM 4-OHT for seven days to delete *Hsf1*, these MEFs were stained with mouse monoclonal anti-HSF1 (E-4) Abs (images of a single experiment). The endogenous AKT-HSF1 interactions (green) were visualized by PLA using the anti-HSF1 (E-4) Ab and the anti-pan AKT (C67E7) Ab in these MEFs (representative images of three experiments performed by two individuals). Actin filaments and nuclei were labeled with phalloidin-Alexa Fluor® 594 conjugates (red) and Hoechst 33342 (blue), respectively. Scale bars: 10μm. (**L**) The consensus AKT phosphorylation sequence and corresponding Ser230 site on both human and mouse HSF1 proteins. (**M**) *In vitro* His-HSF1 Ser230 phosphorylation by recombinant active AKT isoforms (representative images of three experiments). Following co-incubation of 100ng recombinant His-HSF1 proteins with 100ng GST or AKT isoforms at 30°C for 30 min with and without 20μM AKT inhibitors, HSF1 Ser230 phosphorylation was detected by immunoblotting. (**N**) *In vitro* phosphorylation of His-HSF1 by recombinant active MEK1 and AKT1 proteins independently (representative images of three experiments). Phosphorylation was detected by immunoblotting. (**O**) Following heat shock at 43°C for

30 min, HSF1 and AKT phosphorylation in HEK293T cells pre-treated with 20μM PI3K or AKT inhibitors for 3 hr was detected by immunoblotting (images of a single experiment). (**P**) HSF1 and AKT phosphorylation in HEK293T cells stably expressing either scramble or *PTEN*-targeting shRNAs was detected by immunoblotting (images of a single experiment). (**Q**) In HEK293T cells stably expressing a shRNA (A6) that targets the 3' UTR of *HSF1*, indicated plasmids were co-transfected along with the dual HSF1 reporter system. After 48 hr, the reporter activities in culture media were measured, and SEAP activities were normalized against GLuc activities (mean±SD, n=3 experiments, One-way ANOVA). The expression of $HSF1^{WT}$ and $HSF1^{S230A}$ was detected by immunoblotting. (**R**) HEK293T cells stably expressing *HSF1*-targeting shRNAs (A6) were co-transfected with indicated plasmids along with the dual reporter plasmids. After 16 hr, transfected cells were pre-treated with 20μM MK2206 for 3 hr, followed by heat shock at 43°C for 30 min. Forty-eight hours after heat shock, the reporter activities in culture media were measured, and SEAP activities were normalized against GLuc activities (mean±SD, n=3 experiments, One-way ANOVA). (**S**) Following transfection with FLAG-$HSF1^{WT}$ or -$HSF1^{S230A}$ plasmids and heat shock at 43°C for 30 min, the cytosolic and nuclear fractions of HEK293T cells were prepared, and FLAG-HSF1 was detected by immunoblotting (representative images of three experiments). LDH and Lamin A/C were used as the cytosolic and nuclear markers, respectively. C: cytosolic; N: nuclear. (**T**) HEK293T cells stably expressing *HSF1*-targeting shRNAs (A6) were transfected with either FLAG-$HSF1^{WT}$ or -$HSF1^{S230A}$ plasmids. After 48 hr, the binding of HSF1 to the *HSP72* and *HSP27* promoters was quantitated by ChIP-qPCR (mean±SD, n=3 experiments, One-way ANOVA). (**U**) Both heat stress and oncogenic stimuli converge on the AKT-mediated HSF1 activation, which manages to sustain the proteomic stability.
(C), (O), and (P) were done once; all the others were repeated thrice.

# Figure S2

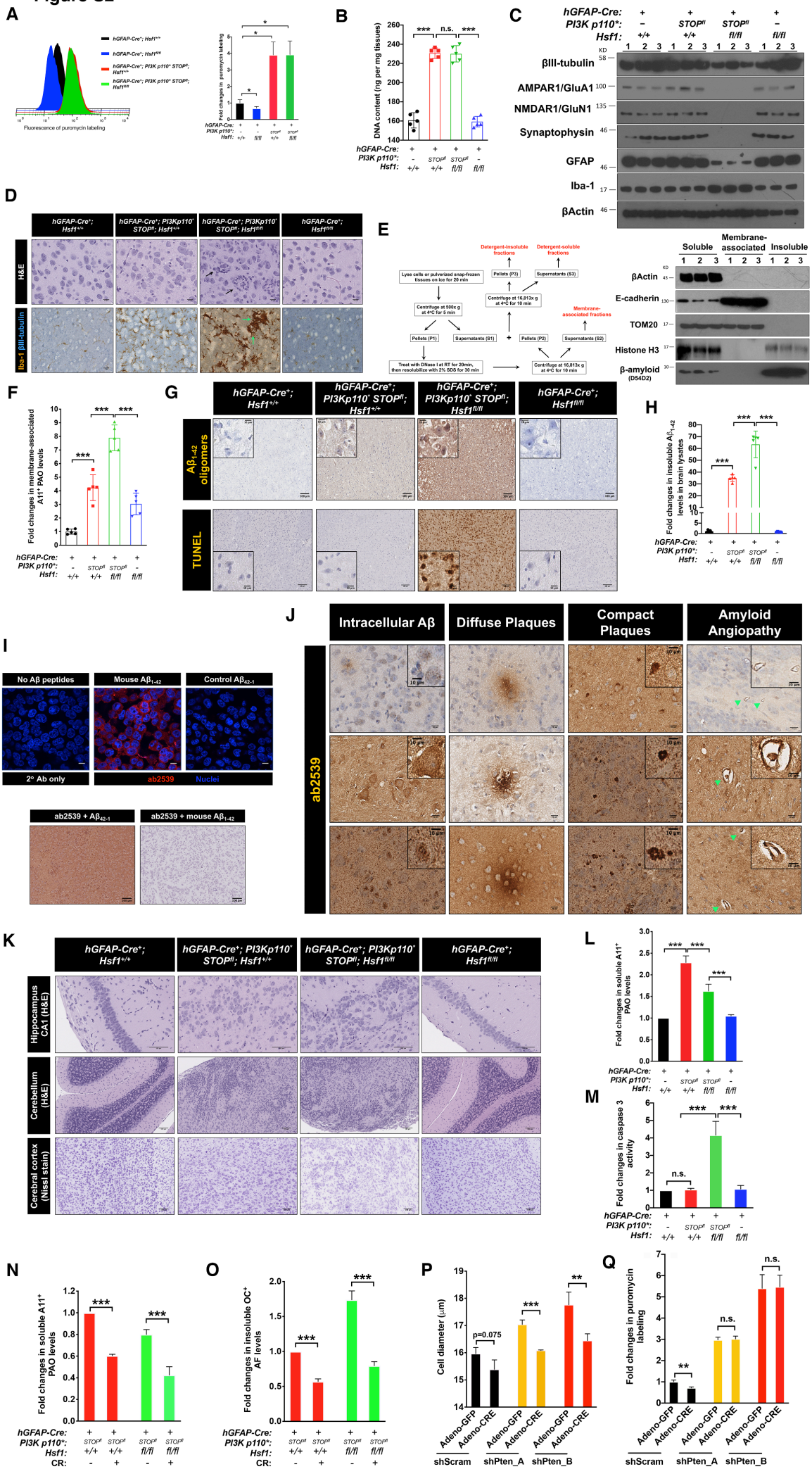
A
B
C
D
E
F
G
H
I
J
K
L
M
N
O
P
Q
hGFAP-Cre:
PI3K p110*:
Hsf1:
DNA content (ng per mg tissues)
n.s.
βIII-tubulin
AMPAR1/GluA1
NMDAR1/GluN1
Synaptophysin
GFAP
Iba-1
βActin
Soluble
Membrane-associated
Insoluble
E-cadherin
TOM20
Histone H3
β-amyloid
(D54D2)
H&E
TUNEL
Aβ1-42 oligomers
Fold changes in membrane-associated A11+ PAO levels
Fold changes in insoluble Aβ1-42 levels in brain lysates
No Aβ peptides
Mouse Aβ1-42
Control Aβ42-1
2° Ab only
ab2539
Nuclei
ab2539 + Aβ42-1
ab2539 + mouse Aβ1-42
Intracellular Aβ
Diffuse Plaques
Compact Plaques
Amyloid Angiopathy
Hippocampus CA1 (H&E)
Cerebellum (H&E)
Cerebral cortex (Nissl stain)
Fold changes in soluble A11+ PAO levels
Fold changes in caspase 3 activity
Fold changes in soluble OC+ AF levels
Cell diameter (μm)
p=0.075
Adeno-GFP
Adeno-CRE
shScram
shPten_A
shPten_B
Fold changes in puromycin labeling

**Figure S2: HSF1 is required for megalencephaly driven by constitutively active PI3K.**
(**A**) Measurement of global protein translation rate in cultured astrocytes by puromycin labeling. The labeling fluorescence intensity (FL1-H) was quantitated by FACS and represented as geometric means (mean±SD, n=3 lines of astrocytes each genotype, One-way ANOVA). The histogram represents a single line. (**B**) Quantitation of DNA content in frozen mouse brain tissues (mean±SD, n=5 mice per group, One-way ANOVA). (**C**) Immunoblotting of neuronal, astrocytic, and microglial markers in the lysates of whole mouse brains (three mice per group). (**D**) Microglial activation and neuronophagia, indicated by the arrows, in $P^{*}H^{-}$ brains (representative images of three brains each genotype). Scale bars: 20μm. (**E**) Flowchart of the fractionation procedures and validation of the fractionation method by immunoblotting using mouse brains. Three individual *p110**-expressing $Hsf1^{+/+}$ brains were tested. β-Actin served as the marker for detergent-soluble fractions, E-cadherin and TOM20 served as the markers for membrane-associated fractions, and β-amyloid served as the marker for detergent-insoluble fractions. For the soluble and insoluble fractions, 40μg proteins were loaded, and only 20μg proteins were loaded for the membrane-associated fractions. Of note, some Histone remained insoluble. Detergent-insoluble fractions were re-solubilized by sonication before loading for SDS-PAGE. **(F**) Quantitation of PAOs in the membrane-associated fractions of brain lysates by ELISA (mean±SD, n=5 mice per group, One-way ANOVA). (**G**) Representative images of frozen brain sections stained with anti-$A\beta_{1\text{-}42}$ oligomer Abs or TUNEL assays (from three brains of each genotype and the TUNEL staining was performed by two individuals). Scale bars: 100μm for main images; 10μm for insets. (**H**) Quantitation of endogenous mouse $A\beta_{1\text{-}42}$ in the insoluble fractions of mouse brain lysates (mean±SD, n=5 mice per group, One-way ANOVA). (**I**) Validation of the specificity of anti-Aβ (ab2539) antibodies. Upper panel: immortalized *Rosa26-CreER*$^{T2}$; $Hsf1^{fl/fl}$ MEFs, treated with 4-OHT to delete *Hsf1*, were transfected with either 10μM control $A\beta_{42\text{-}1}$ or 10μM mouse $A\beta_{1\text{-}42}$ overnight, followed by staining with anti-Aβ (ab2539) Abs (representative images of three experiments). Scale bars: 10μm. Lower panel: the paraffin sections of $P^{*}H^{-}$ brains were stained with the mixture of ab2539 and the control $A\beta_{42\text{-}1}$ or mouse $A\beta_{1\text{-}42}$ peptides at a 1:20 molar ratio (representative images of three brains). Sale bars: 100μm. (**J**) Representative images of intracellular Aβ accumulation, plaque-like Aβ deposits, and amyloid angiopathy in $P^{*}H^{-}$ brains (from three brains). Arrowheads denote amyloid angiopathy. Scale bars: 20μm for main images and 10μm for insets. (**K**) Neurodevelopmental defects and neuronal loss in *p110**-expressing brains revealed by H&E and Nissl staining, respectively (images of a single experiment). Scale bars: 100μm. (**L)** and (**M**) Quantitation of soluble $A11^{+}$ PAOs and caspase 3 activities in cultured astrocytes (mean±SD, n=3 lines of astrocytes each genotype, One-way ANOVA). The caspase 3 activities were measured using a SensoLyte® Homogeneous Rh110 Caspase-3/7 Assay Kit. (**N**) and (**O**) Quantitation of free soluble PAOs and insoluble AFs in *p110**-expressing astrocytes treated with and without 10μM CR for two days, as described in Fig. 2A (mean±SD, n=3 lines of astrocytes each genotype, One-way ANOVA). (**P**) Measurement of the cell size of *Pten*-deficient astrocytes with and without *Hsf1* deletion (mean±SD, n=3 lines of astrocytes each genotype, two-tailed Student's t test). (**Q**) Measurement of the translation rate of *Pten*-deficient astrocytes with and without *Hsf1* deletion by puromycin labeling (mean±SD, n=3 lines of astrocytes each genotype, two-tailed Student's t test).
(B), (C), (H), and (K) were done once; (F) was repeated twice; and all the others were repeated thrice with different sets of astrocytes or brains.

# Figure S3

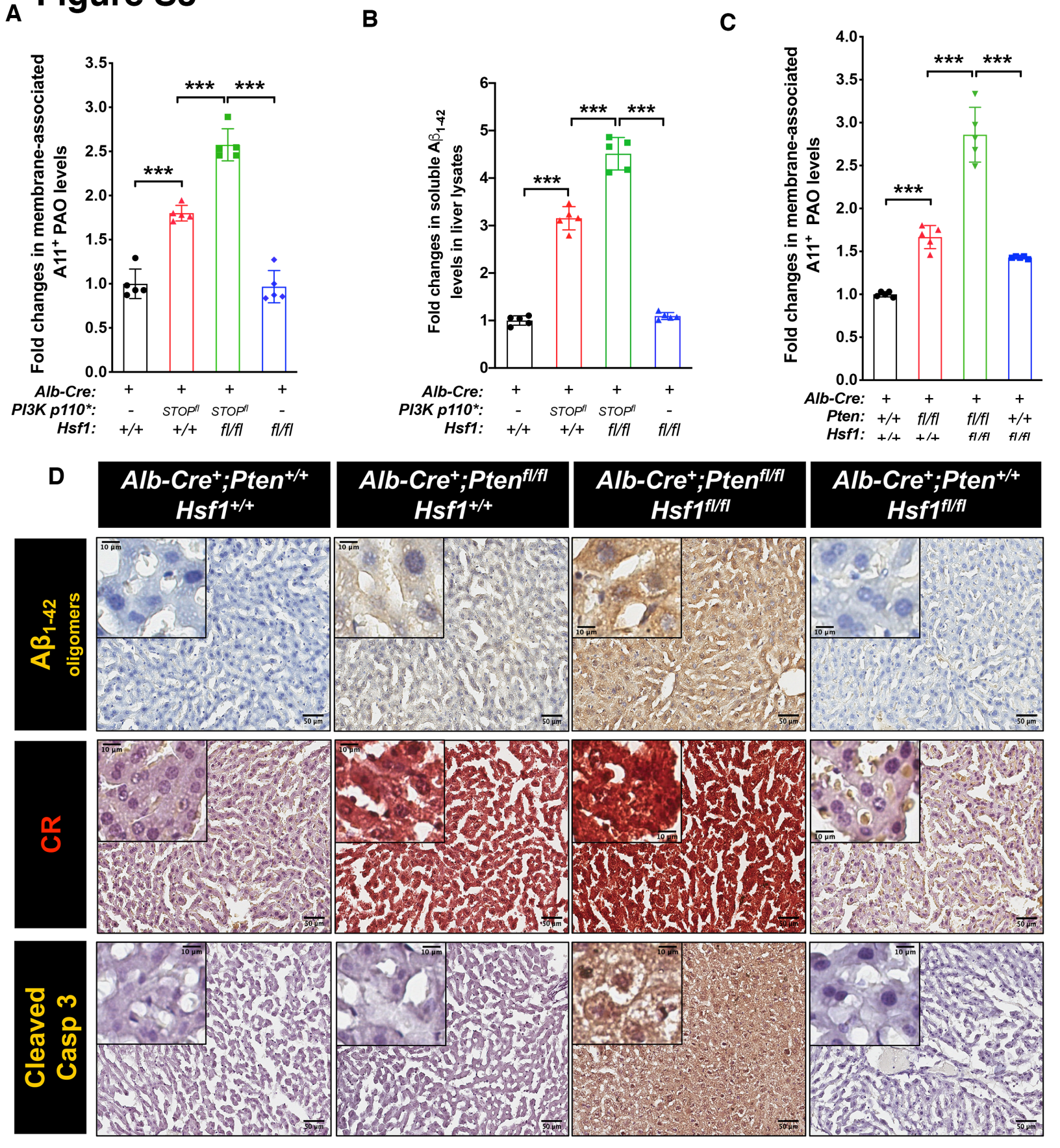
A
Fold changes in membrane-associated A11+ PAO levels
3.5
3.0
2.5
2.0
1.5
1.0
0.5
0.0
***
***
***
Alb-Cre: + + + +
PI3K p110*: - STOPfl STOPfl -
Hsf1: +/+ +/+ fl/fl fl/fl
B
Fold changes in soluble Aβ1-42 levels in liver lysates
6
5
4
3
2
1
0
***
***
***
Alb-Cre: + + + +
PI3K p110*: - STOPfl STOPfl -
Hsf1: +/+ +/+ fl/fl fl/fl
C
Fold changes in membrane-associated A11+ PAO levels
4.0
3.5
3.0
2.5
2.0
1.5
1.0
0.5
0.0
***
***
***
Alb-Cre: + + + +
Pten: +/+ fl/fl fl/fl +/+
Hsf1: +/+ +/+ fl/fl fl/fl
D
Alb-Cre+;Ptenfl/fl Hsf1fl/fl
Alb-Cre+;Ptenfl/fl Hsf1+/+
Alb-Cre+;Ptenfl/fl Hsf1fl/fl
Alb-Cre+;Ptenfl/fl Hsf1fl/fl
Aβ1-42 oligomers
CR
Cleaved Casp 3
10 μm
50 μm

**Figure S3: HSF1 suppresses amyloidogenesis in livers with constitutively active PI3K or PTEN deficiency.**

**(A)** Quantitation of PAOs in the membrane-associated fractions of livers expressing *p110** by ELISA (mean±SD, n=5 mice per group, One-way ANOVA). (**B**) Quantitation of endogenous $A\beta_{1-42}$ levels in the soluble fractions of mouse liver lysates expressing *p110** by ELISA (mean±SD, n=5 mice per group, One-way ANOVA). (**C**) Quantitation of PAOs in the membrane-associated fractions of livers deficient in *Pten* by ELISA (mean±SD, n=5 mice per group, One-way ANOVA). (**D**) Representative images of frozen mouse liver sections stained with anti-$A\beta_{1-42}$ oligomer Ab, Congo red (CR), or anti-cleaved caspase 3 Abs (from three livers of each genotype). Scale bars: 50μm for main images; 10μm for insets.

(B) was done once; (A) and (C) were repeated twice; and (D) was repeated thrice with different sets of livers.

# Figure S4

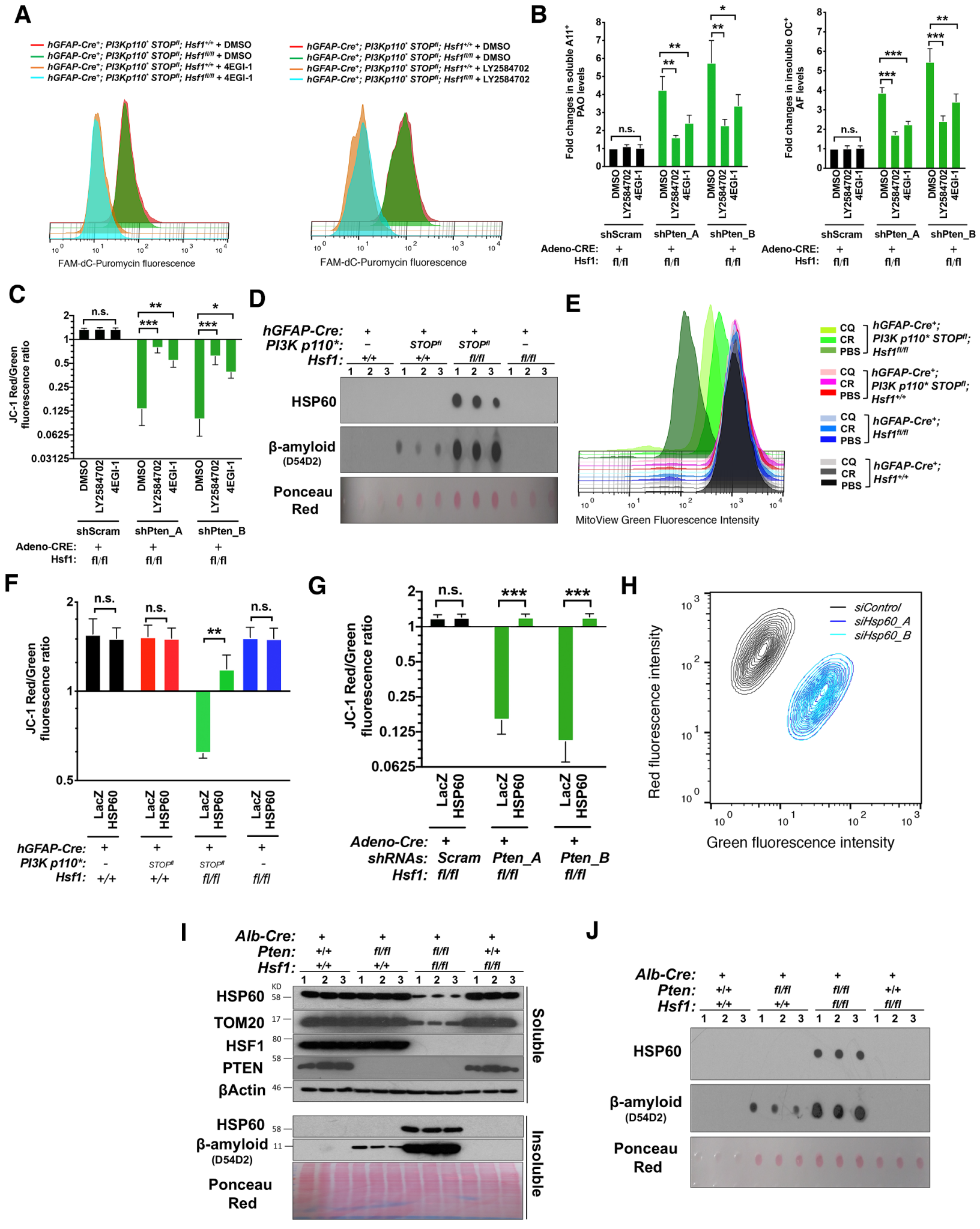
A
hGFAP-Cre+; PI3Kp110* STOPfl; Hsf1+/+ + DMSO
hGFAP-Cre+; PI3Kp110* STOPfl; Hsf1fl/fl + DMSO
hGFAP-Cre+; PI3Kp110* STOPfl; Hsf1+/+ + 4EGI-1
hGFAP-Cre+; PI3Kp110* STOPfl; Hsf1fl/fl + 4EGI-1
FAM-dC-Puromycin fluorescence
hGFAP-Cre+; PI3Kp110* STOPfl; Hsf1+/+ + LY2584702
hGFAP-Cre+; PI3Kp110* STOPfl; Hsf1fl/fl + LY2584702
B
Fold changes in soluble A11+ PAO levels
Fold changes in insoluble OC+ AF levels
n.s.
DMSO
LY2584702
4EGI-1
shScram
shPten_A
shPten_B
Adeno-CRE:
Hsf1:
fl/fl
C
JC-1 Red/Green fluorescence ratio
D
hGFAP-Cre:
PI3K p110*:
Hsf1:
HSP60
β-amyloid (D54D2)
Ponceau Red
E
CQ
CR
PBS
hGFAP-Cre+; PI3K p110* STOPfl; Hsf1fl/fl
hGFAP-Cre+; PI3K p110* STOPfl; Hsf1+/+
hGFAP-Cre+; Hsf1fl/fl
hGFAP-Cre+; Hsf1+/+
MitoView Green Fluorescence Intensity
F
LacZ
HSP60
G
Adeno-Cre:
shRNAs:
Scram
Pten_A
Pten_B
H
siControl
siHsp60_A
siHsp60_B
Red fluorescence intensity
Green fluorescence intensity
I
Alb-Cre:
Pten:
HSP60
TOM20
HSF1
PTEN
βActin
Soluble
Insoluble
J

**Figure S4: Loss of HSP60 function leads to mitochondrial damage, mitophagy, and apoptosis.** (**A**) Measurement of global protein translation rate by puromycin labeling in *p110**-expressing astrocytes treated with and without 50μM 4EGI-1 or 20μM LY2584702 overnight. The histogram represents a single experiment. (**B**) Quantitation of amyloid levels in *Pten*-deficient astrocytes with *Hsf1* deletion treated with and without 50μM 4EGI-1 or 20μM LY2584702 overnight (mean±SD, n=3 lines of astrocytes of each genotype, One-way ANOVA). (**C**) Measurement of the mitochondrial membrane potentials of *Pten*-deficient astrocytes with *Hsf1* deletion treated with and without 50μM 4EGI-1 or 20μM LY2584702 for four days (mean±SD, n=3 lines of astrocytes of each genotype, One-way ANOVA). (**D**) Detection of HSP60 aggregates in whole brain lysates by filter-trap assays (three mice per group). (**E**) Quantitation of mitochondrial mass in astrocytes treated with and without 10μM CR or 20μM CQ for six days by FACS using MitoView™ Green. The histogram depicts a single experiment, and three independent experiments are summarized in Fig. 5A. (**F**) JC-1 Red/Green (FL2-H/FL1-H) fluorescence ratios of *p110**-expressing astrocytes transduced with lentiviral LacZ or HSP60 at a MOI=10 for six days (mean±SD, n=3 lines of astrocytes of each genotype, two-tailed Student's t test). (**G**) JC-1 Red/Green fluorescence ratios of *Pten*-deficient astrocytes with *Hsf1* deletion transduced with lentiviral LacZ or HSP60 at a MOI=10 for six days (mean±SD, n=3 lines of astrocytes of each genotype, two-tailed Student's t test). (**H**) Measurement of the mitochondrial membrane potentials in *hGFAP-Cre*$^{+}$; *Hsf1*$^{+/+}$ astrocytes transfected with control or *Hsp60*-targeting siRNAs for four days (representative contour plot of three lines of astrocytes). (**I**) Detection of HSP60 and TOM20 in the detergent-soluble and detergent-insoluble fractions of *Pten*-deficient livers by immunoblotting (three mice of each genotype). (**J**) Detection of HSP60 aggregates in *Pten*-deficient livers by filter-trap assays (three mice of each genotype).
(A), (D), (I), and (J) were done once; the others were repeated thrice with different sets of astrocytes. (G) was repeated by two individuals.

# Figure S5

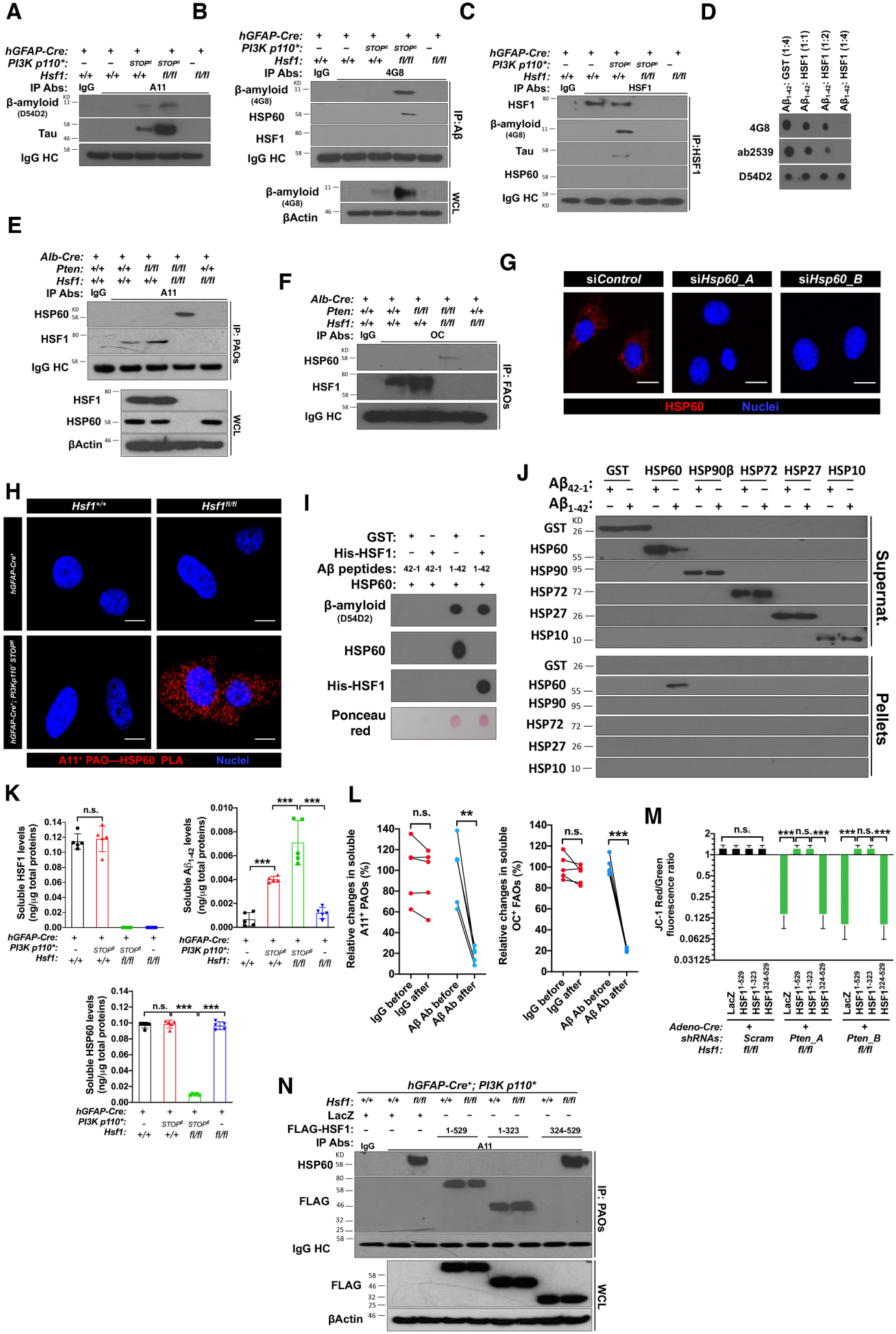
A
hGFAP-Cre:
PI3K p110*:
Hsf1:
IP Abs:
β-amyloid (D54D2)
Tau
IgG HC
B
β-amyloid (4G8)
HSP60
HSF1
IP:Aβ
WCL
βActin
C
IP:HSF1
D
4G8
ab2539
D54D2
E
Alb-Cre:
Pten:
IP: PAOs
F
IP: FAOs
G
siControl
siHsp60_A
siHsp60_B
HSP60
Nuclei
H
Hsf1+/+
Hsf1fl/fl
A11+ PAO—HSP60 PLA
I
GST:
His-HSF1:
Aβ peptides:
HSP60:
Ponceau red
J
Supernat.
Pellets
K
Soluble HSF1 levels (ng/μg total proteins)
Soluble Aβ1-42 levels (ng/μg total proteins)
Soluble HSP60 levels (ng/μg total proteins)
n.s.
L
Relative changes in soluble A11+ PAOs (%)
Relative changes in soluble OC+ FAOs (%)
IgG before
IgG after
Aβ Ab before
Aβ Ab after
M
JC-1 Red/Green fluorescence ratio
Adeno-Cre:
shRNAs:
Scram
Pten_A
Pten_B
N
hGFAP-Cre+; PI3K p110*
LacZ
FLAG-HSF1:
1-529
1-323
324-529
FLAG

**Figure S5: HSF1 protects HSP60 from AO attack.**
**(A)** Detection of PAOs of Aβ and Tau by IP with the EasyBlot® reagents in *p110**-expressing mouse brains (representative images of two sets of brains)**. (B)** and **(C)** Detection of physical Aβ-HSP60 and Aβ-HSF1 interactions in *p110**-expressing mouse brains by co-IP with the EasyBlot® reagents (representative images of three sets of brains). (**D**) Detection of $A\beta_{1\text{-}42}$ co-incubated with and without recombinant HSF1 proteins at increased molar ratios by dot blotting (representative images of three experiments). (**E)** and (**F**) Detection of physical AO-HSF1 and AO-HSP60 interactions in *Pten*-deficient livers by co-IP with the EasyBlot® reagents (representative images of three sets of livers). (**G**) Validation of the mouse monoclonal anti-HSP60 antibody (LK1) used for PLA by immunofluorescence in *hGFAP-Cre*$^{+}$; *Hsf1*$^{+/+}$ astrocytes transfected with control or *Hsp60*-targeting siRNAs for four days (images of a single experiment). Scale bars: 10μm. (**H**) Visualization of PAO-HSP60 interactions in cultured astrocytes by PLA using rabbit anti-PAOs (A11) Abs and mouse monoclonal anti-HSP60 (LK1) Abs (representative images of two lines of astrocytes of each genotype). Scale bars: 10μm. A similar result was also observed in *Pten*-deficient astrocytes following *Hsf1* deletion. (**I**) Detection of HSP60 and HSF1 aggregation due to $A\beta_{1\text{-}42}$ interactions *in vitro*, as described in Fig. 6C, by filter-trap assays (representative images of three experiments). (**J**) Detection of the insolubility of HSPs in the presence of $A\beta_{1\text{-}42}$ *in vitro*. Recombinant HSP60, HSP90β, HSP72, HSP27, and HSP10 proteins were incubated with either $A\beta_{42\text{-}1}$ or $A\beta_{1\text{-}42}$ at a 1:1 molar ratio at RT for 4 hr (representative images of three experiments). (**K)** Quantitation of the absolute levels of HSF1, $A\beta_{42}$, and HSP60 in 10μg of mouse brain lysates by commercial ELISA kits (mean±SD, n=5 mice per genotypic group, One-way ANOVA). (**L)** Quantitation of soluble AOs in *P*H*$^{-}$ mouse brain lysates before and after IP with Aβ (D54D2) Abs (n=5 mice, two-tailed paired Student's t test). Normal rabbit IgG served as the control. (**M**) Measurement of the mitochondrial membrane potentials of *Pten*-deficient astrocytes with *Hsf1* deletion transduced with lentiviral HSF1 at a MOI=10 for six days by JC-1 staining (mean±SD, n=3 lines of astrocytes of each genotype, One-way ANOVA). (**N**) Detection of physical PAO-HSF1 and PAO-HSP60 interactions by co-IP with the EasyBlot® reagents in astrocytes transduced with lentiviral LacZ, $HSF1^{1\text{-}529}$, $HSF1^{1\text{-}323}$, or $HSF1^{324\text{-}529}$ at a MOI=10 for six days (images of a single experiment).
(G), (L), and (N) were done once; (A) and (H) were repeated twice with different sets of brains or astrocytes; (K) was repeated twice; (B), (C), (E), (F), and (M) were repeated thrice with different sets of tissues or astrocytes; and (D), (I), and (J) were repeated thrice with the same reagents.

# Figure S6

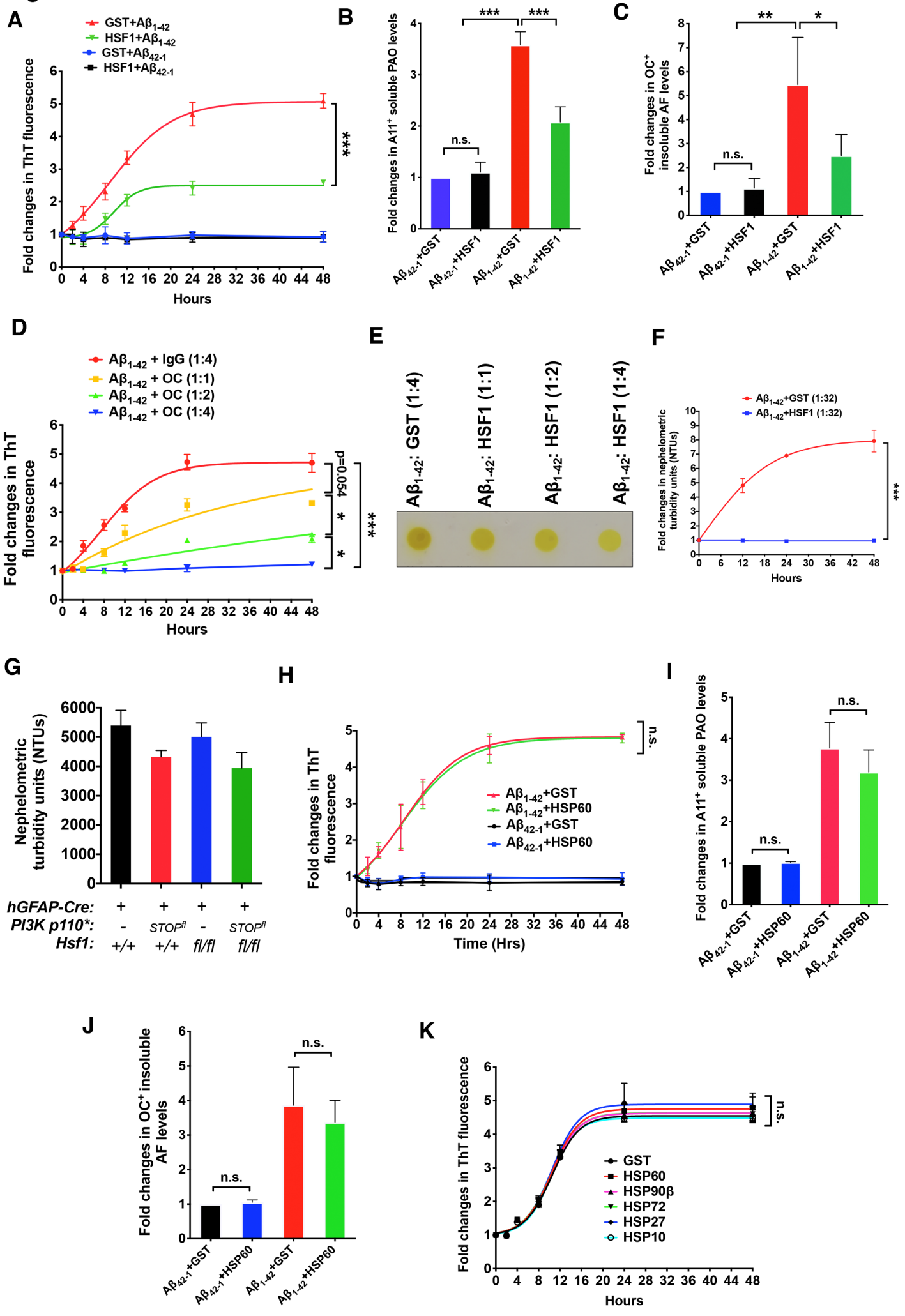
A
GST+Aβ1-42
HSF1+Aβ1-42
GST+Aβ42-1
HSF1+Aβ42-1
Fold changes in ThT fluorescence
Hours
***
B
Fold changes in A11+ soluble PAO levels
n.s.
***
***
Aβ42-1+GST
Aβ42-1+HSF1
Aβ1-42+GST
Aβ1-42+HSF1
C
Fold changes in OC+ insoluble AF levels
n.s.
**
*
D
Aβ1-42 + IgG (1:4)
Aβ1-42 + OC (1:1)
Aβ1-42 + OC (1:2)
Aβ1-42 + OC (1:4)
Fold changes in ThT fluorescence
Hours
p=0.054
*
*
***
E
Aβ1-42: GST (1:4)
Aβ1-42: HSF1 (1:1)
Aβ1-42: HSF1 (1:2)
Aβ1-42: HSF1 (1:4)
F
Aβ1-42+GST (1:32)
Aβ1-42+HSF1 (1:32)
Fold changes in nephelometric turbidity units (NTUs)
Hours
***
G
Nephelometric turbidity units (NTUs)
hGFAP-Cre: + + + +
PI3K p110*: - STOPfl - STOPfl
Hsf1: +/+ +/+ fl/fl fl/fl
H
Fold changes in ThT fluorescence
Time (Hrs)
n.s.
Aβ1-42+GST
Aβ1-42+HSP60
Aβ42-1+GST
Aβ42-1+HSP60
I
Fold changes in A11+ soluble PAO levels
n.s.
n.s.
Aβ42-1+GST
Aβ42-1+HSP60
Aβ1-42+GST
Aβ1-42+HSP60
J
Fold changes in OC+ insoluble AF levels
n.s.
n.s.
Aβ42-1+GST
Aβ42-1+HSP60
Aβ1-42+GST
Aβ1-42+HSP60
K
Fold changes in ThT fluorescence
Hours
n.s.
GST
HSP60
HSP90β
HSP72
HSP27
HSP10

**Figure S6: HSF1 impairs amyloidogenesis through physical interactions.**
**(A)** Measurements of the fibrillation of 2μM $A\beta_{1-42}$ incubated with recombinant GST or HSF1 proteins *in vitro* at a 1:1 molar ratio (mean±SD, n=3 experiments, Two-way ANOVA). Non-amyloidogenic $A\beta_{42-1}$ peptides served as the negative control. The curves are fitted with the Boltzmann sigmoid equation. (**B)** and (**C**) Quantitation of PAOs and AFs formed by 2μM $A\beta_{1-42}$ described in (A) by ELISA (mean±SD, n=3 experiments, One-way ANOVA). (**D**) Measurements of the fibrillation of 0.8μM $A\beta_{1-42}$ incubated with OC Abs *in vitro* at increasing molar ratios (mean±SD, n=3 experiments, Two-way ANOVA). Normal rabbit IgG served as the control. The curves are fitted with the Boltzmann sigmoid equation. (**E**) Detection of protein aggregates in the experiments described in Fig. 8B by filter-trap assays (representative images of three experiments). The yellow color is due to ThT. Photo credit: Zijian Tang, NCI. (**F**) Dynamic measurements of the nephelometric turbidities of 0.2μM $A\beta_{1-42}$ incubated with GST or HSF1 at a 1:32 molar ratio for 48 hr (mean±SD, n=2 experiments, Two-way ANOVA). (**G**) Measurements of the nephelometric turbidities of detergent-soluble brain lysates prior to incubation at 37ºC (mean±SD, n=5 mice per group, One-way ANOVA). (**H**) *In vitro* fibrillation of $A\beta_{1-42}$ incubated with either recombinant GST or HSP60 proteins at a 1:1 molar ratio (mean±SD, n=3 experiments, Two-way ANOVA). Non-amyloidogenic $A\beta_{42-1}$ peptides served as the negative control. The curves are fitted with the Boltzmann sigmoid equation. (**I)** and **(J)** Quantitation of PAOs and AFs formed in (H) by ELISA (mean±SD, n=3 experiments, One-way ANOVA). (**K**) *In vitro* fibrillation of $A\beta_{1-42}$ incubated with either recombinant GST or various HSP proteins at a 1:1 molar ratio (mean±SD, n=3 experiments, Two-way ANOVA). The curves are fitted with the Boltzmann sigmoid equation. (G) was done once; (F) was repeated twice; and all the others were repeated thrice with the same reagents.

Figure S7

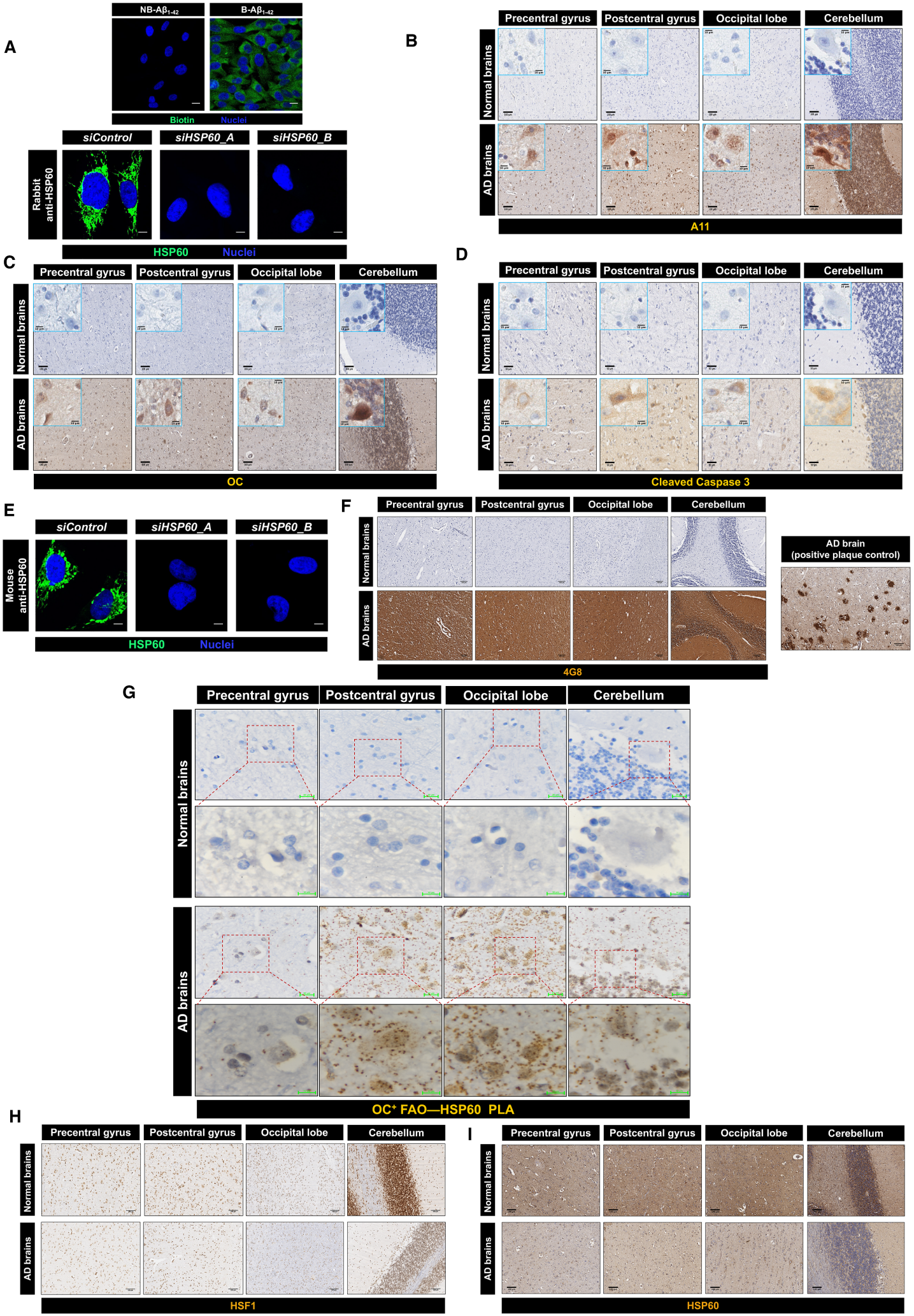
A
NB-Aβ1-42
B-Aβ1-42
Biotin
Nuclei
siControl
siHSP60_A
siHSP60_B
Rabbit anti-HSP60
HSP60
Nuclei
B
Precentral gyrus
Postcentral gyrus
Occipital lobe
Cerebellum
Normal brains
AD brains
A11
C
Precentral gyrus
Postcentral gyrus
Occipital lobe
Cerebellum
Normal brains
AD brains
OC
D
Precentral gyrus
Postcentral gyrus
Occipital lobe
Cerebellum
Normal brains
AD brains
Cleaved Caspase 3
E
siControl
siHSP60_A
siHSP60_B
Mouse anti-HSP60
HSP60
Nuclei
F
Precentral gyrus
Postcentral gyrus
Occipital lobe
Cerebellum
Normal brains
AD brains
4G8
AD brain (positive plaque control)
G
Precentral gyrus
Postcentral gyrus
Occipital lobe
Cerebellum
Normal brains
AD brains
OC+ FAO—HSP60 PLA
H
Precentral gyrus
Postcentral gyrus
Occipital lobe
Cerebellum
Normal brains
AD brains
HSF1
I
Precentral gyrus
Postcentral gyrus
Occipital lobe
Cerebellum
Normal brains
AD brains
HSP60

**Figure S7: Human AD brains display elevated AOs and apoptosis but diminished HSF1 and HSP60 proteins.**

(**A**) Validations of the mouse anti-biotin and rabbit anti-HSP60 Abs in HeLa cells by immunofluorescence (images of a single experiment). Following transfection of 1μM non-biotinylated (NB) or biotinylated $A\beta_{1-42}$ overnight, cells were stained with mouse monoclonal anti-biotin (BTN.4) Abs. Following transfection of 10nM *HSP60*-targetting siRNAs for four days, HeLa cells were stained with rabbit anti-HSP60 (D6F1) Abs. Scale bars: 10μm. (**B)** and **(C)** AD and normal control brain sections on tissue arrays were stained with A11 (B) and OC (C) Abs, respectively (images of a single experiment). Scale bars: 100μm for main images; 10μm for insets. (**D**) AD and normal control brains were stained with rabbit anti-cleaved caspase 3 (Asp175) (representative images of two experiments). Scale bars: 50μm for main images; 10μm for insets. (**E**) Validations of the mouse monoclonal anti-HSP60 (LK1) Ab in HeLa cells, transfected with 10nM *HSP60*-targetting siRNAs for four days, by immunofluorescence (images of a single experiment). Scale bars: 10μm. (**F**) AD and normal control brain sections on tissue arrays were stained with mouse monoclonal anti-$A\beta_{17-24}$ (4G8) Abs (images of a single experiment). A similar result was observed for anti-$A\beta_{1-14}$ (ab2539) Abs. The 4G8 antibody detected numerous amyloid plaques in AD QC control slides. Scale bars: 100μm. (**G**) Visualization of HSP60-FAOs interactions (brown) in AD patients' brains by brightfield PLA using a mouse monoclonal anti-HSP60 Ab (LK1) and the rabbit polyclonal anti-FAOs (OC) Ab (representative images of two experiments). Scale bars: 20μm for low magnification; 10μm for high magnification. (**H)** AD and normal control brains on tissue arrays were stained with rabbit monoclonal anti-HSF1 (EP1710Y) Abs (representative images of three experiments). Scale bars: 100μm. (**I**) AD and normal control brains on tissue arrays were stained with anti-HSP60 (D6F1) Abs (representative images of four experiments). Scale bars: 100μm.

(A)–(C), (E), and (F) were done once; (D) and (G) were repeated twice; and (H) and (I) were repeated three and four times, respectively.

**Figure S8** **Fig. 1C**

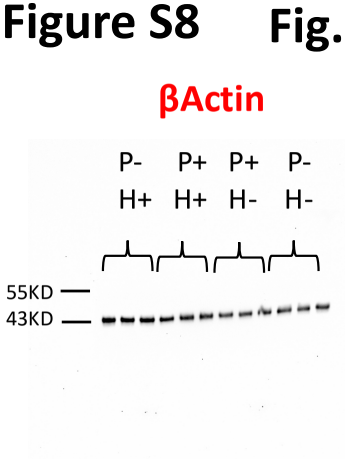


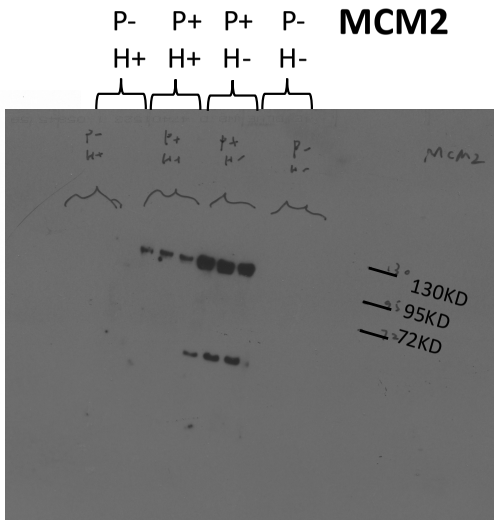


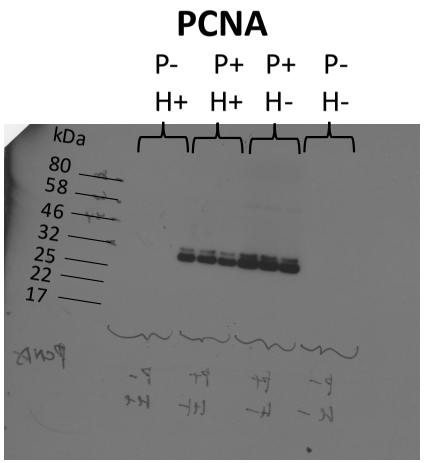


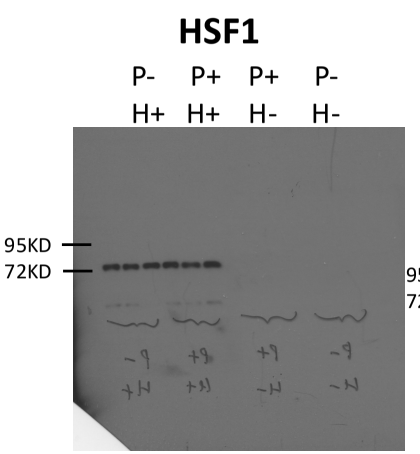


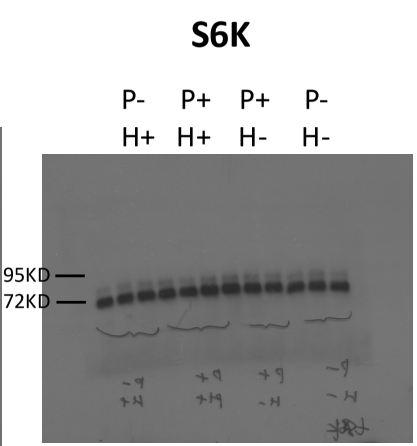


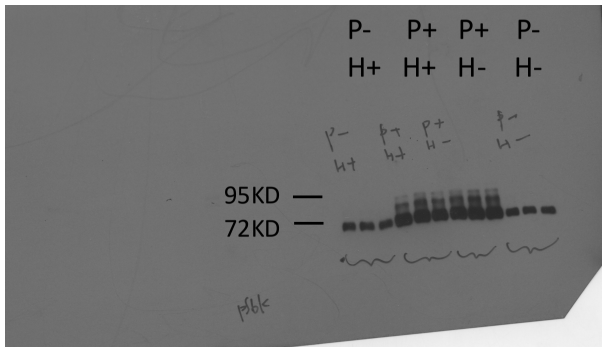


p-S6K T389

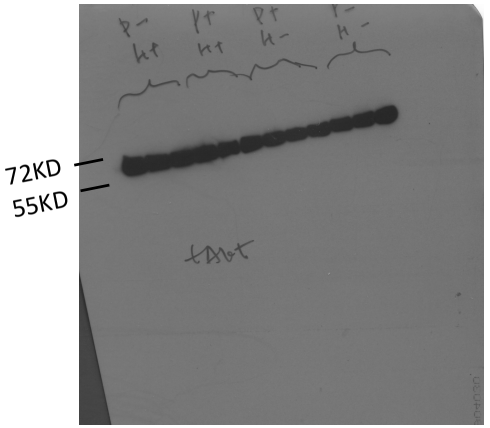


AKT

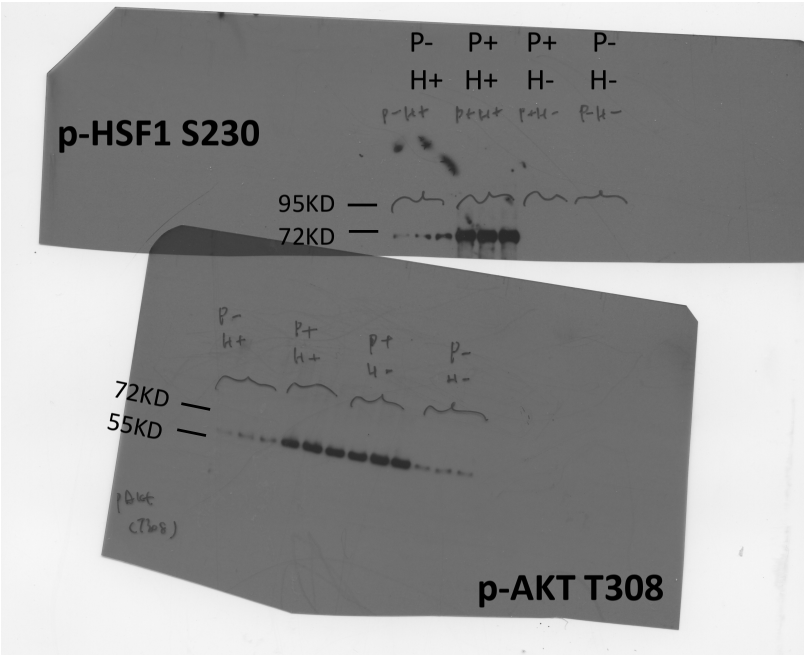

**Fig. 2B**

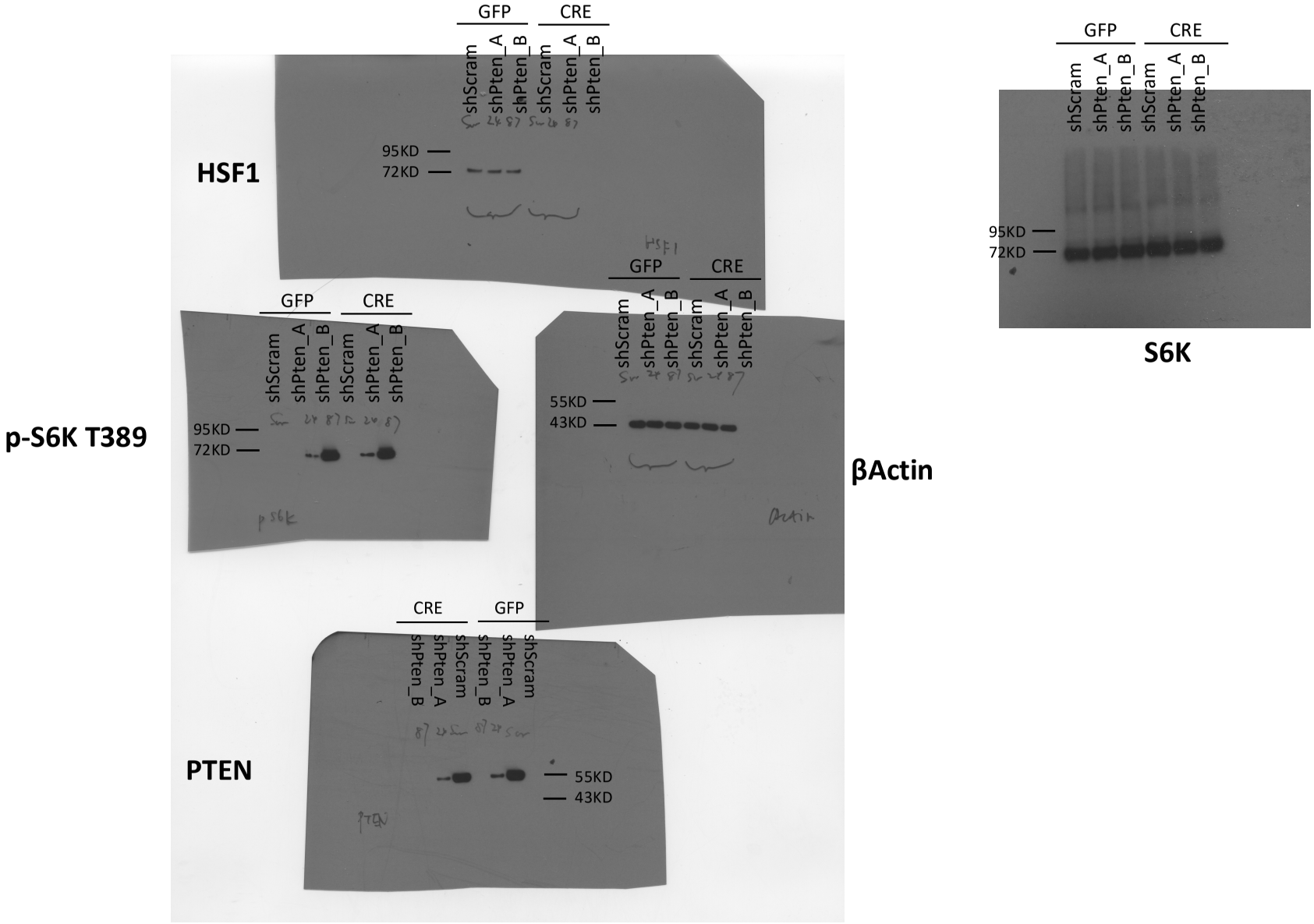
GFP
CRE
shScram
shPten_A
shPten_B
HSF1
95KD
72KD
p-S6K T389
55KD
43KD
βActin
PTEN
S6K

Fig. 4F

Soluble HSP60

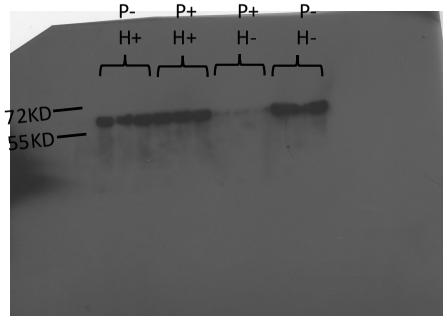


Soluble βActin

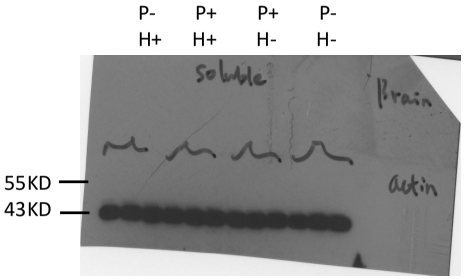


Soluble HSF1

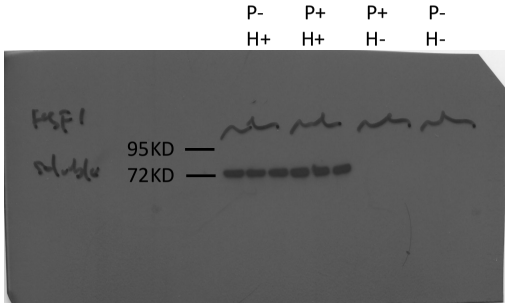


Soluble TOM20

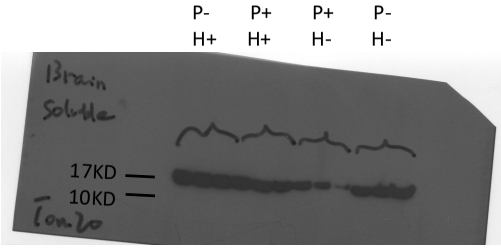


p-Tau S404

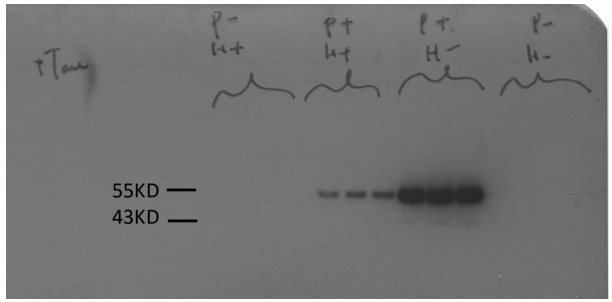


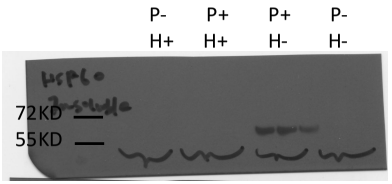


Insoluble HSP60

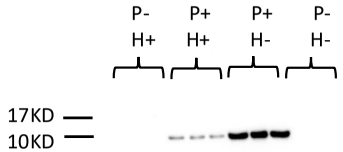


Insoluble Aβ

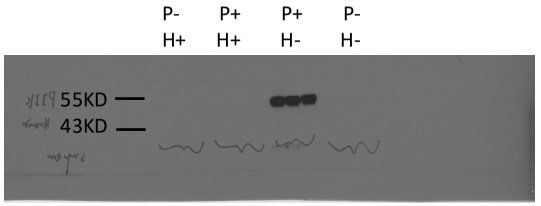


Insoluble Tau

**Fig. 4H**

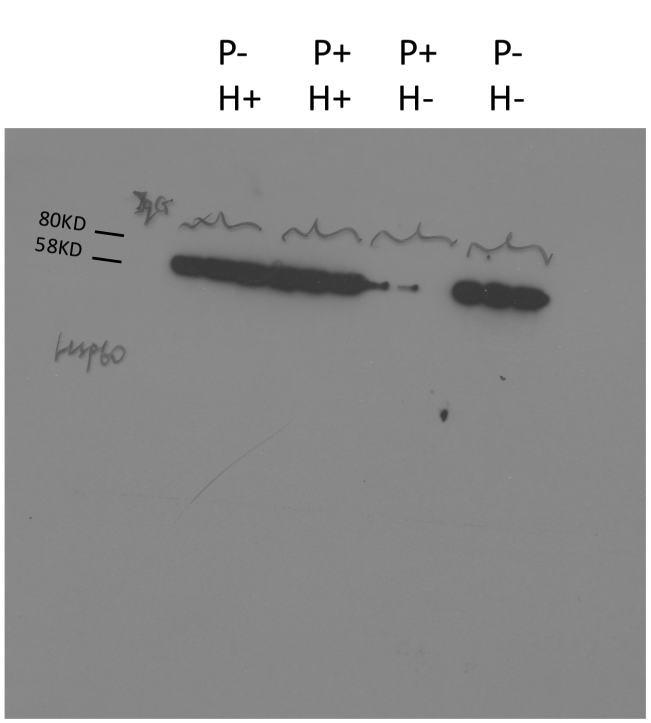


**IPed HSP60**

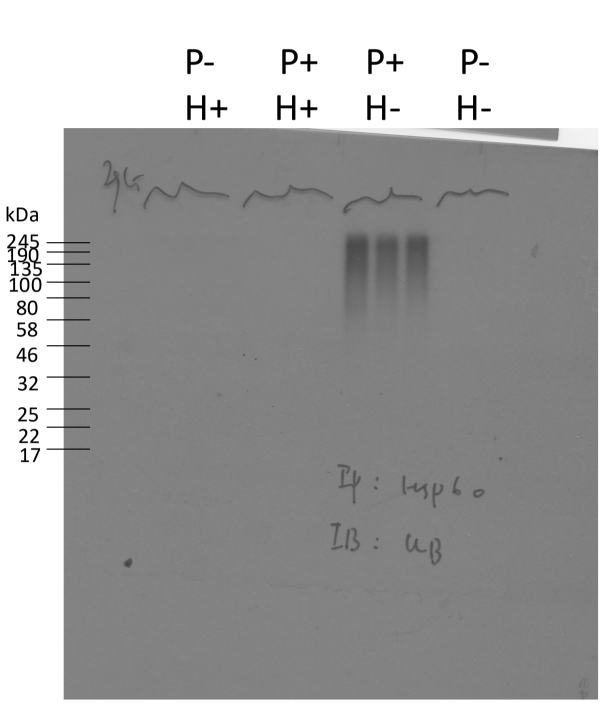


**K48 PolyUb**

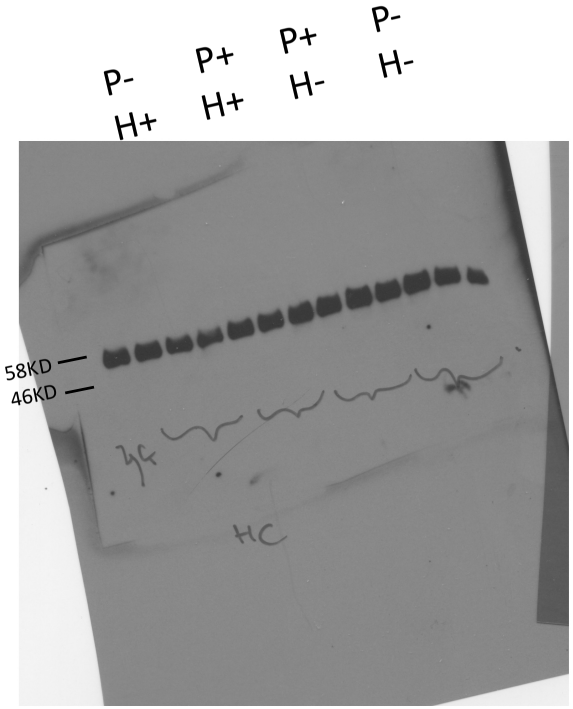


**IgG HC**

**Fig. 4J**

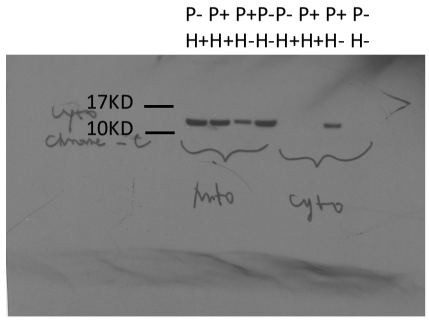


Cyt. C

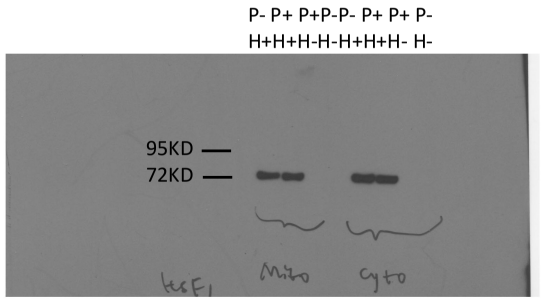


HSF1

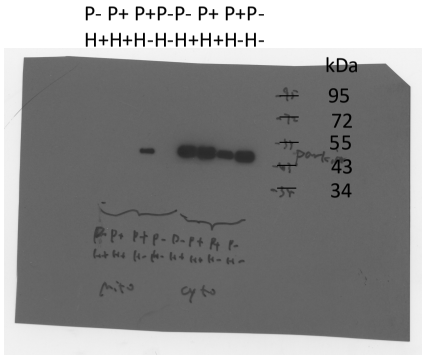


PARKIN

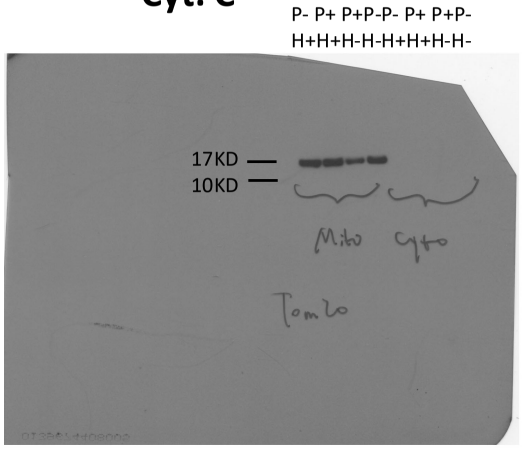


TOM20

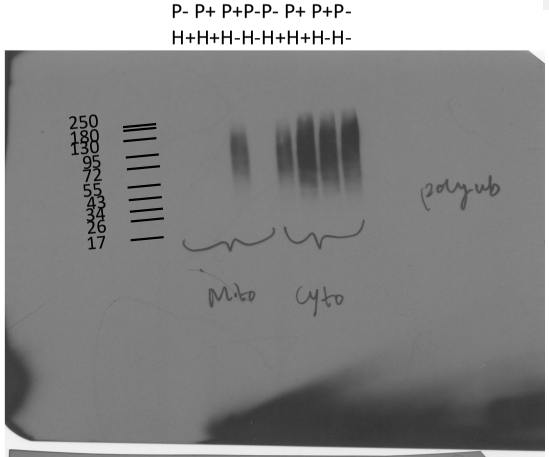


K48 PolyUb

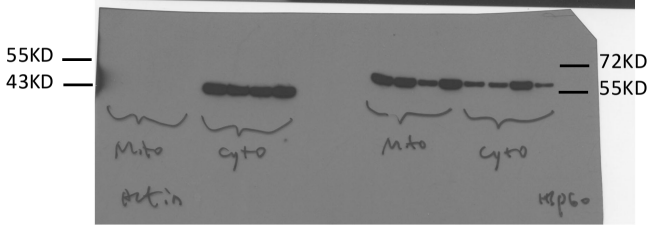


βActin HSP60

Fig. 5B

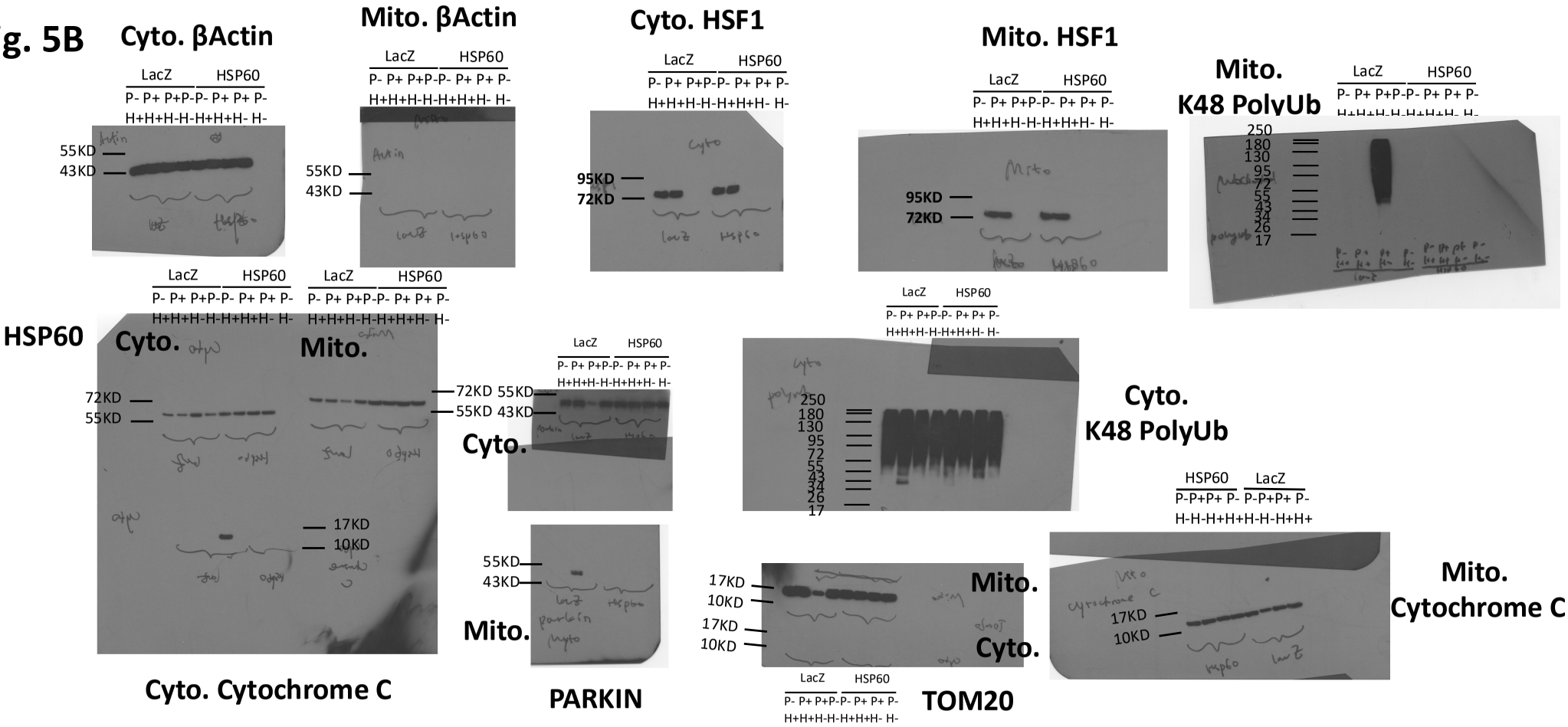
Cyto. βActin
Mito. βActin
Cyto. HSF1
Mito. HSF1
Mito. K48 PolyUb
LacZ
HSP60
P- P+ P+P-P- P+ P+ P-
H+H+H-H-H+H+H- H-
55KD
43KD
95KD
72KD
250
180
130
95
72
55
43
34
26
17
HSP60
Cyto.
Mito.
72KD
55KD
17KD
10KD
Cyto. K48 PolyUb
Cyto. Cytochrome C
PARKIN
Mito.
Cyto.
TOM20
Mito. Cytochrome C

Fig. 5E

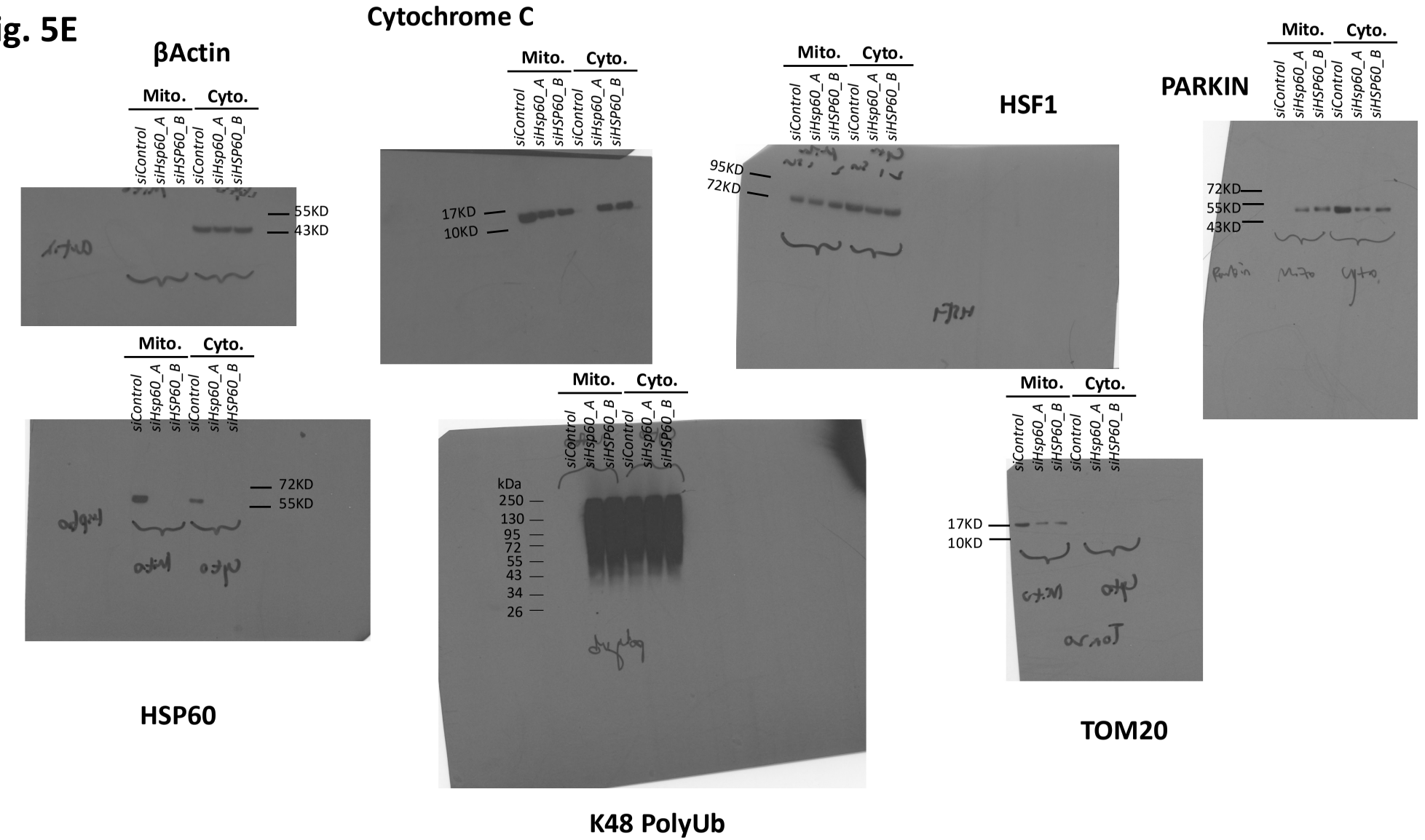
βActin
Mito.
Cyto.
siControl
siHsp60_A
siHSP60_B
55KD
43KD
Cytochrome C
17KD
10KD
HSF1
95KD
72KD
PARKIN
72KD
55KD
43KD
HSP60
72KD
55KD
K48 PolyUb
kDa
250
130
95
72
55
43
34
26
TOM20
17KD
10KD

Fig. 6A

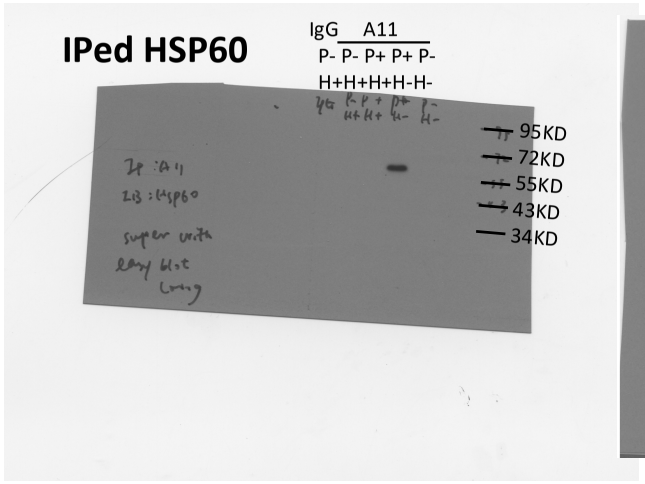


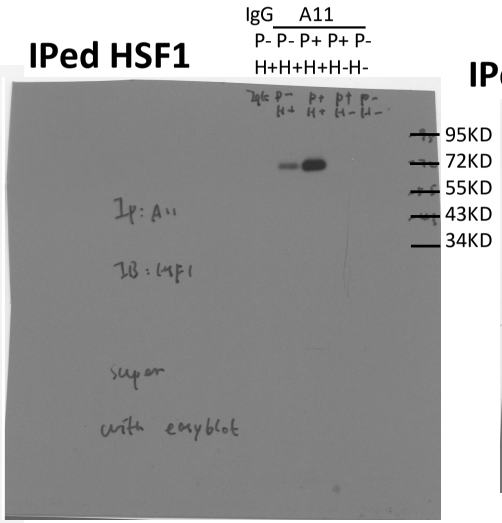


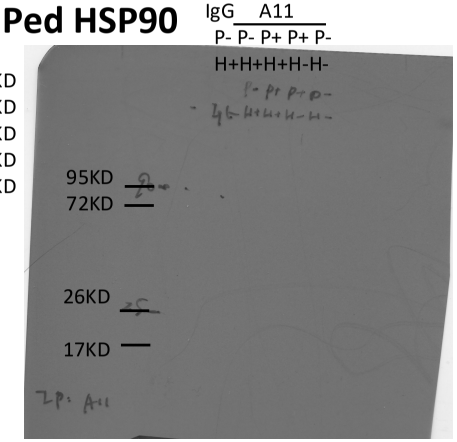


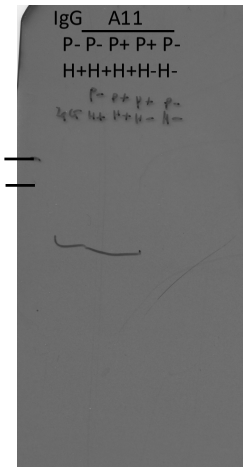


IPed HSP25

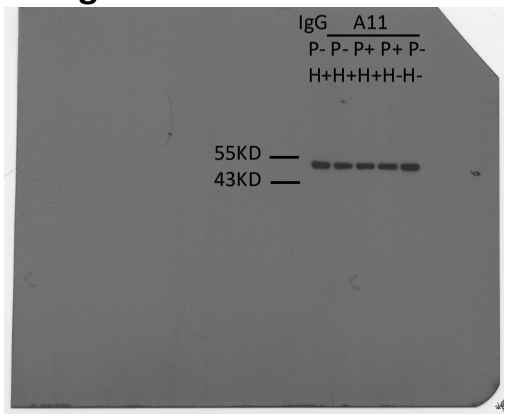


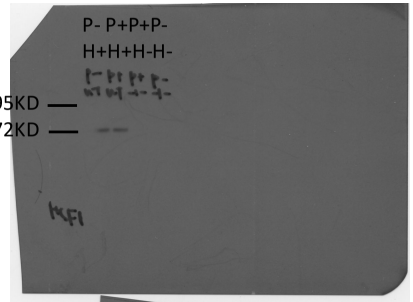


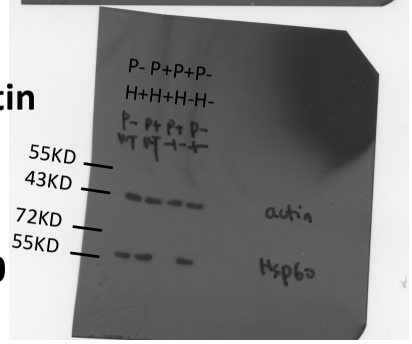

Fig. 6B

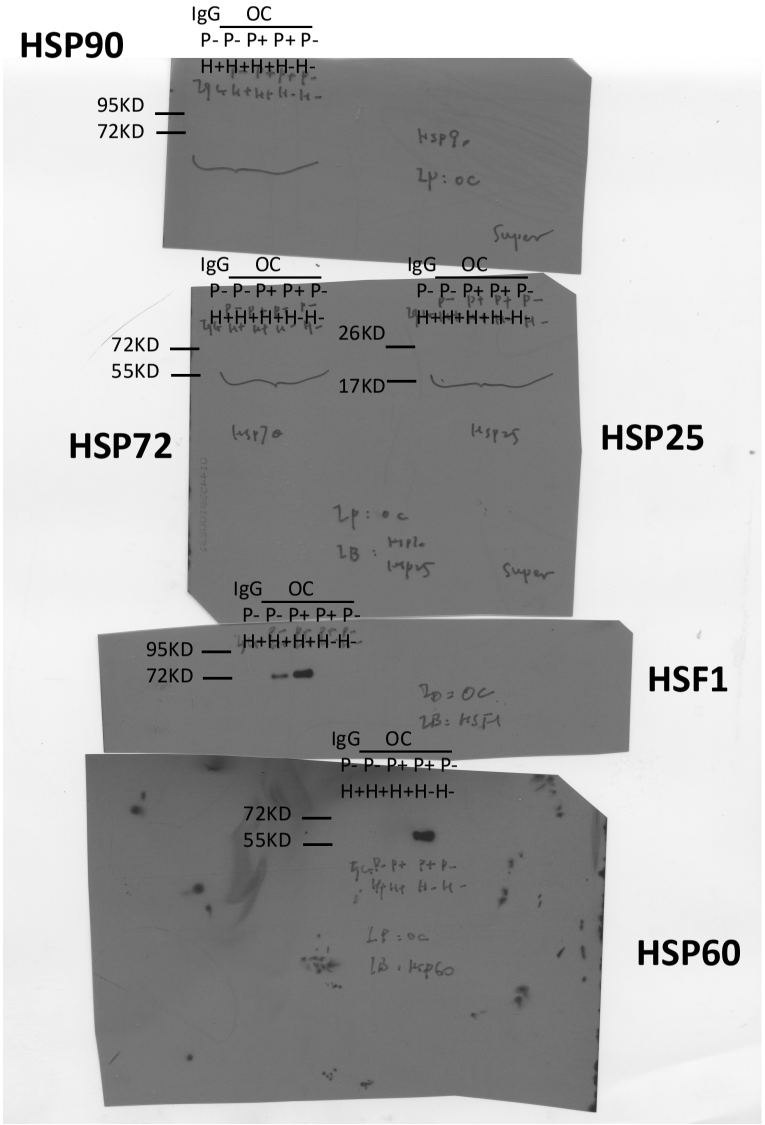
HSP90
IgG OC
P- P- P+ P+ P-
H+H+H+H-H-
95KD
72KD
HSP72
72KD
55KD
IgG OC
P- P- P+ P+ P-
H+H+H+H-H-
26KD
17KD
HSP25
IgG OC
P- P- P+ P+ P-
H+H+H+H-H-
95KD
72KD
HSF1
IgG OC
P- P- P+ P+ P-
H+H+H+H-H-
72KD
55KD
HSP60

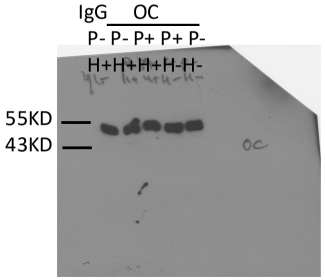
IgG OC
P- P- P+ P+ P-
H+H+H+H-H-
55KD
43KD
IgG HC

# Fig. 6C

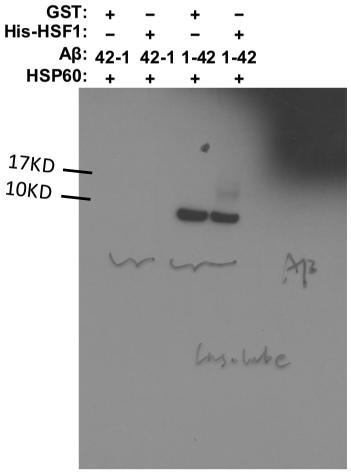


Pellet Aβ

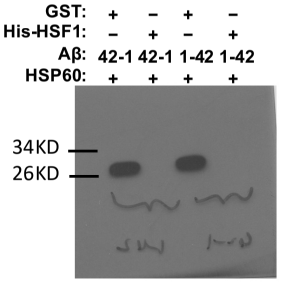


Supernatant GST

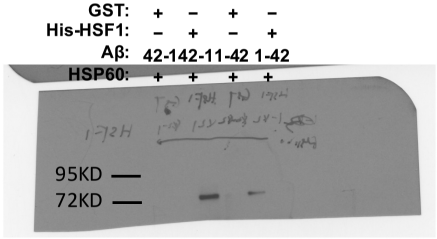


Supernatant HSF1

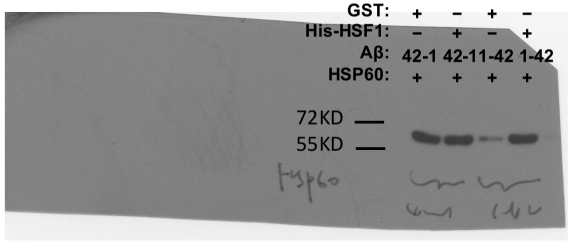


Supernatant HSP60

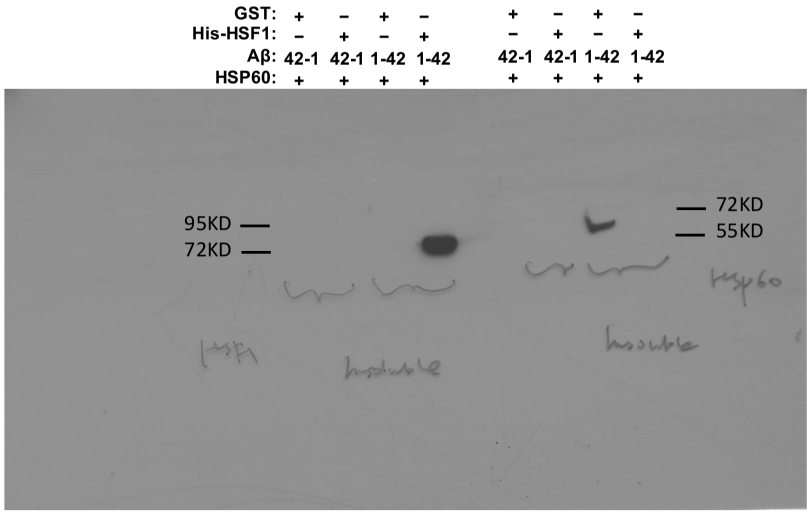


Pellet HSF1

Pellet HSP60

**Fig. 6D**

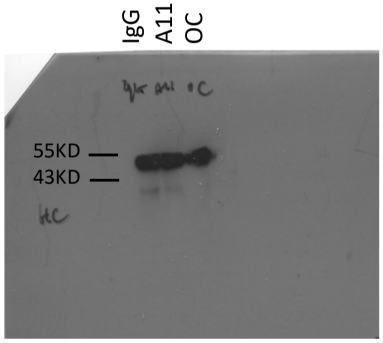


**Supernatant IgG HC**

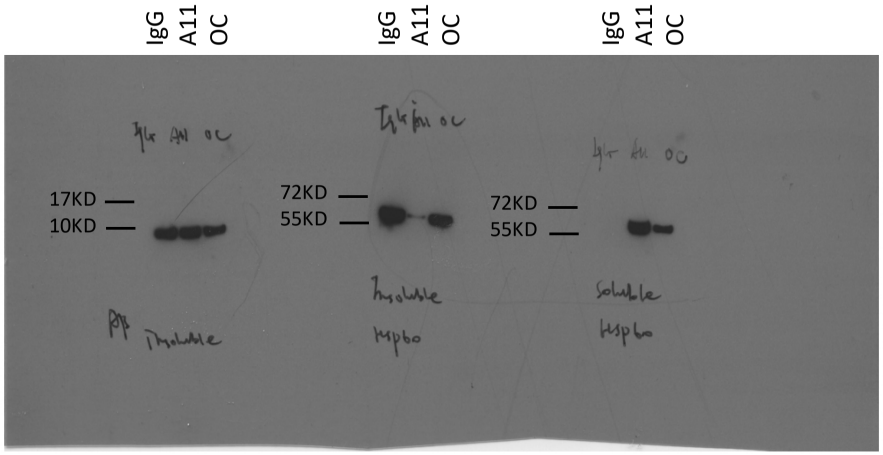


**Pellet Aβ** **Pellet HSP60** **Supernatant HSP60**

Fig. 6E

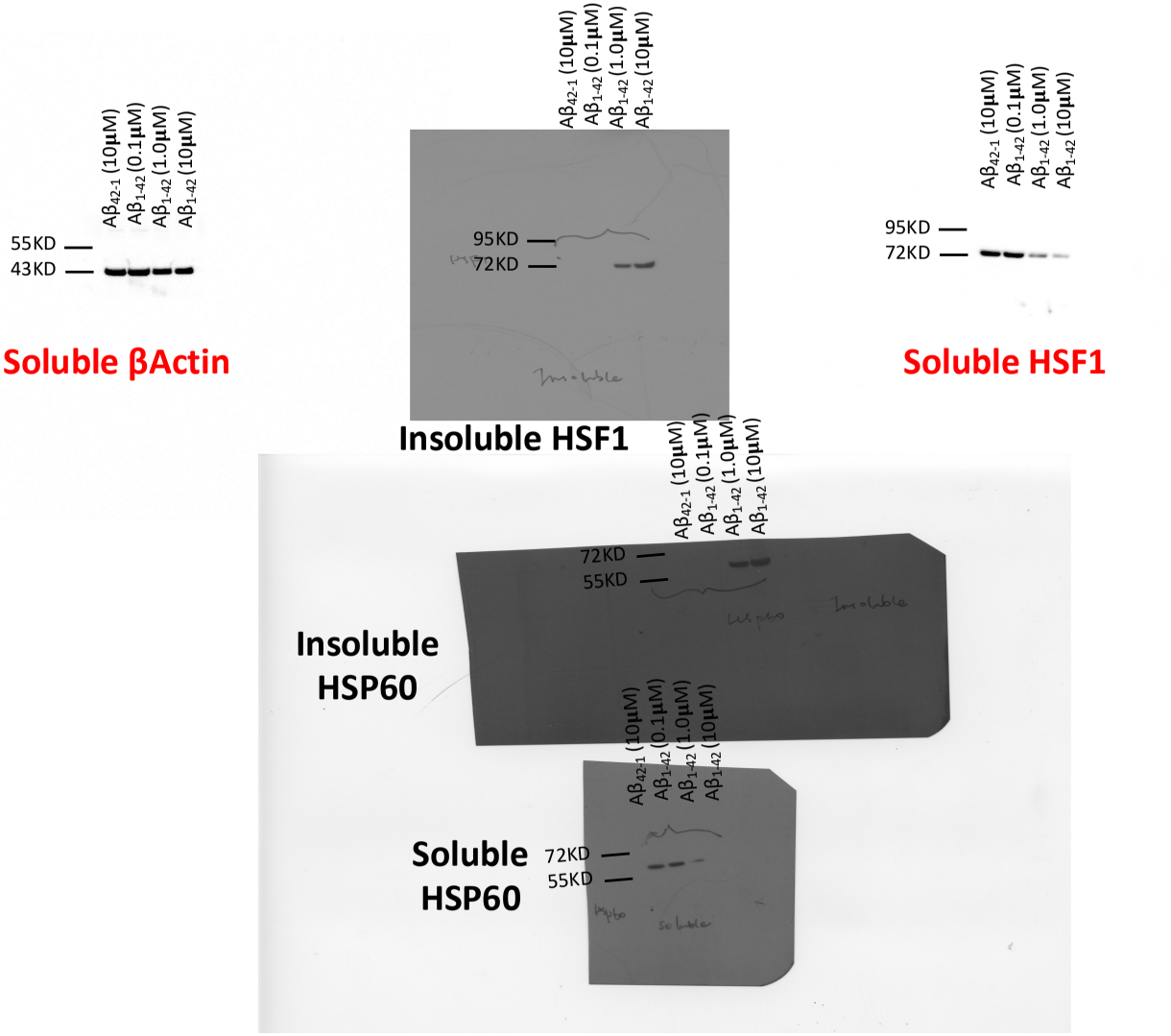
Aβ42-1 (10μM)
Aβ1-42 (0.1μM)
Aβ1-42 (1.0μM)
Aβ1-42 (10μM)
55KD
43KD
Soluble βActin
95KD
72KD
Insoluble HSF1
95KD
72KD
Soluble HSF1
Insoluble HSP60
72KD
55KD
Soluble HSP60
72KD
55KD

**Fig. 6G**

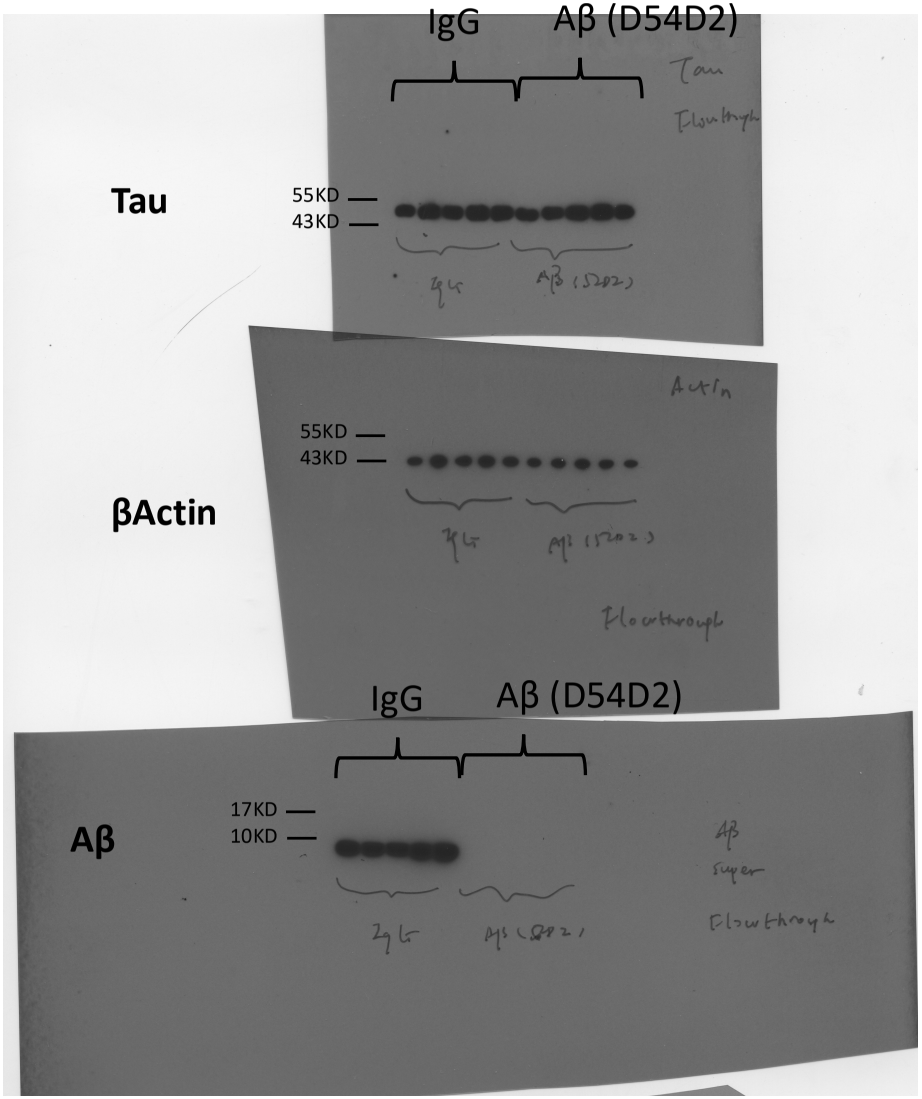
IgG
Aβ (D54D2)
Tau
55KD
43KD
βActin
Actin
Aβ
17KD
10KD
Flowthrough

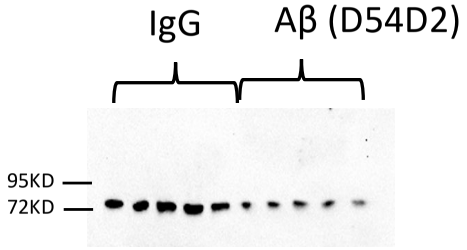
IgG
Aβ (D54D2)
95KD
72KD

HSF1

# Fig. 11A

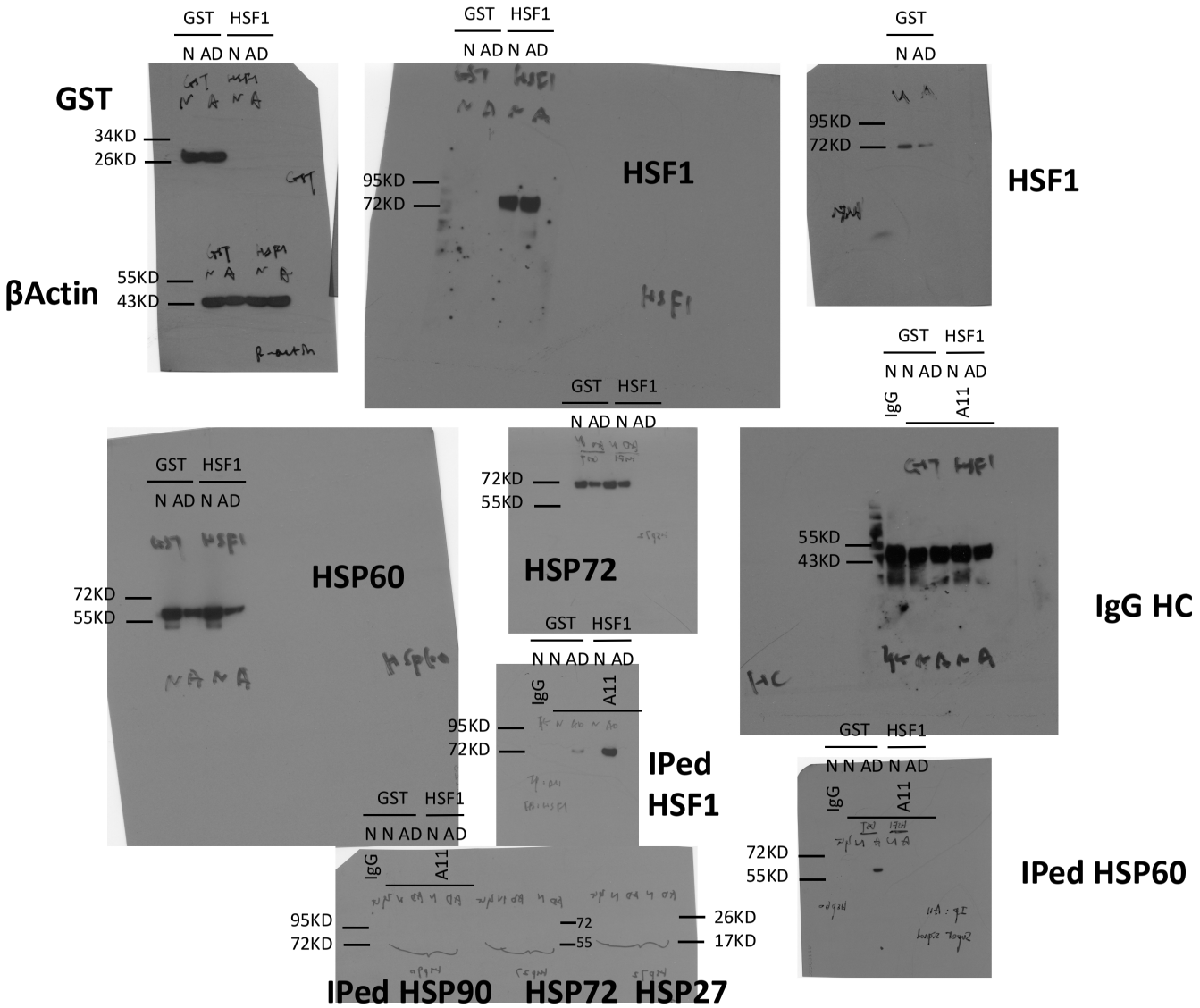
Whole brain
GST
HSF1
N AD N AD
34KD
26KD
βActin
55KD
43KD
95KD
72KD
HSF1
N AD
HSP60
HSP72
IgG
A11
N N AD N AD
IgG HC
IPed HSF1
IPed HSP60
IPed HSP90
HSP72
HSP27
72
55
26KD
17KD

# Fig. 11A

**Hippocampus**

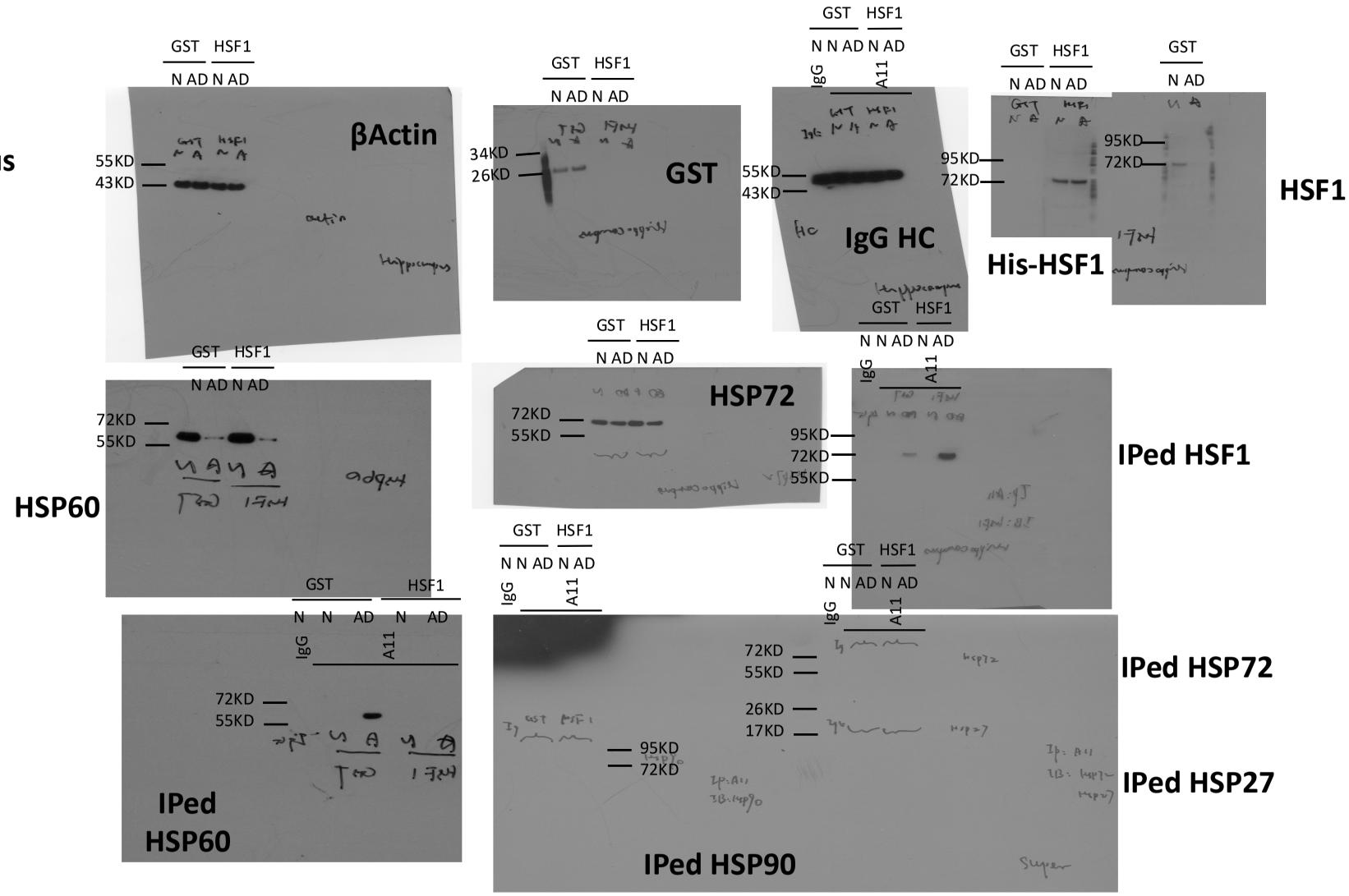

Fig. 11B

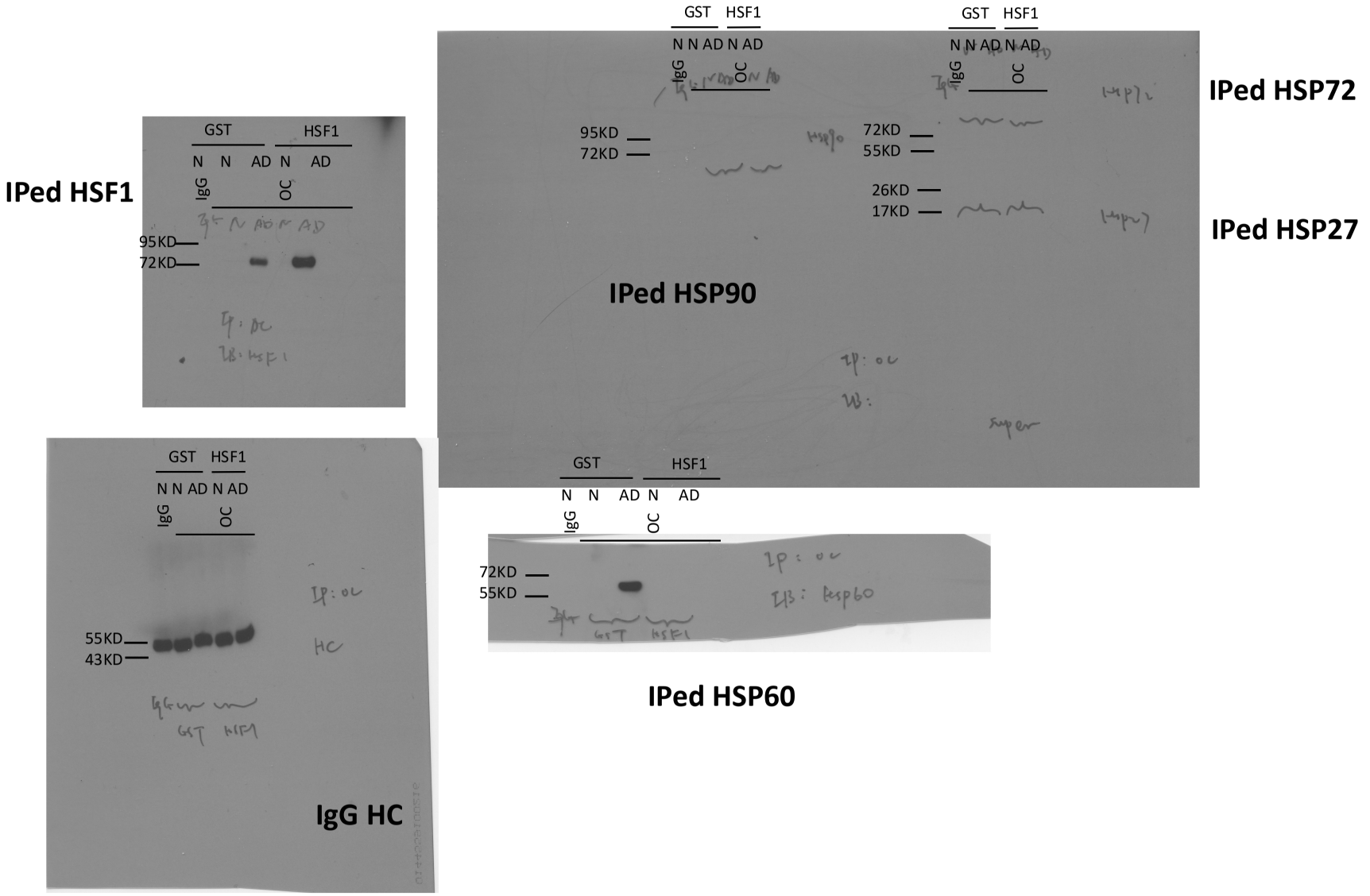
GST
HSF1
N N AD N AD
IgG
OC
IPed HSF1
95KD
72KD
IPed HSP90
72KD
55KD
26KD
17KD
IPed HSP72
IPed HSP27
55KD
43KD
HC
IgG HC
IPed HSP60

# Fig. 11C

**Whole brain**

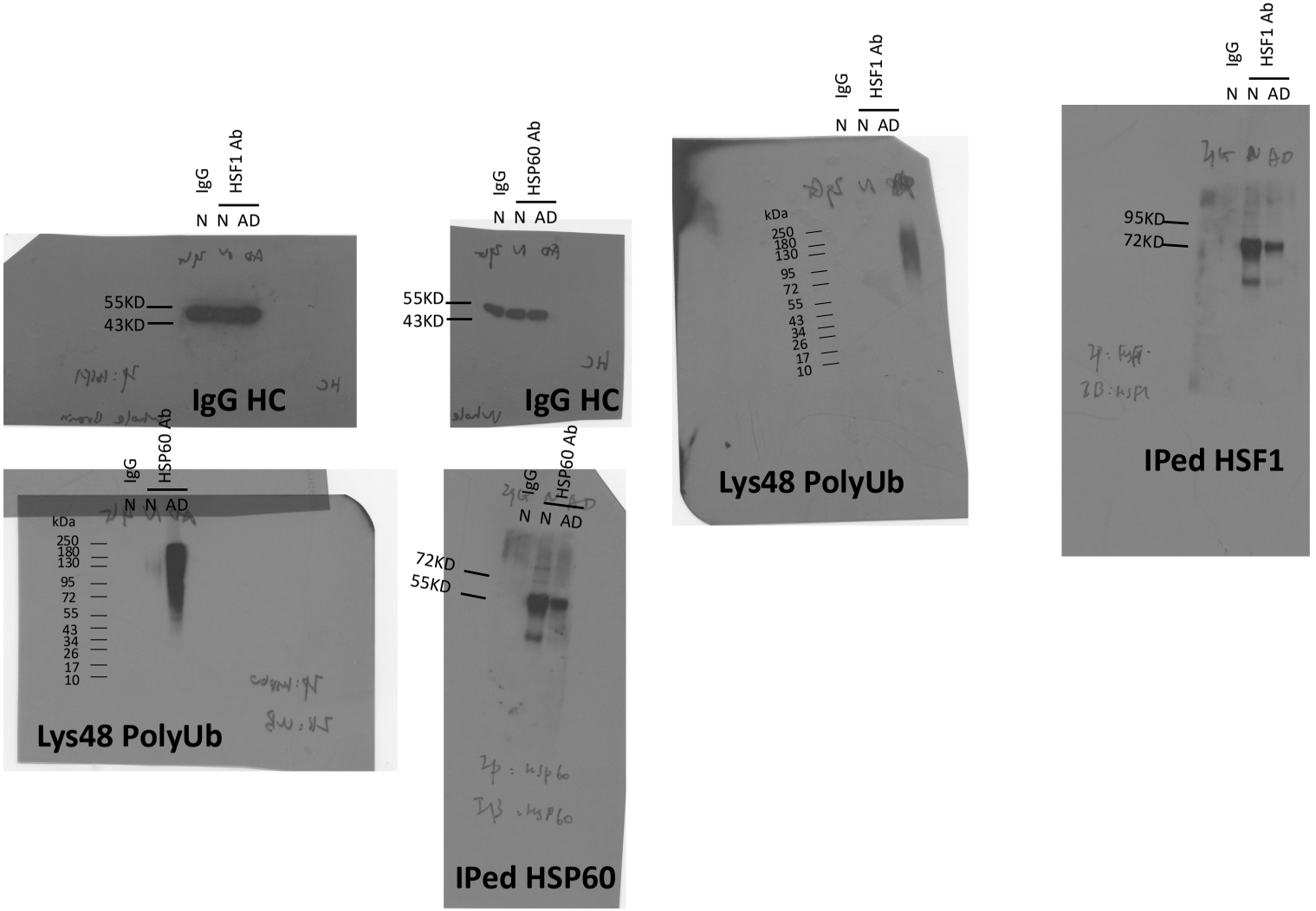

# Fig. 11C

**Hippocampus**

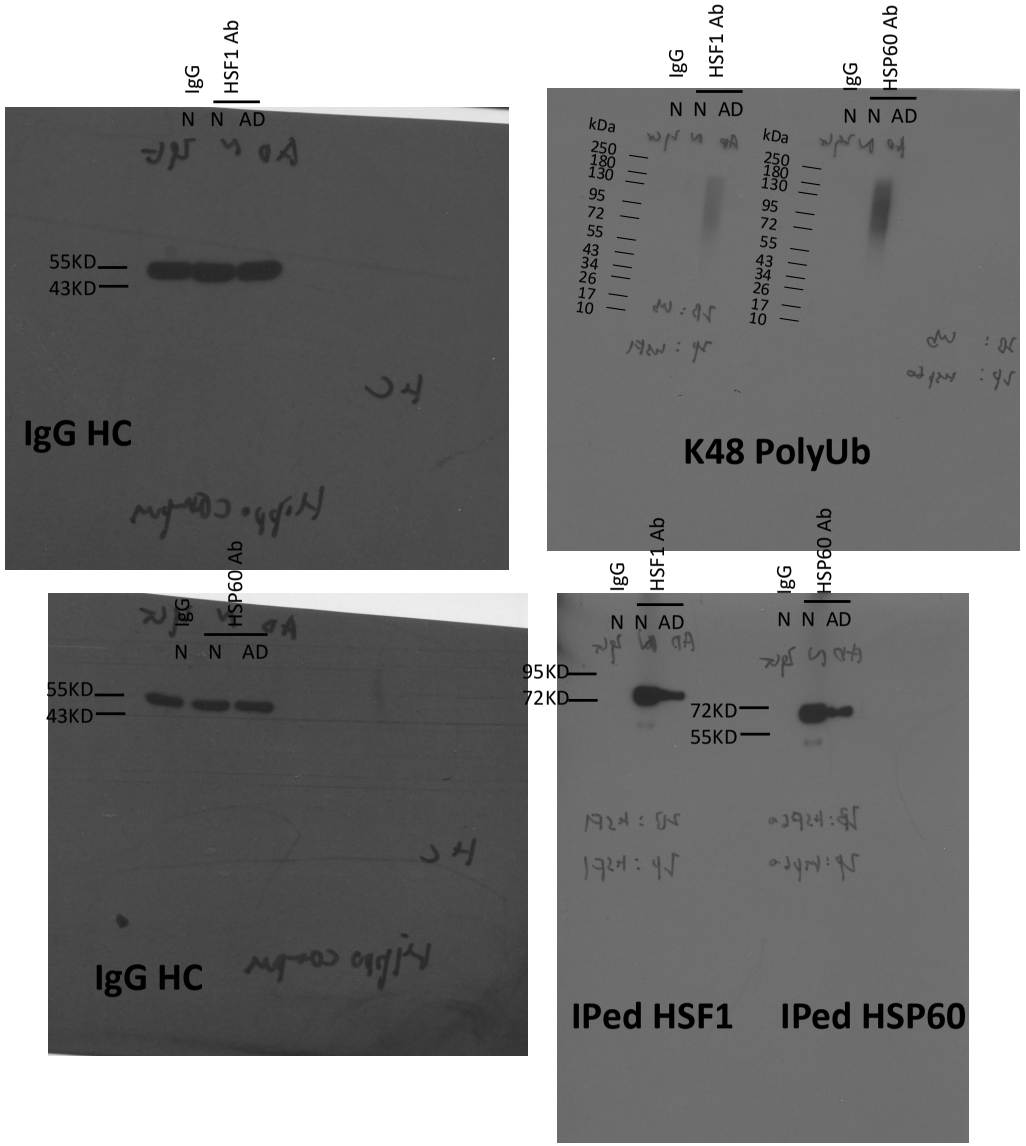

Fig. 11D

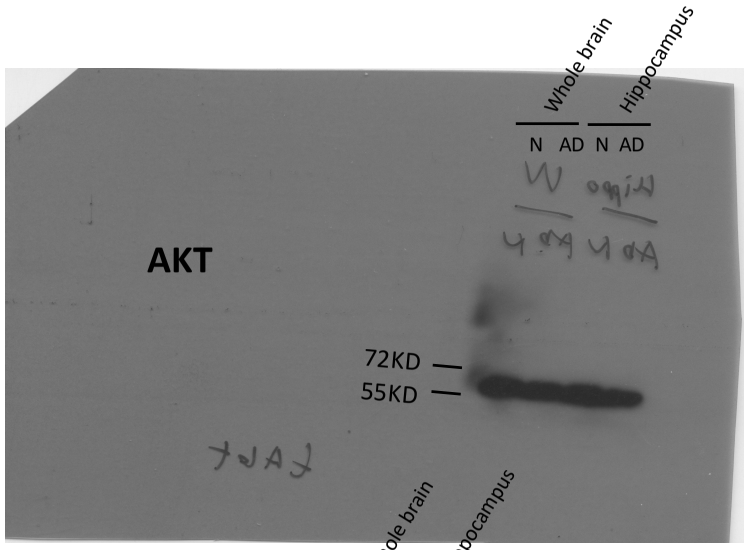


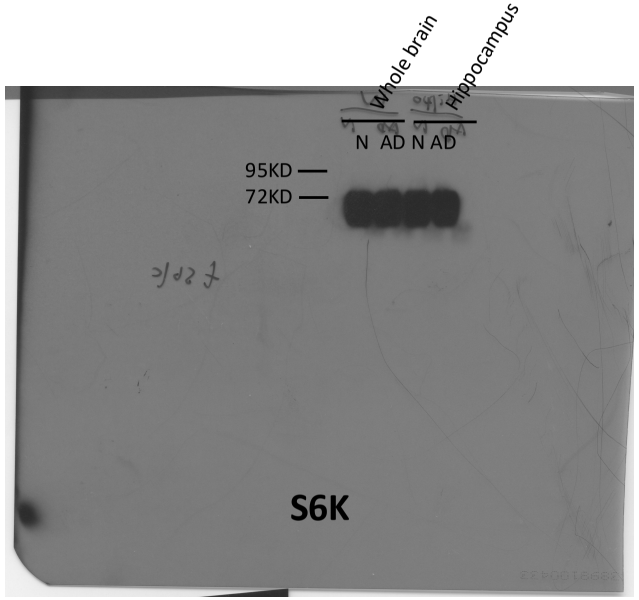


p-AKT T308

p-AKT S473

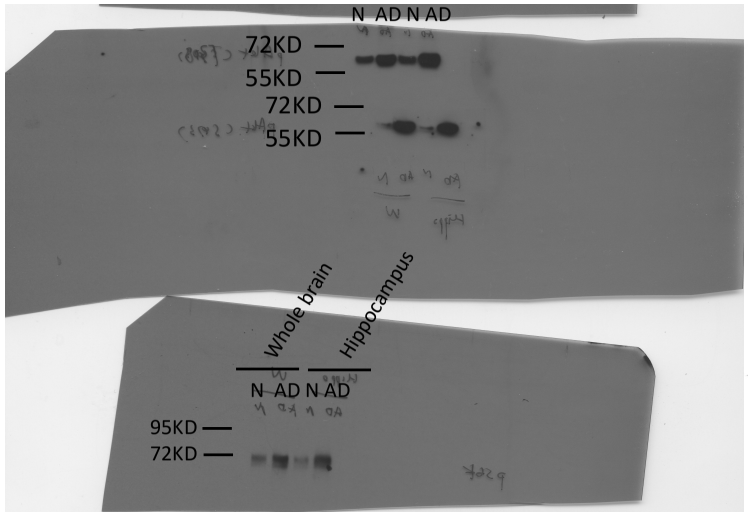


p-S6K T389




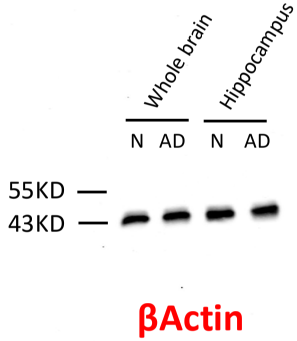


βActin

# Fig. S1C

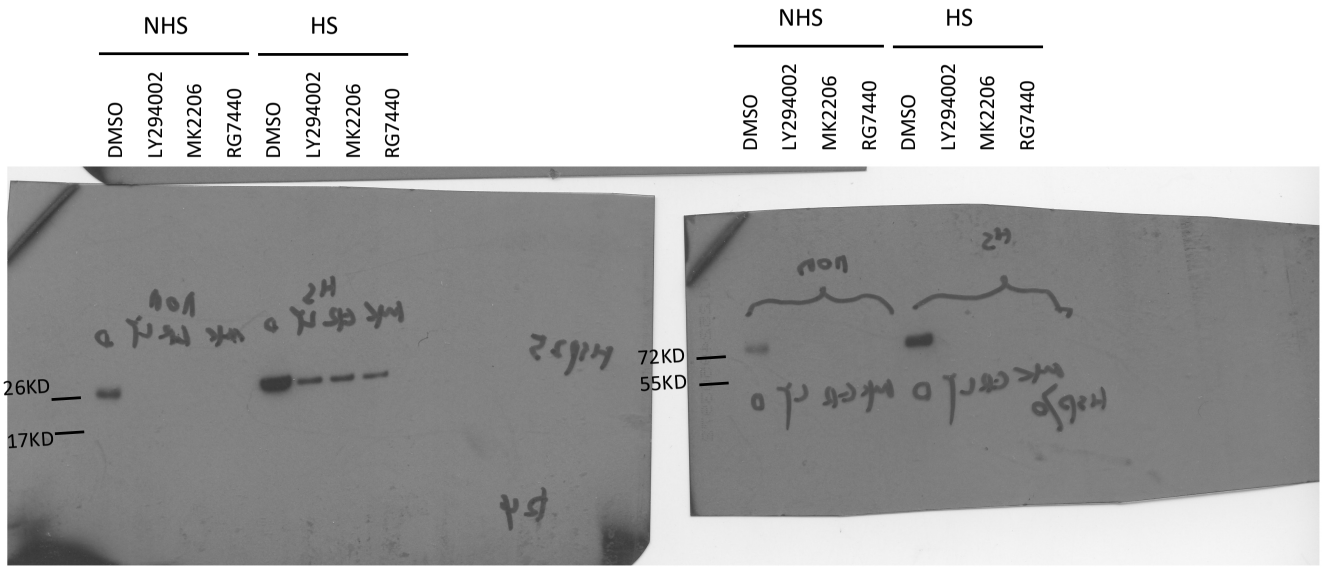


HSP25

HSP72

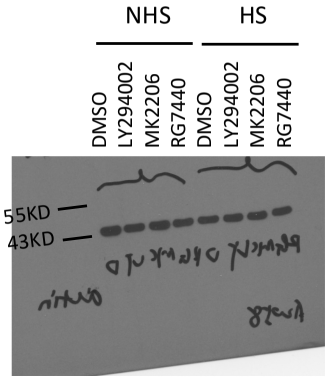


βActin

**Fig. S1J**

**HSF1**

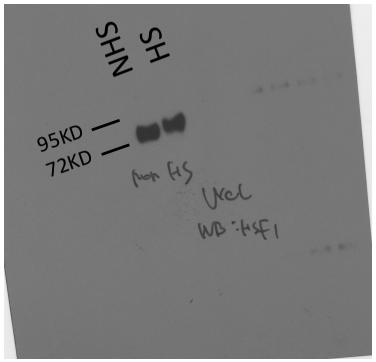


**p-AKT T308**

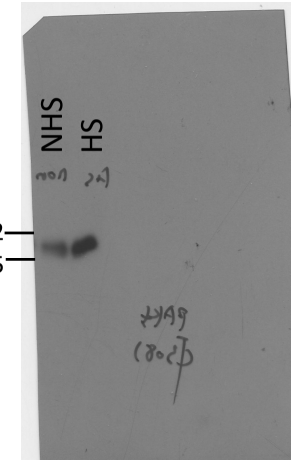


**p-AKT S473**

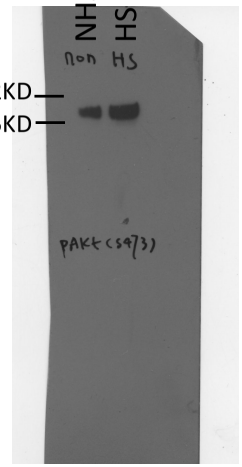


**AKT**

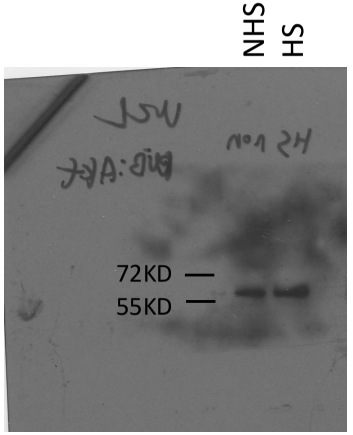


**βActin**

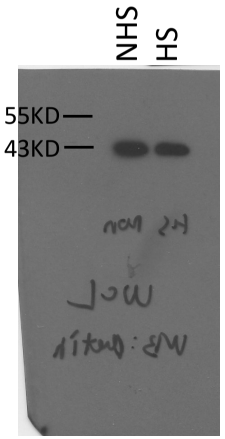


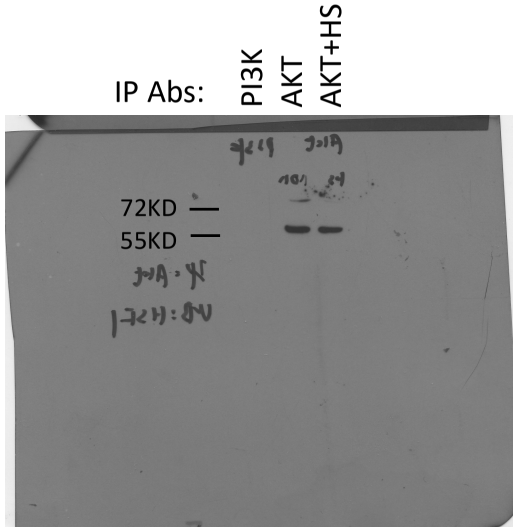


**IPed AKT**

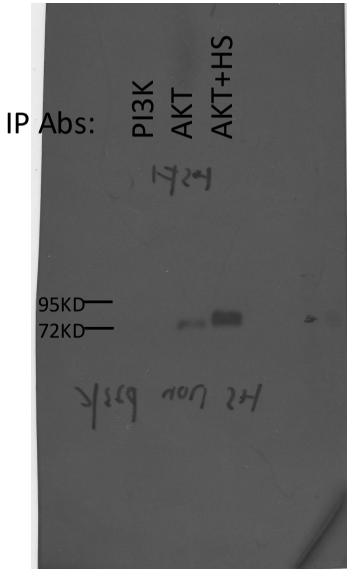


**IPed HSF1**

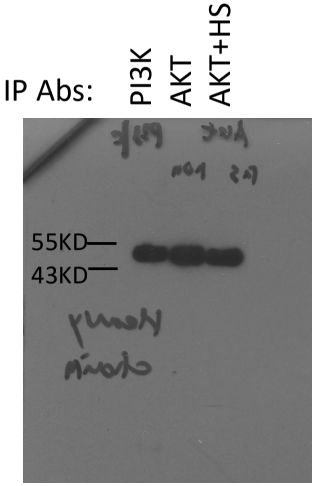


**IgG HC**

# Fig. S1M

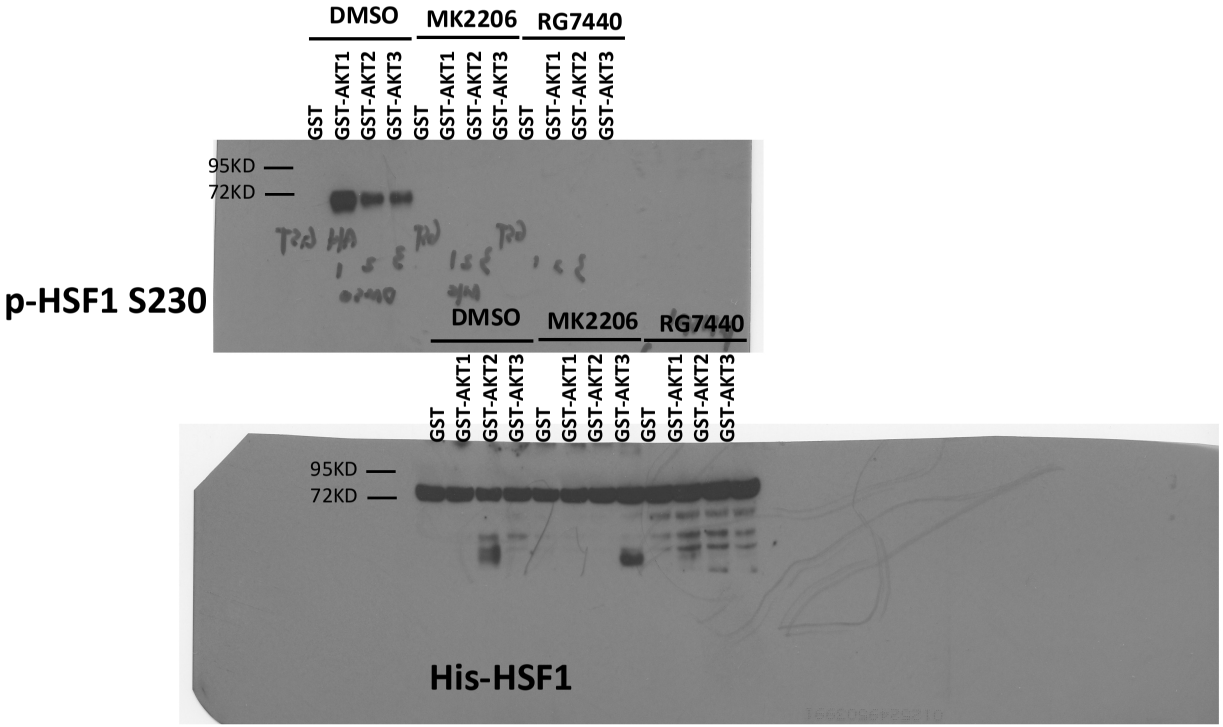
DMSO
MK2206
RG7440
GST
GST-AKT1
GST-AKT2
GST-AKT3
95KD
72KD
p-HSF1 S230
DMSO
MK2206
RG7440
GST
GST-AKT1
GST-AKT2
GST-AKT3
95KD
72KD
His-HSF1

**Fig. S1N**

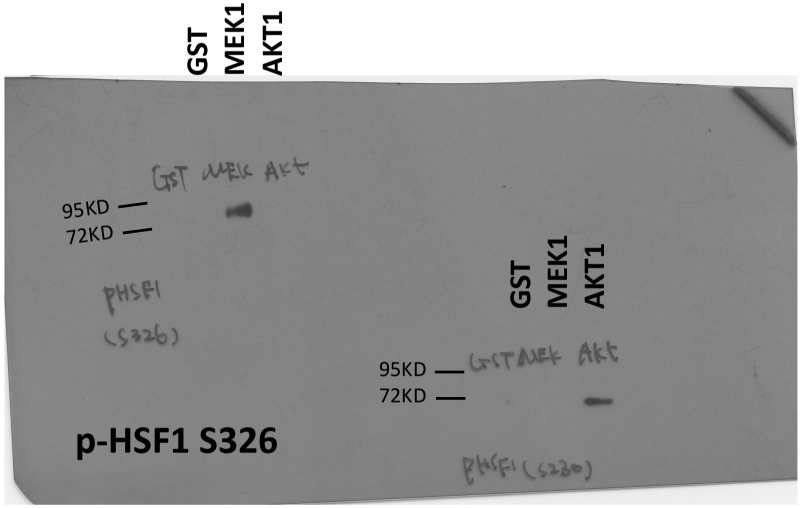


p-HSF1 S230

**Fig. S1O**

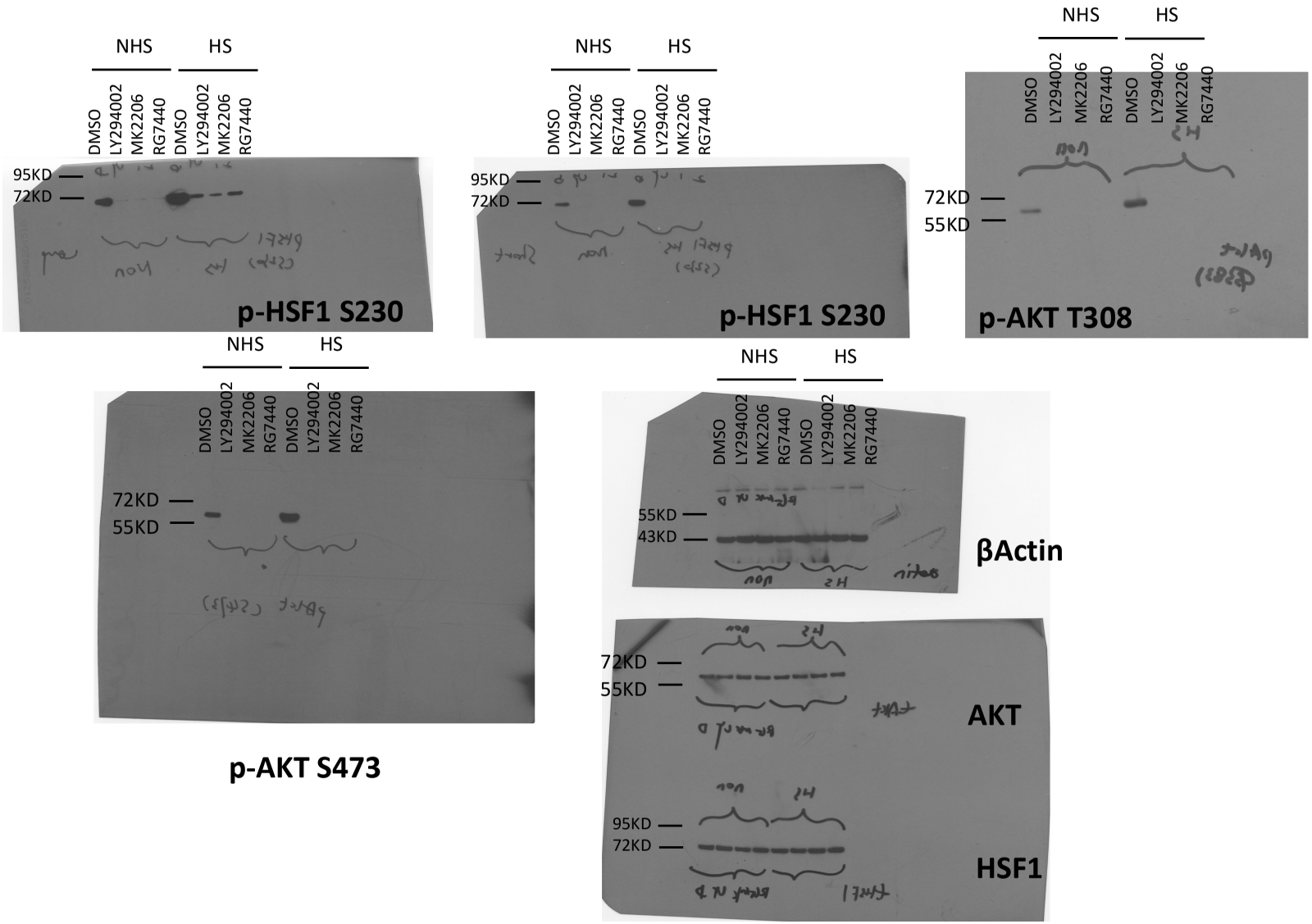
NHS
HS
DMSO
LY294002
MK2206
RG7440
95KD
72KD
p-HSF1 S230
p-HSF1 S230
55KD
p-AKT T308
p-AKT S473
43KD
βActin
AKT
HSF1

# Fig. S1P

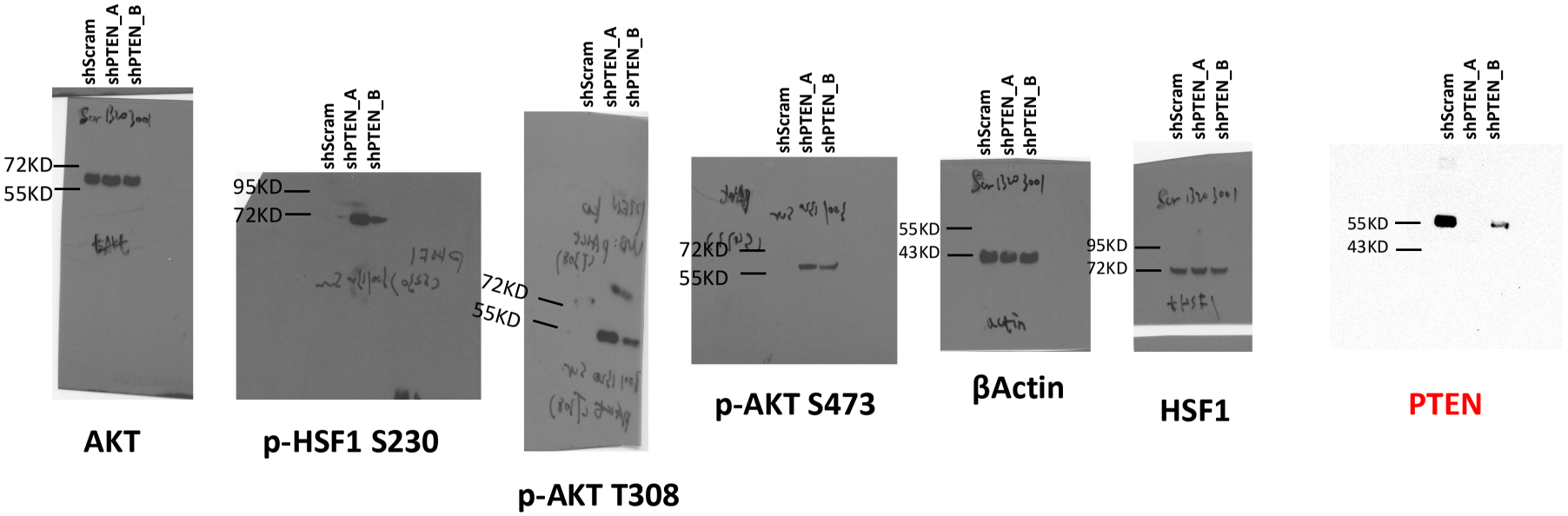
shScram
shPTEN_A
shPTEN_B
72KD
55KD
AKT
95KD
72KD
p-HSF1 S230
72KD
55KD
p-AKT T308
72KD
55KD
p-AKT S473
55KD
43KD
βActin
95KD
72KD
HSF1
55KD
43KD
PTEN

# Fig. S1Q

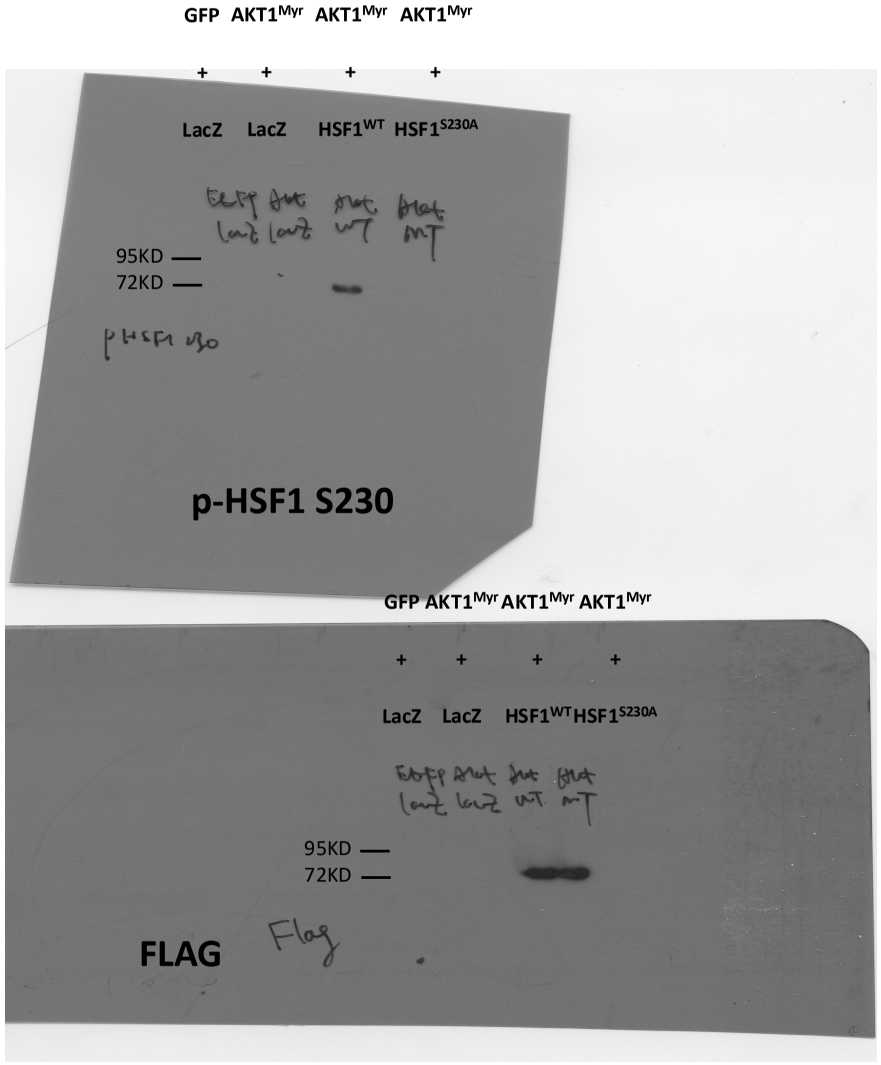
GFP AKT1Myr AKT1Myr AKT1Myr
+ + + +
LacZ LacZ HSF1WT HSF1S230A
95KD
72KD
p-HSF1 S230
GFP AKT1Myr AKT1Myr AKT1Myr
+ + + +
LacZ LacZ HSF1WT HSF1S230A
95KD
72KD
FLAG
Flag

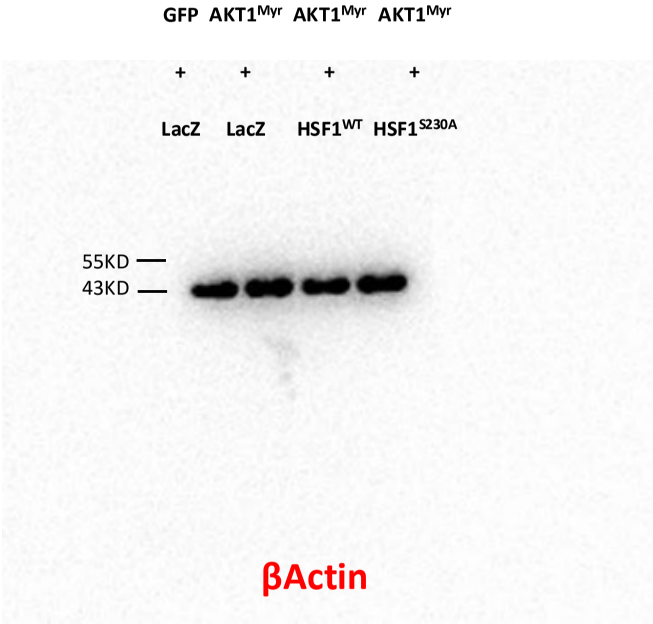
GFP AKT1Myr AKT1Myr AKT1Myr
+ + + +
LacZ LacZ HSF1WT HSF1S230A
55KD
43KD
βActin

Fig. S1S

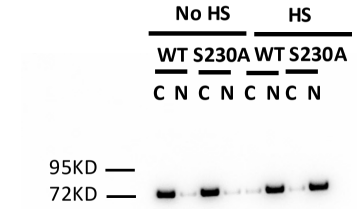


FLAG

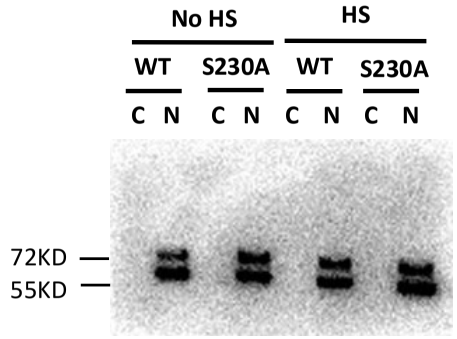


Lamin A/C

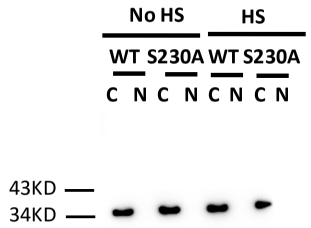


LDH

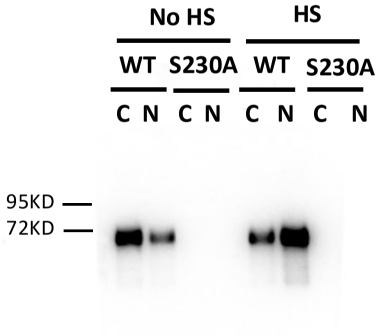


p-HSF1 S230

Fig. S2C

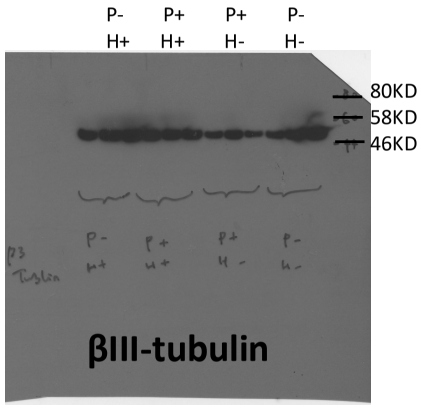


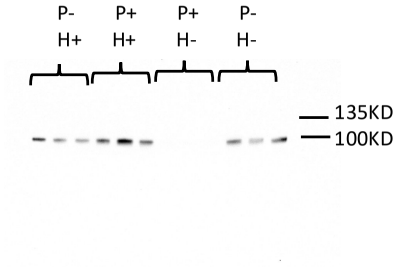


AMPAR1

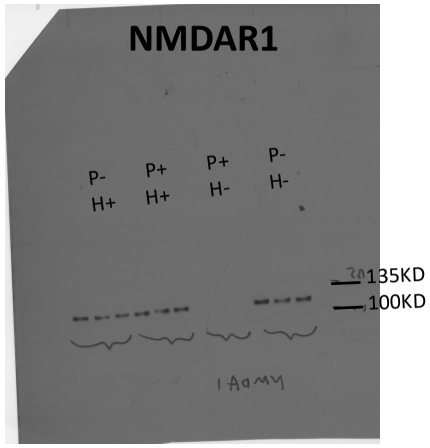


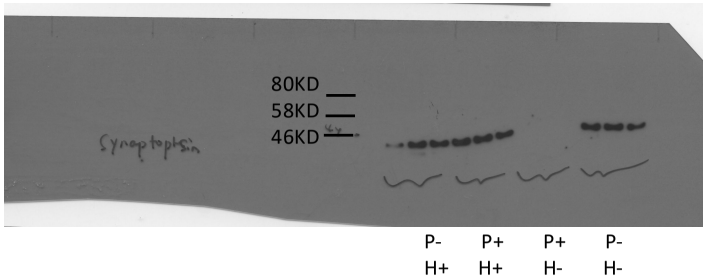


Synaptophysin

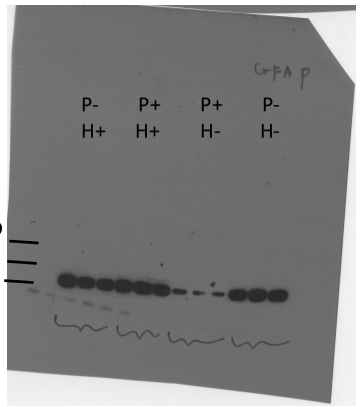


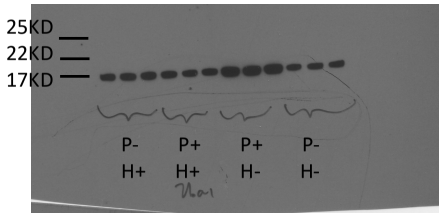


Iba-1

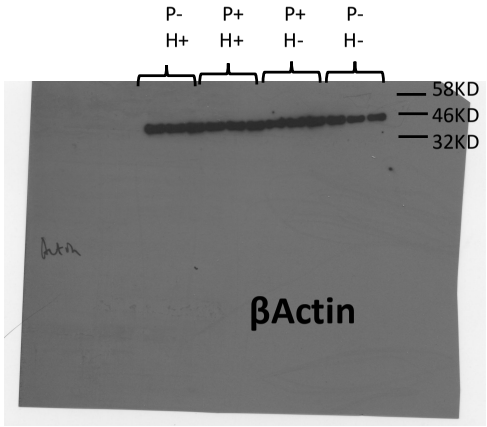

# Fig. S2E

βActin

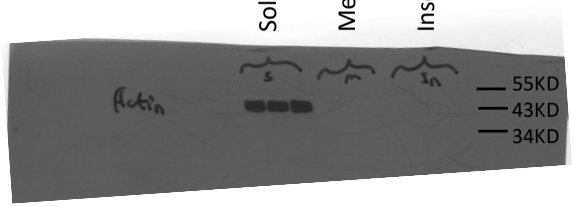


TOM20

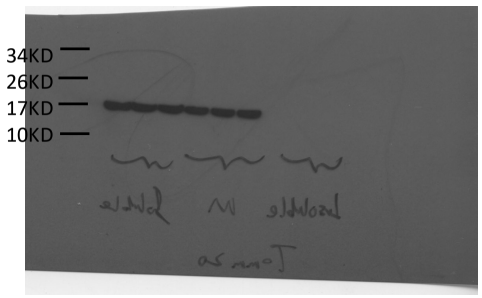


E-Cadherin

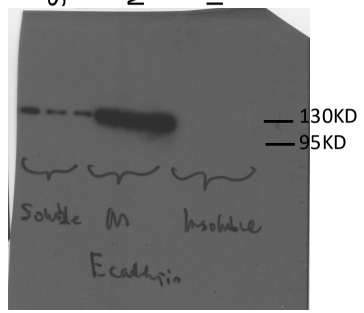


Aβ

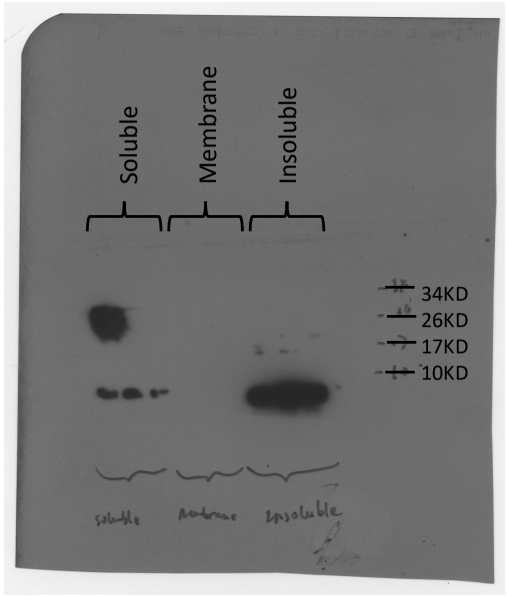


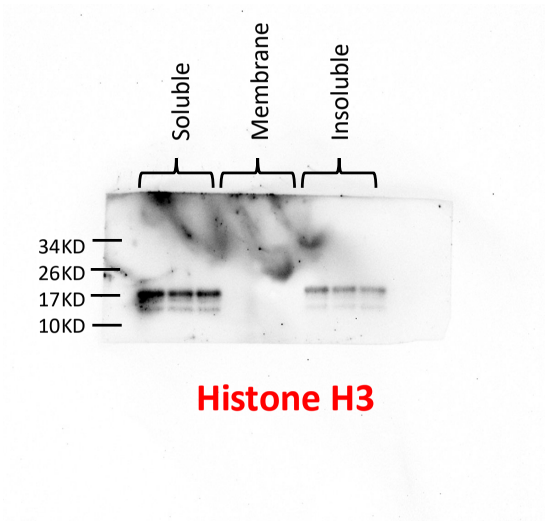

# Fig. S4l

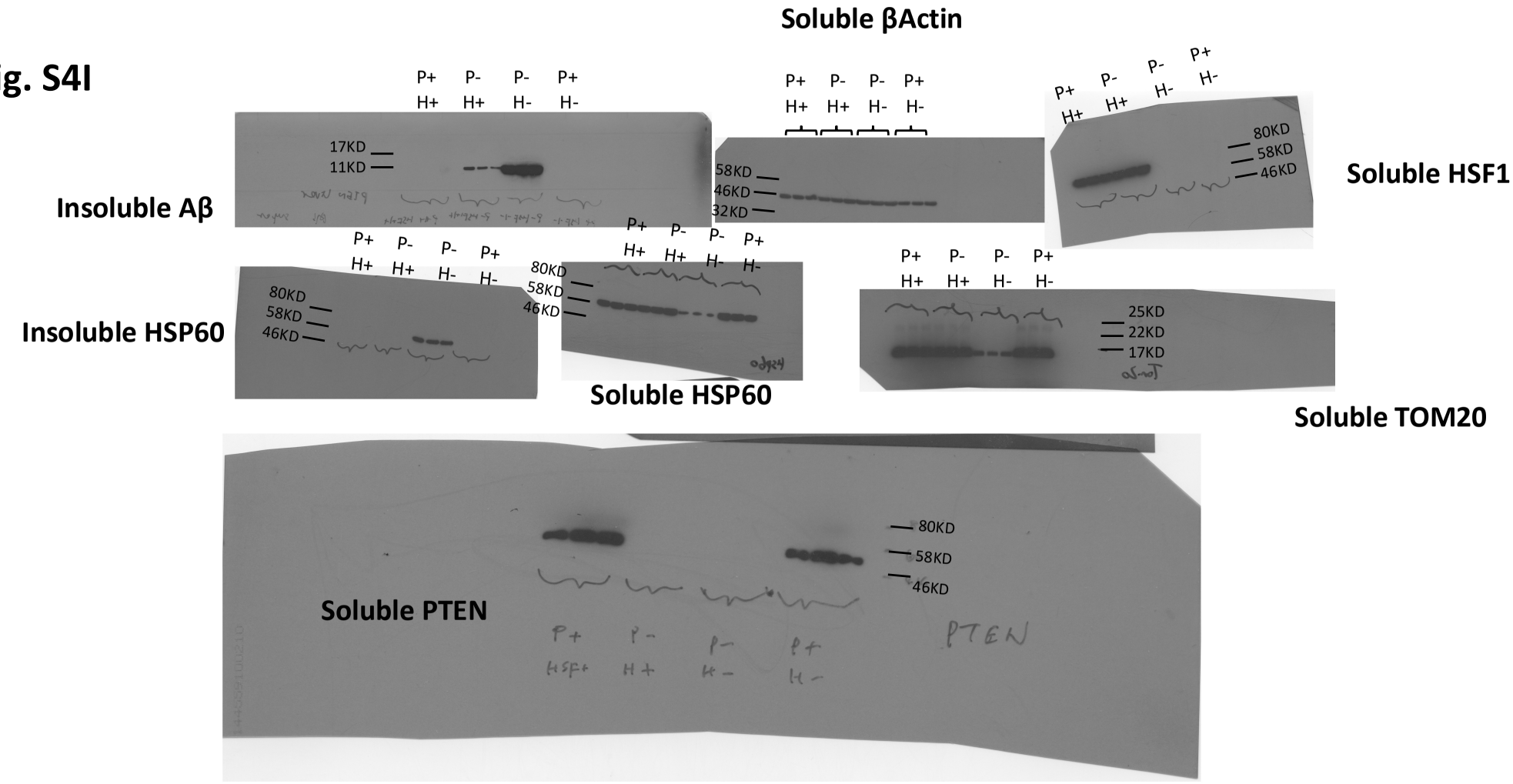
Soluble βActin
Insoluble Aβ
P+ P- P- P+
H+ H+ H- H-
17KD
11KD
58KD
46KD
32KD
Soluble HSF1
80KD
58KD
46KD
Insoluble HSP60
80KD
58KD
46KD
Soluble HSP60
25KD
22KD
17KD
Soluble TOM20
Soluble PTEN
80KD
58KD
46KD
PTEN

# Fig. S5A

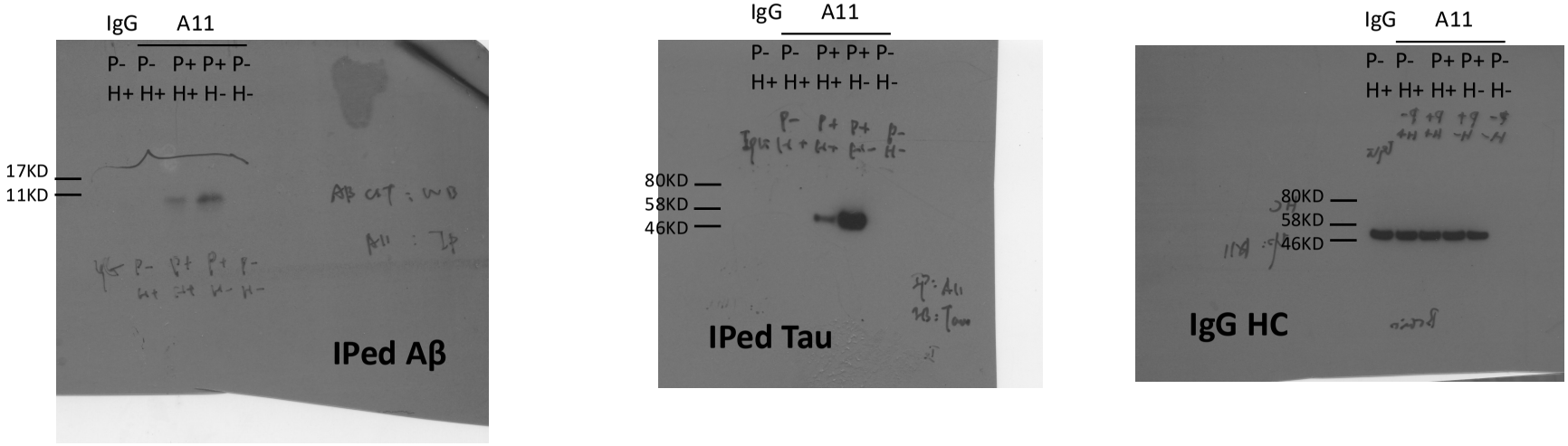
IgG
A11
P- P- P+ P+ P-
H+ H+ H+ H- H-
17KD
11KD
IPed Aβ
IgG
A11
P- P- P+ P+ P-
H+ H+ H+ H- H-
80KD
58KD
46KD
IPed Tau
IgG
A11
P- P- P+ P+ P-
H+ H+ H+ H- H-
80KD
58KD
46KD
IgG HC

# Fig. S5B

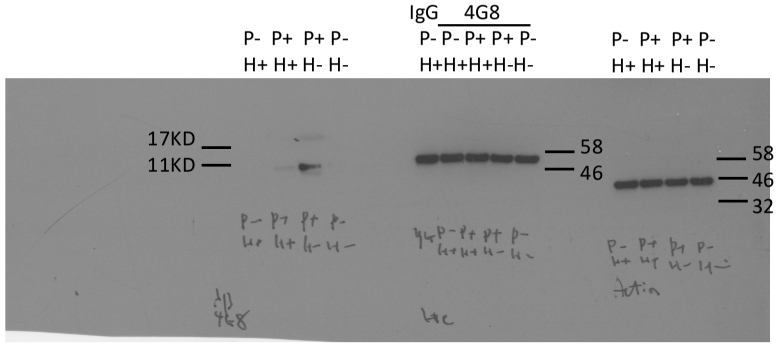


Aβ IgG HC βActin

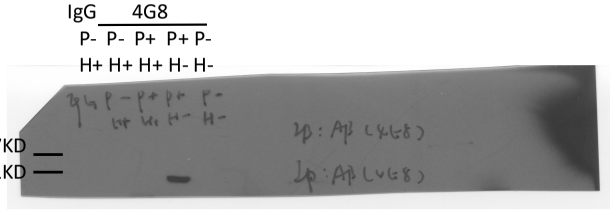


IPed Aβ

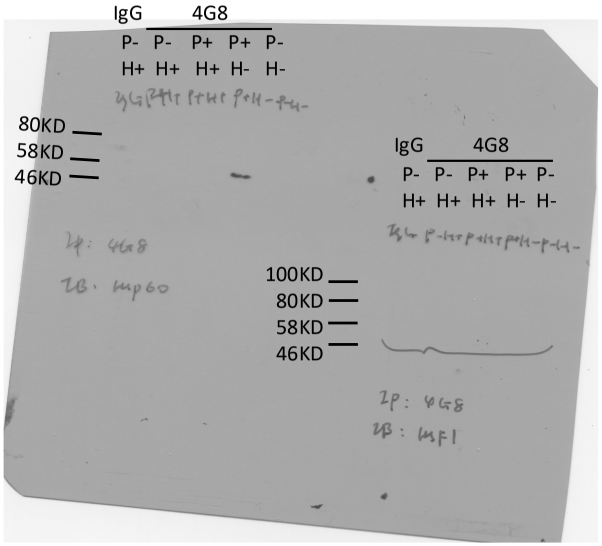


IPed HSP60

IPed HSF1

**Fig. S5C**

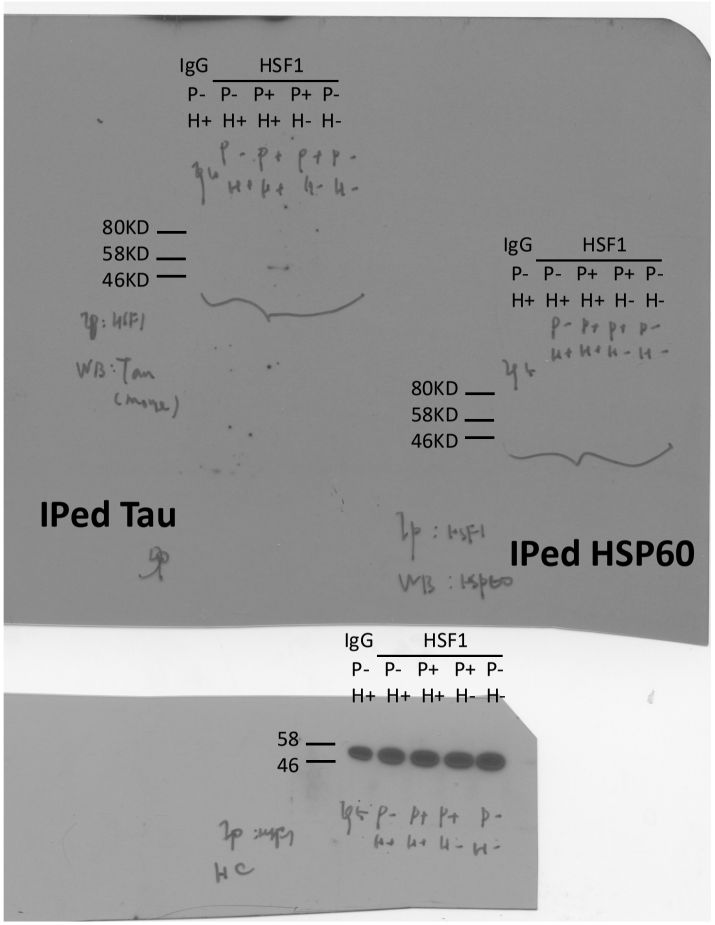
IgG
HSF1
P- P- P+ P+ P-
H+ H+ H+ H- H-
80KD
58KD
46KD
IPed Tau
IPed HSP60
58
46
IgG HC

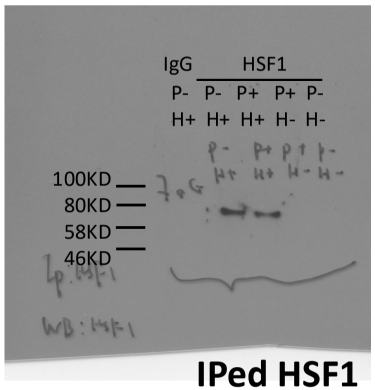
IgG
HSF1
P- P- P+ P+ P-
H+ H+ H+ H- H-
100KD
80KD
58KD
46KD
IPed HSF1

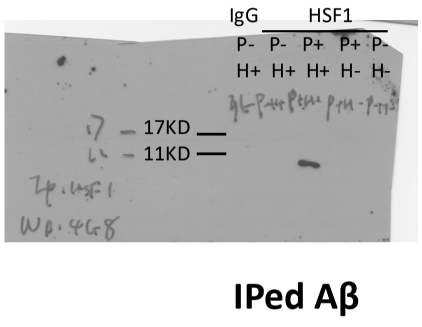
IgG
HSF1
P- P- P+ P+ P-
H+ H+ H+ H- H-
17KD
11KD
IPed Aβ

# Fig. S5E

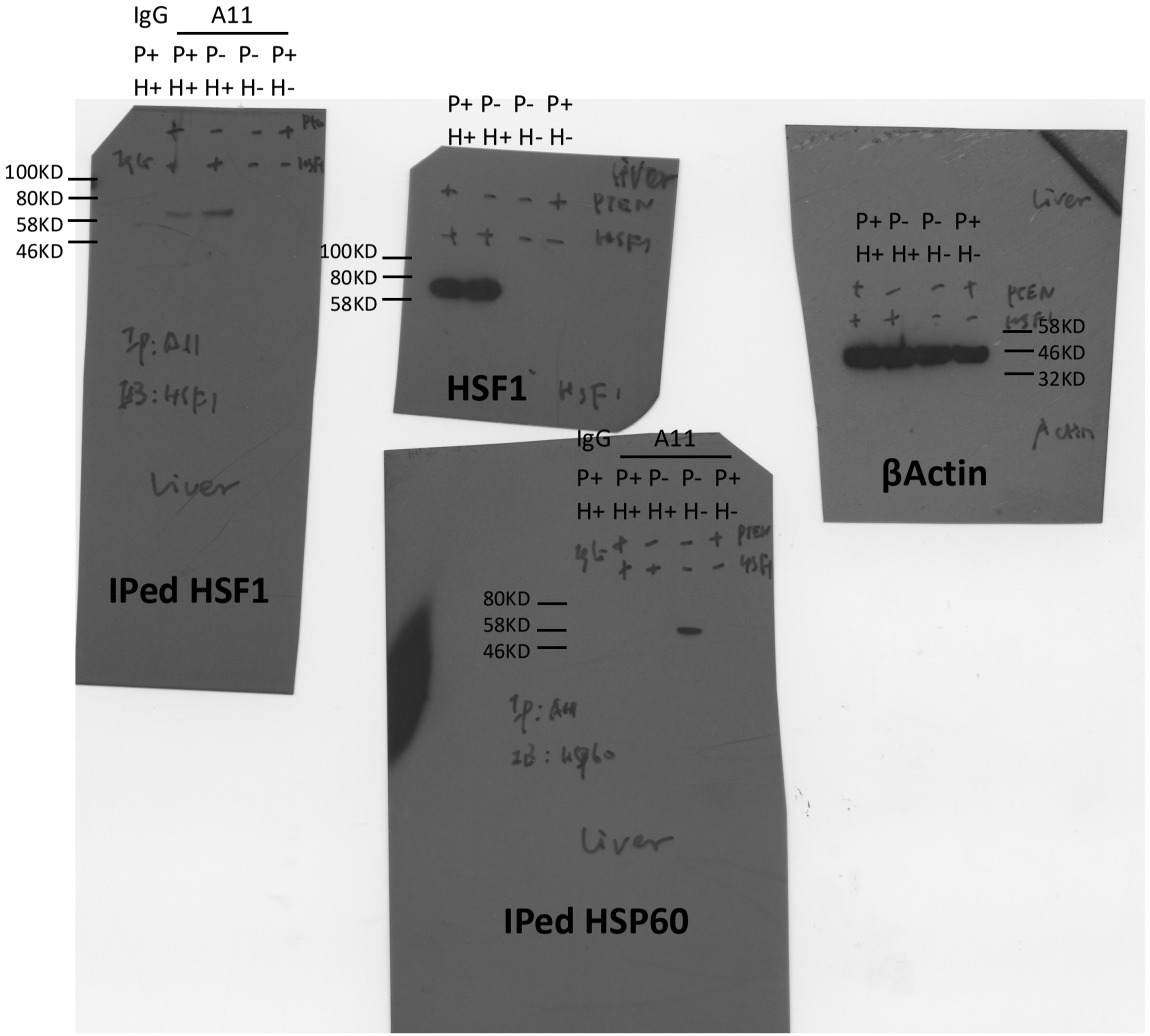
IgG A11
P+ P+ P- P- P+
H+ H+ H+ H- H-
100KD
80KD
58KD
46KD
IPed HSF1
HSF1
βActin
58KD
46KD
32KD
IPed HSP60
80KD
58KD
46KD

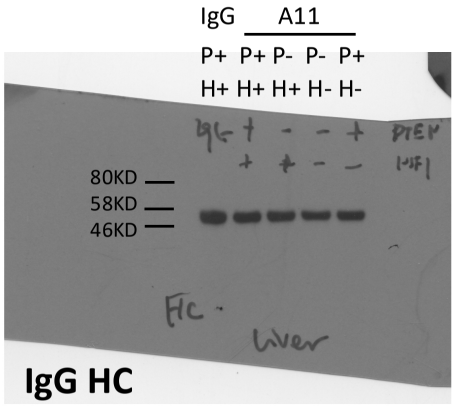
IgG A11
P+ P+ P- P- P+
H+ H+ H+ H- H-
80KD
58KD
46KD
IgG HC

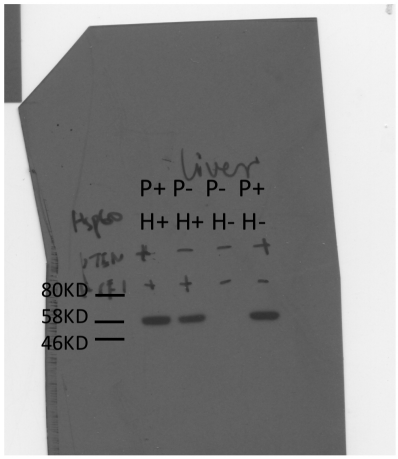
P+ P- P- P+
H+ H+ H- H-
80KD
58KD
46KD
HSP60

**Fig. S5F**

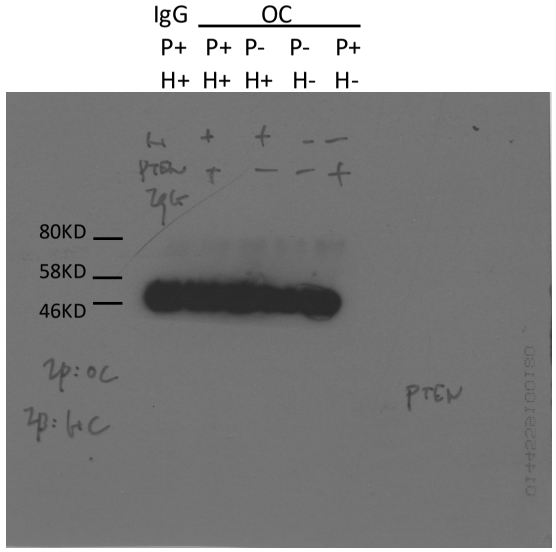


**IgG HC**

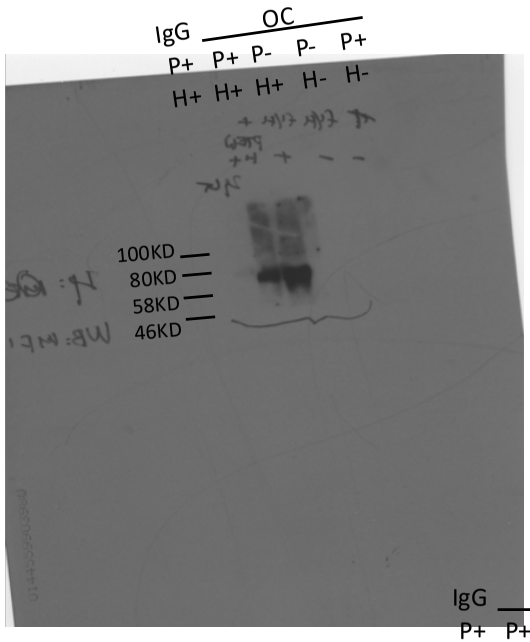


**IPed HSF1**

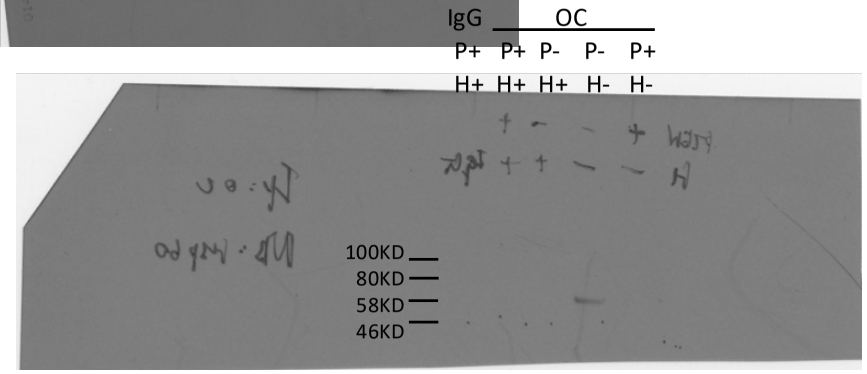


**IPed HSP60**

**Fig. S5J**

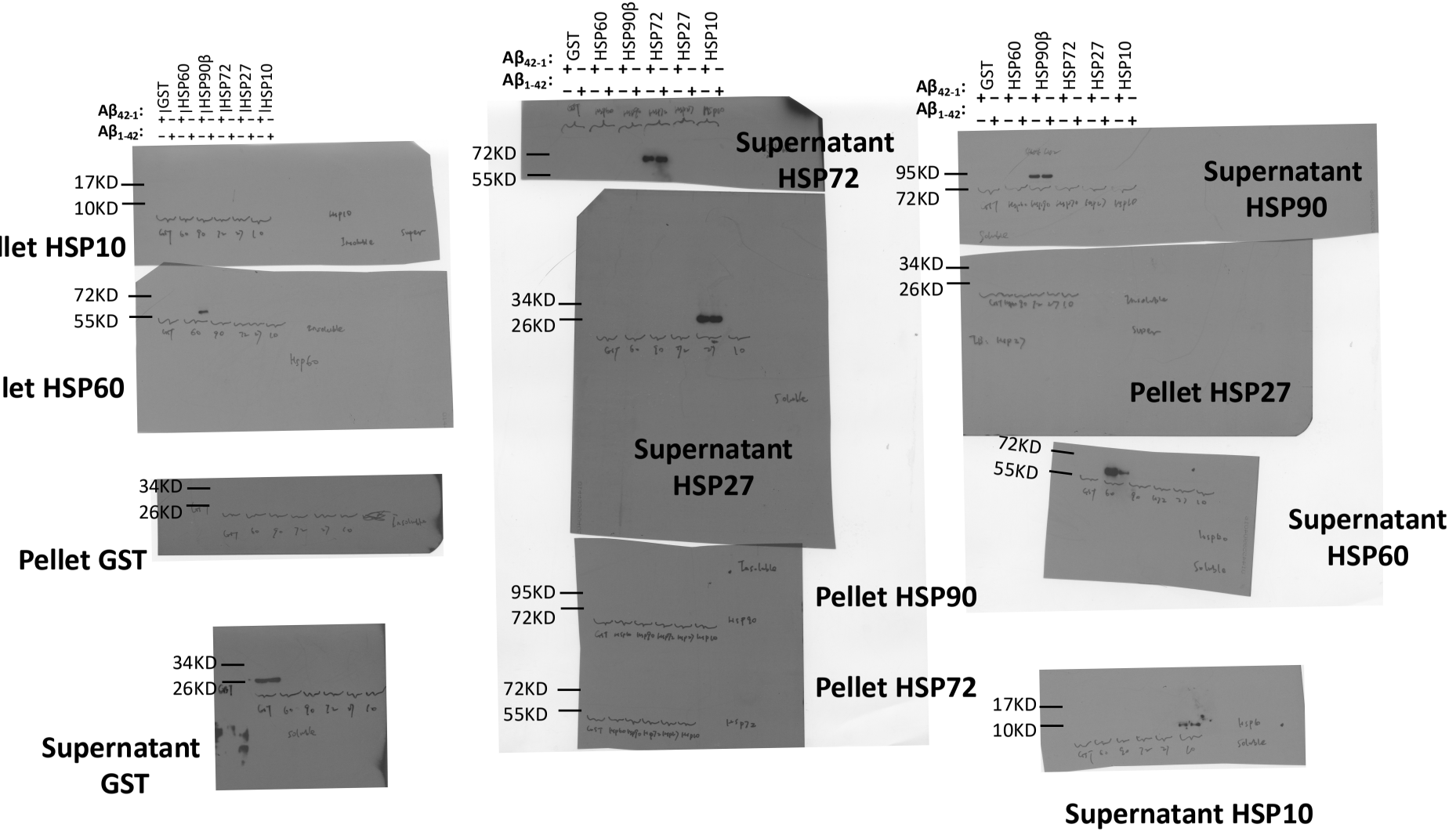
Aβ42-1: + − + − + − + − + − + −
Aβ1-42: − + − + − + − + − + −
GST
HSP60
HSP90β
HSP72
HSP27
HSP10
17KD
10KD
Pellet HSP10
72KD
55KD
Pellet HSP60
34KD
26KD
Pellet GST
34KD
26KD
Supernatant GST
72KD
55KD
Supernatant HSP72
34KD
26KD
Supernatant HSP27
95KD
72KD
Pellet HSP90
72KD
55KD
Pellet HSP72
95KD
72KD
Supernatant HSP90
34KD
26KD
Pellet HSP27
72KD
55KD
Supernatant HSP60
17KD
10KD
Supernatant HSP10

# Fig. S5N

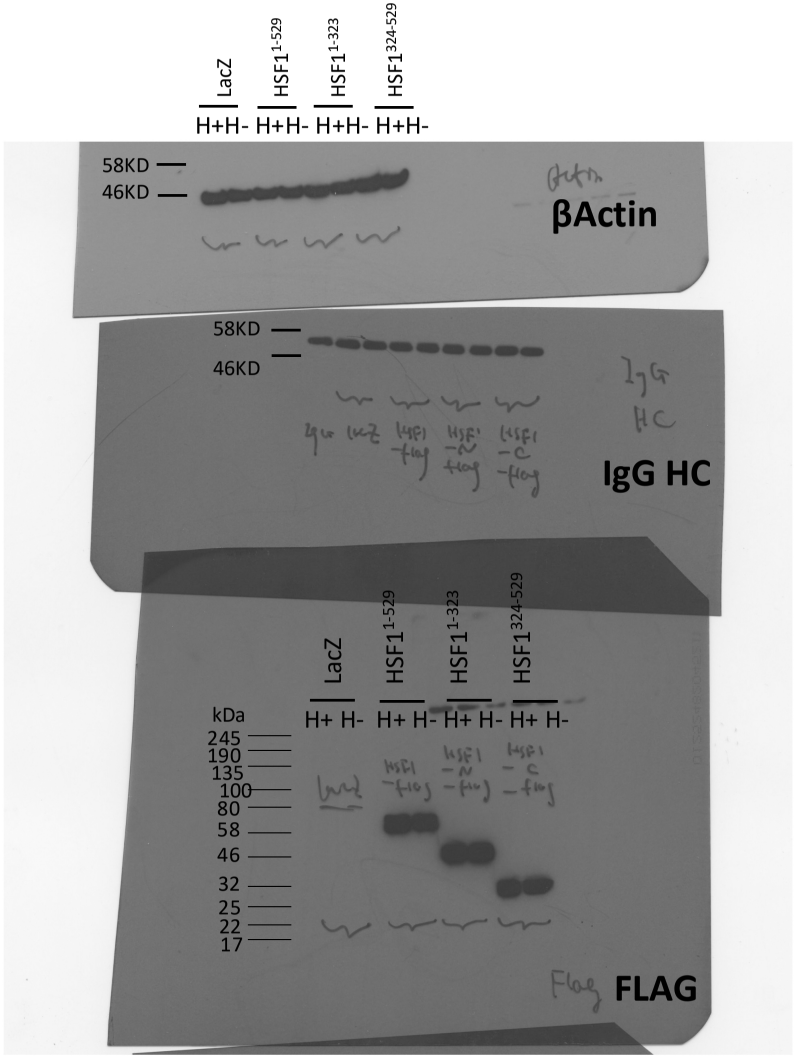
LacZ
HSF1 1-529
HSF1 1-323
HSF1 324-529
H+H- H+H- H+H- H+H-
58KD
46KD
βActin
58KD
46KD
IgG HC
IgG HC
kDa
245
190
135
100
80
58
46
32
25
22
17
FLAG

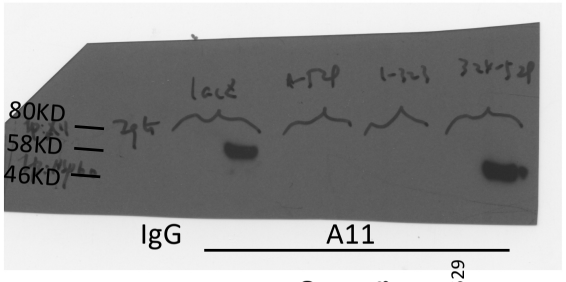
IPed HSP60
80KD
58KD
46KD
IgG
A11
LazZ
LacZ
HSF1 1-529
HSF1 1-323
HSF1 324-529
H+ H+ H- H+ H- H+ H- H+ H-

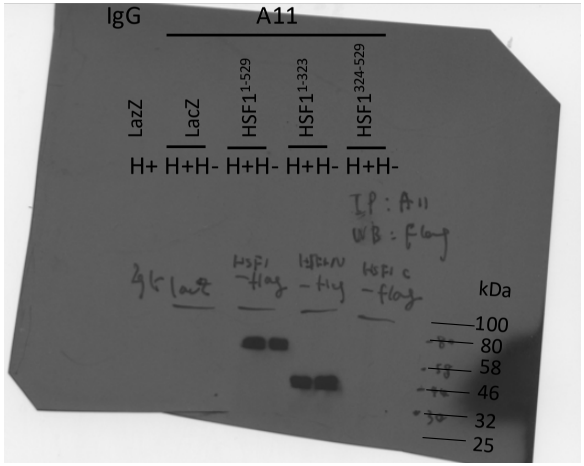
IgG
A11
LazZ
LacZ
HSF1 1-529
HSF1 1-323
HSF1 324-529
H+ H+H- H+H- H+H- H+H-
kDa
100
80
58
46
32
25
IPed FLAG

**Figure S8: Uncropped immunoblot images.**
Images highlighted in red fonts were captured by an iBright™ FL1000 imaging system. Photo credit: Zijian Tang, NCI.l.

**Table S1: Information of human tissues used in this study.**

| Tissue Types | Disease State | Sex | Age (years) |
|---|---|---|---|
| **Brain (paraffin sections)** | Alzheimer's | M | 73 |
| **Brain (paraffin sections)** | Alzheimer's | M | 72 |
| **Brain (paraffin sections)** | Alzheimer's | M | 88 |
| **Brain (paraffin sections, positive control for amyloid plaques)** | Alzheimer's | N/A | N/A |
| **Brain (total lysates)** | Alzheimer's | M | 65 |
| **Brain (Hippocampus lysates)** | Alzheimer's | F | 93 |
| **Brain (paraffin sections)** | Normal aged control | M | 54 |
| **Brain (paraffin sections)** | Normal aged control | F | 54 |
| **Brain (paraffin sections)** | Normal aged control | M | 73 |
| **Brain (total lysates)** | Normal aged control | M | 82 |
| **Brain (Hippocampus lysates)** | Normal aged control | M | 71 |

**Table S2: Detailed information of all experimental materials.**

| REAGENTS OR RESOURCE | SOURCE | IDENTIFIER |
|---|---|---|
| **Antibodies** | | |
| Anti-phospho-AKT Thr380 (D25E6) | Cell Signaling Technology | Cat#: 13038 |
| Anti-phospho-AKT Ser473 (D9E) | Cell Signaling Technology | Cat#: 4060 |
| Anti-HSF1 (H-311) | Santa Cruz Biotechnology | Cat#: sc-9144 |
| Anti-PI3K p110α (C73F8) | Cell Signaling Technology | Cat#: 4249 |
| Anti-AKT (pan) (C67E7) | Cell Signaling Technology | Cat#: 4691 |
| Anti-HSF1 (E-4) | Santa Cruz Biotechnology | Cat#: sc-17757 |
| Anti-HSF1 (10H8) | Santa Cruz Biotechnology | Cat#: sc-13516 |
| Anti-phospho-HSF1 Ser230 | Santa Cruz Biotechnology | Cat#: sc-30443-R |
| Anti-βActin (GT5512) | GeneTex | Cat#: GTX629630 |
| Anti-PTEN (D4.3) | Cell Signaling Technology | Cat#: 9188 |
| Anti-DYKDDDDK Tag (FLAG) (D6W5B) | Cell Signaling Technology | Cat#: 14793 |
| Anti-HSP72 | Enzo Life Science | Cat#: ADI-SPA-812 |
| Anti-HSP25 | Enzo Life Science | Cat#: ADI-SPA-801 |
| Anti-phospho-HSF1 Ser326 (EP1713Y) | Abcam | Cat#: ab76076 |
| Anti-LDH (EP1563Y) | Abcam | Cat#: ab134187 |
| Anti-Lamin A/C (4C11) | Cell Signaling Technology | Cat#: 4777 |
| Anti-MCM2 (D7G11) | Cell Signaling Technology | Cat#: 3619 |
| Anti-PCNA (PC10) | Cell Signaling Technology | Cat#: 2586 |
| Anti-phospho-p70 S6K Thr389 (108D2) | Cell Signaling Technology | Cat#: 9234 |
| Anti-p70 S6K (49D7) | Cell Signaling Technology | Cat#: 2708 |
| Anti-β III tubulin (AA10) | STEMCELL Technologies | Cat#: 60100 |
| Anti-AMPAR1/GluA1 (D4N9V) | Cell Signaling Technology | Cat#: 13185 |
| Anti-NMDAR1/GluN1) (D65B7) | Cell Signaling Technology | Cat#: 5704 |
| Anti-PSD95 (D27E11) | Cell Signaling Technology | Cat#: 3450 |
| Anti-GFAP (E4L7M) | Cell Signaling Technology | Cat#: 80788 |
| Anti-Synaptophysin (D8F6H) | Cell Signaling Technology | Cat#: 36406 |
| Anti-Iba-1/AIF1 | GeneTex | Cat#: GTX100042 |
| Anti-amyloid oligomer (A11) | StressMarq Biosciences | Cat#: SPC-506D |
| Biotin-conjugated Anti-amyloid oligomer (A11) | StressMarq Biosciences | Cat# SPC-506D-BI |
| Anti-amyloid fibrils (OC) | StressMarq Biosciences | Cat#: SPC-507D |
| Biotin-conjugated Anti-amyloid fibrils (OC) | StressMarq Biosciences | Cat# SPC-507D-BI |
| Anti-cleaved caspase 3 (Asp175) (5A1E) | Cell Signaling Technology | Cat#: 9664 |
| Anti-E-cadherin (24E10) | Cell Signaling Technology | Cat#: 3195 |
| Anti-TOM20 (D8T4N) | Cell Signaling Technology | Cat#: 42406 |
| Anti-Histone H3 (D1H2) | Cell Signaling Technology | Cat#: 4499 |
| Anti-β-amyloid, 17-24 (4G8) | BioLegend | Cat#: 800701 |
| Anti-β-amyloid, 1-14 | Abcam | Cat#: ab2539 |

| | | |
|---|---|---|
| Anti-β-amyloid (D54D2) | Cell Signaling Technology | Cat#: 8243 |
| Anti-$A\beta_{1\text{-}42,}$ oligomer specific | GeneTex | Cat#: GTX134510 |
| Anti-HSP60 (D6F1) | Cell Signaling Technology | Cat#: 12165 |
| Anti-HSP60 (LK1) | EMD Millipore | Cat#: MAB3514 |
| Anti-Tau (Tau46) | Cell Signaling Technology | Cat#: 4019 |
| Anti-phospho-Tau (Ser404) (D2Z4G) | Cell Signaling Technology | Cat#: 35834 |
| Anti-Lys48 polyubiquitin (Apu2) | EMD Millipore | Cat#: 05-1307 |
| Anti-β III tubulin (2G10-TB3), Alexa Fluor 488 | Thermo Fisher Scientific | Cat#: 53-4510-80 |
| Anti-Parkin (Prk8) | Cell Signaling Technology | Cat#: 4211 |
| Anti-Cytochrome C (7H8.2C12) | Thermo Fisher Scientific | Cat#: 33-8500 |
| Anti-HSP90α/β | Enzo Life Science | Cat#: ADI-SPA-846-D |
| Anti-GST (91G1) | Cell Signaling Technology | Cat#: 2625 |
| Anti-HSP27 | Enzo Life Science | Cat#: ADI-SPA-803 |
| Anti-HSP10 | Enzo Life Science | Cat#: ADI-SPA-110-D |
| Anti-Biotin (BTN.4) | Thermo Fisher Scientific | Cat#: MA5-11251 |
| Anti-DYKDDDDK Tag, DyLight 680 | Thermo Fisher Scientific | Cat#: MA1-91878-D680 |
| Anti-DYKDDDDK Tag, Alexa Fluro 488 | Cell Signaling Technology | Cat#: 15008 |
| Anti-HSF1 (EP1710Y) | Abcam | Cat#: ab52757 |
| Anti-$A\beta_{1\text{-}42}$ (mOC98) | Abcam | Cat#: ab201061 |
| Normal mouse and rabbit IgG | Santa Cruz Biotechnology | Cat#: sc-2025 and sc-2027 |
| Peroxidase AffiniPure Goat Anti-Rabbit IgG (H+L) | Jackson ImmunoResearch | Cat#: 111-035-144 |
| Peroxidase AffiniPure Goat Anti-Mouse IgG (H+L) | Jackson ImmunoResearch | Cat#: 115-035-003 |
| Peroxidase AffiniPure Goat Anti-Rat IgG (H+L) | Jackson ImmunoResearch | Cat#: 112-035-143 |
| Duolink® In Situ PLA® anti-rabbit Plus probes | Sigma-Aldrich | Cat#: DUO92002 |
| Duolink® In Situ PLA® anti-mouse MINUS probes | Sigma-Aldrich | Cat#: DUO92004 |
| CF®594 Donkey anti-mouse IgG (H+L) | Biotium | Cat#: 20115 |
| CF®594 Donkey anti-rabbit IgG (H+L) | Biotium | Cat#: 20152 |
| CF®488A Donkey anti-mouse IgG (H+L) | Biotium | Cat#: 20014 |
| CF®488A Donkey anti-rabbit IgG (H+L) | Biotium | Cat#: 20015 |
| **Cell Culture Reagents, Chemicals, Peptides, and Recombinant Proteins** | | |
| Accumax Cell Dissociation Solution | Innovative Cell Technologies | Cat# AM105 |
| HyClone™ bovine growth serum | HyClone Laboratories | Cat# SH30541.03IR |
| LY294002 | Selleck Chemicals | Cat#: S1105 |
| MK2206 | ApexBio | Cat#: A3010 |
| RG7440 (Ipatasertib) | ApexBio | Cat#: A3006 |

| | | |
|---|---|---|
| Halt™ phosphatase inhibitor cocktail | Thermo Fisher Scientific | Cat#: 78420 |
| Halt™ protease inhibitor cocktail | Thermo Fisher Scientific | Cat#: 87785 |
| ActinRed™ 555 ReadyProbes™ Reagent | Thermo Fisher Scientific | Cat#: R37112 |
| Hoechst 33342 | Thermo Fisher Scientific | Cat# H1399 |
| 2% uranyl acetate solution | Electron Microscopy Sciences | Cat# 22400-2 |
| SuperSignal West Pico PLUS or Femto chemiluminescent substrates | Thermo Fisher Scientific | Cat#34580 or 34095 |
| Protein G MagBeads | GenScript | Cat#L00274 |
| Recombinant active AKT1, AKT2, and AKT3 proteins | SignalChem | Cat#: A16-10G-10, A17-10G-10, A18-10G-10 |
| Recombinant active MEK1 proteins | SignalChem | Cat#: M02-10G-10 |
| TurboFect™ transfection reagents | Thermo Fisher Scientific | Cat#R0531 |
| Mission® siRNA transfection reagent | Sigma-Aldrich | Cat#: S1452 |
| jetPRIME® transfection reagent | Polyplus-transfection® SA | Cat#: 114-15 |
| RNA STAT-60™ reagent | Tel-Test, Inc. | Cat#: CS-111 |
| Xfect™ Protein Transfection Reagent | Takara Bio USA | Cat#: 631324 |
| 6-FAM-dc-puromycin | Jena Bioscience | Cat#: NU-925-6FM |
| 1-Step™ Ultra TMB-ELISA substrates | Thermo Fisher Scientific | Cat#: 34029 |
| Synthetic human $A\beta_{1-42}$ peptides | GenScript | Cat#: RP10017 |
| Thioflavin T (ThT) | Thermo Fisher Scientific | Cat#: AC211760050 |
| BLOXALL blocking solution | Vector Laboratories | Cat#: SP-6000 |
| Mouse on mouse (M.O.M) blocking reagents | Vector Laboratories | Cat#MKB-2213 |
| Congo Red (CR) | Thermo Fisher Scientific | Cat#: C580-25 |
| 4EGI-1 | EMD Millipore | Cat#: 324517-10MG |
| LY2584702 | BioVision | Cat#: 9445-25 |
| Pan-caspase inhibitor (CI), Q-VD-OPH | APExBIO | Cat#: A1901 |
| MitoView™ Green dyes | Biotium | Cat#: 70054 |
| Chloroquine diphosphate (CQ) | Axxora | Cat#: LKT-C2950-G025 |
| Synthetic $A\beta_{42-1}$ peptides | AnaSpec | Cat#: AS-27275 |
| Recombinant GST proteins | SignalChem | Cat#: G52-30U-50 |
| Recombinant human HSF1 proteins | Enzo Life Science | Cat#: ADI-SPP-900-F |
| Recombinant human HSP60 proteins | R&D Systems | Cat#: AP-140-050 |
| Recombinant human HSP90β | Enzo Life Science | Cat#: ALX201147C025 |
| Recombinant human HSP72 proteins | Enzo Life Science | Cat#: ADI-SPP-715-D |
| Recombinant human HSP27 proteins | Enzo Life Science | Cat#: ADI-NSP-555-D |
| Recombinant human HSP10 proteins | Enzo Life Science | Cat#: ADI-SPP-110-D |
| HiLyte™ Fluor 488-labeled human $A\beta_{1-42}$ | AnaSpec | Cat#: AS-60479-01 |
| DABCYL acid, SE | AnaSpec | Cat#: AS-81801 |
| Synthetic human Biotin-$A\beta_{1-42}$ peptides | AnaSpec | Cat#: AS-23523-05 |

| | | |
|---|---|---|
| Synthetic human Biotin-$A\beta_{42-1}$ peptides | GenScript | Custom synthesis |
| Poly-L-Lysine | ScienCell Research Laboratories | Cat#: 0403 |
| Purified mouse laminin | EMD Millipore | Cat#: CC095 |
| **Commercial Kits** | | |
| EasyBlot anti-Rabbit or anti-Mouse IgG Kits | GeneTex | Cat# GTX225856-01, GTX225857-01 |
| MycoAlert™ Mycoplasm Detection kits | Lonza | Cat# LT07-418 |
| normocin | Invivogen | Cat# ant-nr-1 |
| Complete neuronal medium | ScienCell Research Laboratories | Cat# 1521 |
| Pierce™ BCA Protein Assay Kit | Thermo Fisher Scientific | Cat#: 23225 |
| NovaBright™ Phospha-Light™ EXP Assay Kit for SEAP | Thermo Fisher Scientific | Cat#: N10578 |
| Pierce™ Gaussia Luciferase Glow Assay Kit | Thermo Fisher Scientific | Cat#: 16160 |
| Duolink® In Situ Detection Reagents Red, Green, or Brightfield | Sigma-Aldrich | Cat#: DUO92008, DUO92014 DUO92012 |
| Verso cDNA Synthesis kit | Thermo Fisher Scientific | Cat#: AB1453B |
| DyNAmo HS SYBR Green qPCR kit | Thermo Fisher Scientific | Cat#: F410L |
| Q5® Site-Directed Mutagenesis Kit | New England Biolabs | Cat#: E0554S |
| NE-PER™ Nuclear and Cytoplasmic Extraction Kit | Thermo Fisher Scientific | Cat#: 78835 |
| NucleoSpin® TriPrep Kit | Takara Bio USA | Cat#: 740966.50 |
| Detergent-free Nuclei Isolation Kit | 101Bio, LLC | Cat#: P524-20 |
| Caspase-3 Colorimetric Assay Kit | R&D Systems | Cat#: K106-100 |
| Caspase 3 DEVD-R110 Fluorometric and Colorimetric Assay Kit | Biotium | Cat#: 30008-2 |
| NeuroTACS™ In Situ Apoptosis Detection Kit | R&D Systems | Cat#: 4823-30-K |
| JC-1 Mitochondrial Membrane Potential Detection Kit | Biotium | Cat#: 30001 |
| NovaUltra Nissl Stain Kit | IHCWORLD | Cat#: IW-3007 |
| ImmPRESS™ HRP horse anti-rabbit IgG Polymers Detection Kit | Vector Laboratories | Cat#: MP-7401-15 |
| ImmPRESS™-AP Anti-Mouse IgG (alkaline phosphatase) Polymer Detection Kit | Vector Laboratories | Cat#: MP-5402-15 |
| ImmPACT™ DAB Peroxidase (HRP) Substrate Kit | Vector Laboratories | Cat#: SK-4105 |
| ImmPACT™ NovaRED™ Peroxidase (HRP) Substrate Kit | Vector Laboratories | Cat#: SK-4805 |

| | | |
|---|---|---|
| ImmPACT® Vector Red Alkaline Phosphatase (AP) substrate | Vector Laboratories | Cat#: SK-5105 |
| Vector Blue Alkaline Phosphatase (Blue AP) Substrate Kit | Vector Laboratories | Cat#: SK-5300 |
| ImmPRESS™ Excel Amplified HRP Polymer Staining Kit (Anti-Rabbit IgG) | Vector Laboratories | Cat#: MP-7601 |
| HSF1 ELISA Kit | Enzo Life Sciences | Cat# ADI-900-198 |
| Amyloid beta 42 Mouse ELISA Kit | Thermo Fisher Scientific | Cat#: KMB3441 |
| Mouse HSP60 ELISA Kit | Abcam | Cat# Ab208344 |
| Mitochondrial Isolation Kit | Sigma-Aldrich | Cat#: MITOISO2-1KT |
| Molecular Probes Alexa Fluor™ 594 Microscale Protein Labeling Kit | Thermo Fisher Scientific | Cat#: A30008 |
| Lenti-X™ GoStix™ Plus | Takara Bio USA | Cat#: 631280 |
| CellTiter-Blue® Cell Viability Assay | Promega | Cat# G8080 |
| **Cell Lines and Mouse Strains** | | |
| HEK293T cells | GE Dharmacon | Cat#: HCL4517 |
| HeLa cells | ATCC | Cat#: CCL-2 |
| A2058 cells | ATCC | Cat#: CRL-11147 |
| NIH3T3 cells | Lab Collection | N/A |
| HEK293T cells stably expressing *HSF1*-targeting lentiviral shRNAs (A6) | Lab Collection | N/A |
| *Rosa26-CreER$^{T2}$*; *Hsf1$^{fl/fl}$* MEFs (male) | Lab Collection | N/A |
| *hGFAP-Cre$^{+}$*; *PI3K p110* STOP$^{fl}$*; *Hsf1$^{+/+\ or\ fl/fl}$* astrocytes | This study | N/A |
| *Hsf1$^{fl/fl}$* astrocytes stably expressing Scramble or *Pten*-targeting shRNAs | This study | N/A |
| Primary human neurons | ScienCell Research Laboratories | Cat#: 1520 |
| *Hsf1$^{fl/fl}$* mice | Lab Collection | N/A |
| *R26Stop$^{FL}$P110** | The Jackson Laboratory | Stock#: 012343 |
| *hGFAP-Cre* mice | The Jackson Laboratory | Stock#: 004600 |
| *Alb-Cre* mice | The Jackson Laboratory | Stock#: 016832 |
| *Pten$^{fl/fl}$* mice | The Jackson Laboratory | Stock#: 006440 |
| **Oligonucleotides** | | |
| All listed in Table S3 | Fisher Scientific and IDT | N/A |
| **Recombinant DNAs, shRNAs, and siRNAs** | | |
| pHSE-SEAP | Clontech Laboratories | Cat#: 631910 |
| pCMV-Gaussia Luc | Thermo Fisher Scientific | Cat#: 16147 |
| pcDNA3-Myr-HA-AKT1 | Addgene | Cat#: 9008 |
| pcDNA3-Myr-HA-AKT2 | Addgene | Cat#: 9016 |
| pcDNA3-Myr-HA-AKT3 | Addgene | Cat#: 9017 |
| pCMV-dR8.2 dvpr | Addgene | Cat#: 8455 |
| pCMV-VSV-G | Addgene | Cat#: 8454 |
| pLKO.1-shScramble | Addgene | Cat#: 1864 |

| | | |
|---|---|---|
| pLKO.1-shPTEN_A | Addgene | Cat#: 25638 |
| pLKO.1-shPTEN_B | Addgene | Cat#: 25639 |
| pLKO-shPten_A | Sigma-Aldrich | Cat#: TRCN0000322421 |
| pLKO-shPten_B | Sigma-Aldrich | Cat#: TRCN0000322487 |
| pLenti6-LacZ | Lab Collection | N/A |
| pLenti6-FLAG-HSF1$^{WT}$ | Lab Collection | N/A |
| pLenti6-FLAG-HSF1$^{S230A}$ | This study | N/A |
| pLX304-HSP60 | DNASU repository | Cat#: HsCD00442045 |
| siControl | Thermo Fisher Scientific | Cat#: D-001810-01 |
| siAkt1 | Sigma-Aldrich | Cat#: SIHK0096 |
| siAkt2 | Sigma-Aldrich | Cat#: SIHK0099 |
| siAkt3 | Sigma-Aldrich | Cat#: SIHK0102 |
| siHsp60_A | Sigma-Aldrich | Cat#: SASI_Hs01_00136360 |
| siHsp60_B | Sigma-Aldrich | Cat#:SASI_Mm01_00146428 |
| siHSP60_A | Sigma-Aldrich | Cat#: SASI_Hs01_00136360 |
| siHSP60_B | Sigma-Aldrich | Cat#: SASI_Hs01_00136363 |
| pLenti6-FLAG-HSF1$^{1-323}$ | This study | N/A |
| pLenti6-FLAG-HSF1$^{324-529}$ | This study | N/A |
| **Software and Algorithm** | | |
| Prism 8 | GraphPad Software | N/A |
| FlowJo v10 | FlowJo, LLC | N/A |
| Fiji v1.0 | NIH | N/A |
| **Others** | | |
| Ad5CMVhr-GFP and Ad5CMVCre viral particles | University of Iowa Gene Transfer Vector Core | Cat#: VVC-U of Iowa-2161 and -5 |
| Immobilon® PVDF membranes, 0.45µm pore size | EMD Millipore | Cat# IPVH07850 |
| 200-mesh carbon-coated nickel grid | Electron Microscopy Sciences | Cat# CF200-Ni |
| 8-well Nunc™ Lab-Tek™ II CC2™ Chamber Slides | Thermo Fisher Scientific | Cat# 154941 |
| Tissue arrays, Alzheimer's Disease | US Biological | Cat#: T5595-6325 |
| Alzheimer QC control slides | StatLab Medical Products, LLC | Cat#: CSA0224P |

**Table S3: Nucleotide sequences of primers and target sequences of siRNAs and shRNAs.**

**qRT-PCR primers**

| Primer ID | Primer sequences (5'→3') |
|---|---|
| **Mouse_Hspa1a/Hsp72_ Forward** | ATGGACAAGGCGCAGATCC |
| **Mouse_Hspa1a/Hsp72_ Reverse** | CTCCGACTTGTCCCCCAT |
| **Mouse_Hspb1/Hsp25_ Forward** | ATCCCCTGAGGGCACACTTA |
| **Mouse_Hspb1/Hsp25_ Reverse** | GGAATGGTGATCTCCGCTGAC |
| **Mouse_Hsp90aa1/Hsp90α_ Forward** | AATTGCCCAGTTAATGTCCTTGA |
| **Mouse_Hsp90aa1/Hsp90α_ Reverse** | CGTCCGATGAATTGGAGATGAG |
| **Mouse_Hspd1/Hsp60_ Forward** | CACAGTCCTTCGCCAGATGAG |
| **Mouse_Hspd1/Hsp60_ Reverse** | CTACACCTTGAAGCATTAAGGCT |
| **Mouse_βActin_Forward** | GGCTGTATTCCCCTCCATCG |
| **Mouse_βActin_Reverse** | CCAGTTGGTAACAATGCCATGT |
| **Human_HSPA1A/HSP72_Forward** | CAAGATCACCATCACCAACG |
| **Human_HSPA1A/HSP72_ Reverse** | TCGTCCTCCGCTTTGTACTT |
| **Human_HSPB1/HSP27_ Forward** | GGACGAGCTGACGGTCAAG |
| **Human_HSPB1/HSP27_ Reverse** | AGCGTGTATTTCCGCGTGA |
| **Human_βACTIN_Forward** | CATGTACGTTGCTATCCAGGC |
| **Human_βACTIN_Reverse** | CTCCTTAATGTCACGCACGAT |

**ChIP qPCR primers**

| Primer ID | Primer sequences (5'→3') |
|---|---|
| **Human_HSP72_HSE Forward** | GGCGAAAACCCTGGAATATTCCCGA |
| **Human_HSP72_HSE Reverse** | AGCCTTGGGACAACGGGAG |
| **Human_HSP27_HSE_ Forward** | GTCGCGCTCTCGAATTCAT |
| **Human_HSP27_HSE_ Reverse** | CCTCCCCATGCACTCCTC |

**Mutagenesis primers**

| Primer ID | Primer sequences (5'→3') |
|---|---|
| **HSF1_1-323_ Forward** | GACTACAAGGACGACGATGACAAGTAG |
| **HSF1_1-323_ Reverse** | GGTGTCCACGGAAGATGG |
| **HSF1_324-529_ Forward** | CTCTTGTCCCCGAC |
| **HSF1_324-529_ Reverse** | CATCTCGAGCAAGGA |
| **HSF1_S230A_Forward** | CGGCAGTTCGCCCTGGAGCACGTC |
| **HSF1_S230A_ Reverse** | GCTATACTTGGGCATGGAATGTGC |

**siRNAs**

| Gene ID | Sequences | Vector | Vendor | Cat# |
|---|---|---|---|---|
| ***Akt1*** | Proprietary | N/A | Sigma-Aldrich | SIHK0096 |

| | | | | |
|---|---|---|---|---|
| ***Akt2*** | Proprietary | N/A | Sigma-Aldrich | SIHK0099 |
| ***Akt3*** | Proprietary | N/A | Sigma-Aldrich | SIHK0102 |
| ***HSPD1/HSP60_A*** | Proprietary | N/A | Sigma-Aldrich | SASI_Hs01_00136360 |
| ***HSPD1/HSP60_B*** | Proprietary | N/A | Sigma-Aldrich | SASI_Hs01_00136363 |
| ***Hspd1/Hsp60_A*** | Proprietary | N/A | Sigma-Aldrich | SASI_Mm01_00146427 |
| ***Hspd1/Hsp60_B*** | Proprietary | N/A | Sigma-Aldrich | SASI_Mm01_00146428 |
| **Non-targeting control** | Proprietary | N/A | Thermo Fisher Scientific | D-001810-01 |

**shRNAs**

| Gene ID | Sequences | Vector | Vendor | Cat# |
|---|---|---|---|---|
| ***PTEN_A*** | CCACAGCTAGAACTTATCAAA | pLKO | Addgene | #25638 |
| ***PTEN_B*** | CCACAAATGAAGGGATATAAA | pLKO | Addgene | #25639 |
| ***Pten_A*** | CGACTTAGACTTGACCTATAT | pLKO | Sigma-Aldrich | TRCN0000322421 |
| ***Pten_B*** | ACATTATGACACCGCCAAATT | pLKO | Sigma-Aldrich | TRCN0000322487 |
| **Scramble control** | CCTAAGGTTAAGTCGCCCTCG | pLKO | Addgene | #1864 |